



Wisconsin Electric POWER COMPANY
231 W. MICHIGAN, P.O. BOX 2046, MILWAUKEE, WI 53201

May 27, 1981

Mr. Harold R. Denton, Director
Office of Nuclear Reactor Regulation
U. S. NUCLEAR REGULATORY COMMISSION
Washington, D. C. 20555

Attention: Mr. Robert A. Clark, Chief
Operating Reactor Branch No. 3

Gentlemen:



DOCKET NO. 50-301
REPORT OF STEAM GENERATOR TUBE INSPECTION
POINT BEACH NUCLEAR PLANT, UNIT NO. 2

In our Licensee Event Report No. 81-002/01T-01 we reported that a segment of steam generator tube R15C73 had been removed from the Point Beach Nuclear Plant Unit 2 "A" steam generator for detailed metallographic inspection and examination. Attached is a report of the results and observations from this inspection. These results were discussed with Mr. Emmitt Murphy of your Staff on May 22, 1981.

We have also enclosed an additional report on the evaluation of the April 1981 eddy current inspection results. The principal objective of this report was to determine the average growth of the eddy current indications since the previous spring 1980 inspection. Comparisons of reported eddy current results as well as comparisons of eddy current signals were made during this evaluation. This evaluation concludes, as we had concluded in our May 11, 1981 report, that there has been little or no change in eddy current indicator signals since 1974, and that corrosion rates over the period from spring 1980 to spring 1981 are not substantially changed from previous years in Unit 2.

Finally, as requested by Mr. Murphy, we have enclosed eddy current inspection maps for both the steam generator "A" and "B" inlets. If you have any questions regarding this information, please let me know.

Very truly yours,

CW Fay

C. W. Fay, Director
Nuclear Power Department

*Doc 2
5/11*

Copy to NRC Resident Inspector
Mr. C. F. Riederer (PSCW)
Mr. Peter Anderson (WED)

8106030 **308**
Attachment

EXAMINATION OF POINT BEACH UNIT #2

STEAM GENERATOR TUBE SAMPLE

SG A R15-C73 HL

May 18, 1981

SG A KID-4-1-14

During the April 1981 outage at Point Beach Unit #2, one steam generator tube sample was removed from steam generator A inlet (hot leg) side, designated Row 15, Column 73. The tube showed the presence of an eddy current indication of 41 percent wall penetration, prior to removal, at the top of the tubesheet.

For extraction of the sample, the tube was cut using a ID cutting device at a short distance below the first (lowest) tube support plate. The seal weld at the primary face of the tubesheet was also removed, thus freeing the tube for extraction. An extraction tool was inserted and a load of ~11,000 lbs was applied. As the sample was moved from the tubesheet, a fracture occurred that separated the tube into two pieces. Extraction was continued until the entire sample was removed in three pieces; a second ID cut being made to accommodate the sample's length. Figure A1 is a schematic of the three pieces of the sample, with dimensional measurements after complete removal.

In the laboratory, additional dimensional measurements were made (Figure A2) and numerical reconstruction of the tube was made (Figure B) to locate the elevation of the fracture that occurred during extraction. From the dimensional measurements, the tube had been stretched in length approximately 10 inches, based on an original cut length of 68.5 inches, compared to a final length of 78.125 inches. From outside diameter measurements, most of the stretch occurred in pieces 2 and 3.

As given in Figure B, the fracture location is judged to be at 0.5 inches above the top of the tubesheet.

Radiography of each piece was performed as a guide to metallography. A number of indications were found due to ID scoring from the tube cutting and tube extraction tooling. One of these indications at ~7-1/2 inches above the tubesheet, was examined by metallographic techniques and confirmed to be a tool mark on the tube ID.

The sample was subjected then to metallographic and microscopic attention to the fractured ends.

Metallographic and Microscopic Examinations

The fractured ends were photographed at 4 views each (90° apart). The fracture surface at the upper end of Section 1 (the first section to be removed) was then examined by scanning electron microscope (SEM) fractography and selected-area energy-dispersive X-ray spectral analyses (EDAX). Axial cross sections upward and downward from both fracture faces were then examined by optical metallography. The OD surface immediately below the fracture at the area of maximum apparent wall thickness reduction (which also contained the deepest intergranular penetrations) was cathodically descaled (in 5% H_2SO_4 with "Rodine" inhibitor) and examined by the SEM. An additional axial cross section through this zone was then prepared.

Additional metallographic samples included two transverse sections within the tubesheet region, one located 1-1/2 in. below the fracture and a second located 11 in. above the lowest end of the as-received Section 1. The remaining metallographic sample was an axial cross-section above the top of the tubesheet, 6-3/4 to 7-3/4 in. above the fracture edge.

All examinations and sample locations are synopsized in Figure 1.

Figure 2 shows the as-received appearance of the 1-1/2 in. of tubing which extended from the fracture downward. The sectioning in this region and photomicrographs of the fracture edge appear in Figures 3-5 for axial planes located at 90° and 270°. (The zero degree orientation reportedly faced the divider plate.) The third plane, located at about 210° (and prepared after descaling and SEM examination) is shown in Figures 6-8.

The deepest penetrations by intergranular attack (IGA) at the fracture edge were noted in the 270° micro (Figure 3) at 0.016 in., and in the 210° micro (Figure 7) as 0.010-0.012 in. The "necking" at the fracture requires these

observations, particularly at 210° , to be estimates, since the original OD edges may have been distorted due to the elongation. Essentially, no IGA was observed on the fracture edge at 90° (Figure 5). The axial extent of IGA below the fracture, as shown by Figures 4, 5, 7, and 8, was about 0.10-0.15 in. (for any IGA of ± 0.001 in.).

The zone extending upward from the fracture is shown in the photographs and photomicrographically of Figures 9-12. The results, for the 90° and 270° edges, are, of course, the same as preceeding at the fracture edge. The axial extent of IGA upward was greater at 270° (0.83 in.) than at 90° (0.4 in.) see Figure 10. The deepest IGA (on the 270° edge, Figure 11), was about 0.016 in.

The SEM fractographs of the upper end of Section 1 (taken prior to the axial sectioning above) are collected in Figures 13-18. Examinations were made 0° and at 45° intervals (with 2 added increments between 225° and 270°). Zones of IGA existed in the fractographs at 135° to 270° , with maximum apparent depths of IGA at 180° to 250° . Shear zones were present at all locations; the fracture faces at 0° , 45° , 90° , and 315° were predominantly-to-exclusively shear. The fractional depths of IGA in the fractographs is not useful in determining the fractional penetration by IGA prior to tube removal because the shear zones are narrower than the original ligament of unaffected base metal, owing to the "necking down" by elongation.

The absolute depths of IGA, inferable from the fractographs, are subject to the magnification distortions arising from the sample tilt on the SEM stage. (The 6 to 8 mils of apparent IGA shown in the 270° fractograph does not compare well with approx. 16 mils found metallographically, whereas the 13 mils that appear in the 235° - 250° fractographs closely agrees with the metallography.)

To investigate the possibility of pre-existing OD thinning at the fracture zone, the downward-extending axial micro was descaled and examined with the SEM on the 0° - 180° - 270° side. The observations appear in Figure 19-22 and are supportive of both mechanical elongation and chemical (etching" or attack

grinding), suggests chemical thinning. When this observation is coupled with the appearance of the axial sections at 270° and 210°, it appears that a thinning phenomenon had been present at the fracture zone.

The condition of the tube within the tubesheet is shown in the photomicrographs of the 2 transverse cross-sections in Figures 23-26. At 11 in. above the bottom end, a single penetration of 0.009 in. existed; this was the deepest found (Figure 23). At 1-1/2 in. below the fracture, some extremely shallow (0.6 mil deep) grain boundary penetrations existed (Figure 26).

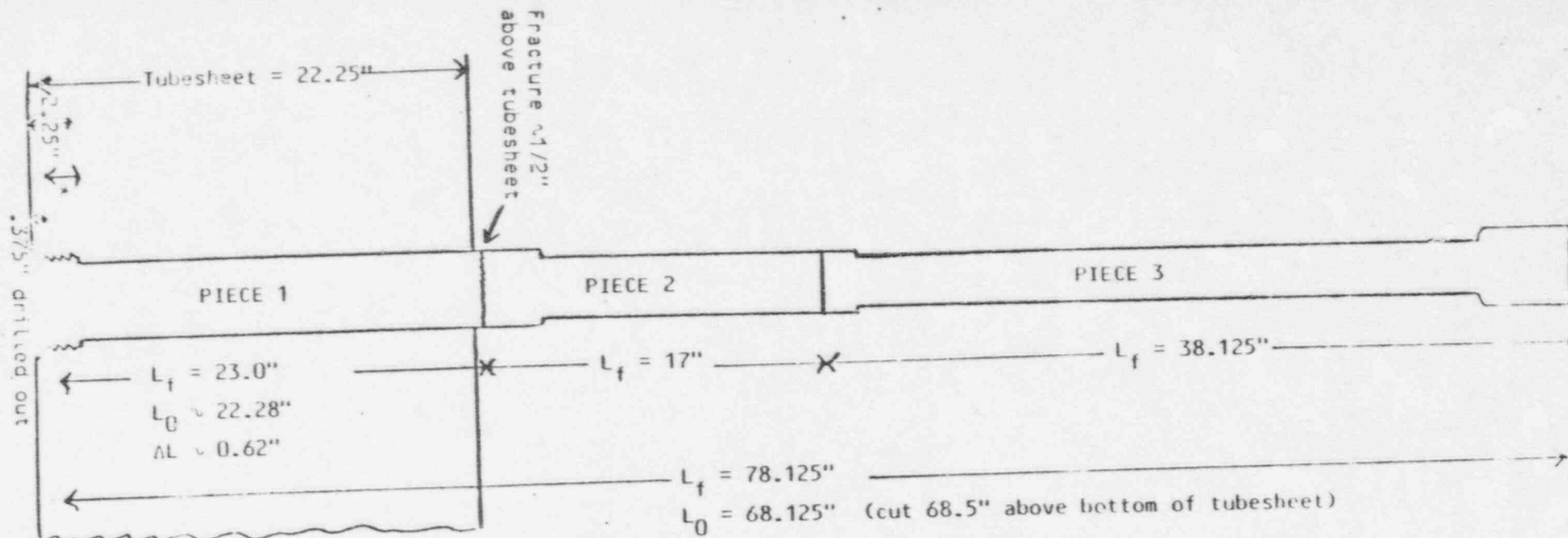
No IGA or other degradations existed in a zone 6-3/4 to 7-3/4 in. above the fracture, above the top of the tubesheet. Figures 27 and 28 present these observations.

The EDAX analyses of materials on the fracture face that was studied by SEM appear in Figure 30-36. Typical elements (Na, Al, Si, S, Cl, K and Ca) were observed.

Summary of Observations

1. The tube sample fractured at about 0.5 inches above the top of the tubesheet due to extraction loads.
2. Intergranular attack was noted in a relatively narrow axial zone part way around the tube outside perimeter.
3. The maximum depth of penetration by IGA is estimated to be 0.016 inches (approx. 32% of original wall thickness). In-situ eddy current testing estimated 41 percent wall penetration.
4. Some localized tube wall OD thinning was suggested by the metallographic results. The depth of thinning could not be determined owing to the elongation of the tube wall at the point of fracture.

5. One transverse metallographic section at 11 inches from the bottom of tube 1 (approx. mid way in tubesheet crevice) showed a single penetration from the OD surface of about 15 percent wall thickness.
6. No significant IGA was observed on the tube by metallography at about one inch below the top surface of the tubesheet within the crevice.

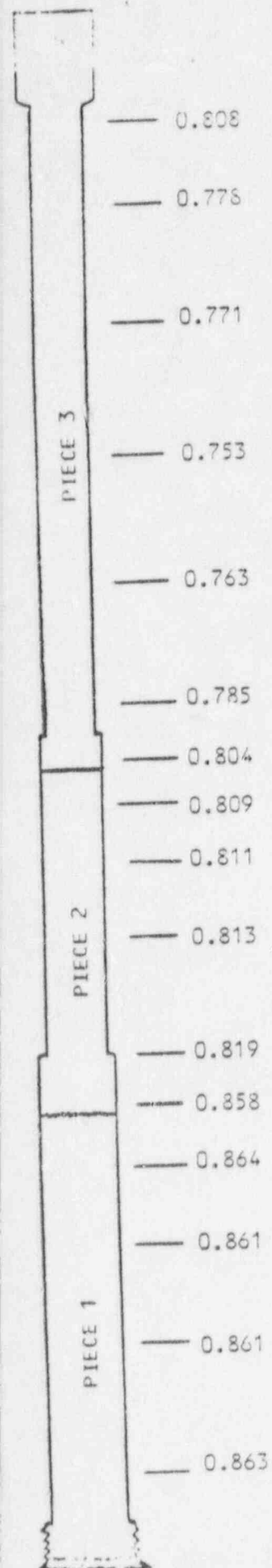


*1.875" threaded to transition

FIGURE 1

Tube R15073 Point Beach Unit 2 - OD Measurements

171



average OD for all three pieces = 0.818"

average OD piece 1 = 0.862"

1. $V_0 = V_6$

2. Assume no wall thinning

$$\text{then } V_0 = D_0^2 L_0 = D_f^2 L_f = V_f$$

3. Original length of piece 1 = L_0

$$D_0 = 0.875''$$

$$L_0 = 23.0''$$

$$L_{f \text{ effective}} = 23.0 - 1.875 = 21.125''$$

$$D_{f \text{ average}} = 0.862''$$

$$4. \quad L_{0 \text{ effective}} = \frac{D_f^2 L_f}{D_0^2} = \frac{(0.862)^2 \cdot 21.125}{(0.875)^2} = 20.5$$

$$L_0 = L_{0 \text{ effective}} + 1.875 = 22.375$$

Location of fracture above bottom of tubesheet = $L_0 + 0.375 = 22.75''$
or 0.5" above nominal top of tubesheet

Check of Wall Thinning Assumption

1. Measured average OD of entire cut tube = 0.818"

$$\text{Calculated average OD} = \left[\frac{D_0^2 L_0}{L_f} \right]^{1/2} = \left[\frac{(0.875)^2 \cdot 66.25}{76.25} \right]^{1/2} = 0.816''$$

$$\text{where: } L_{0 \text{ effective}} = 68.125'' - 1.875'' = 66.25''$$

$$L_{f \text{ effective}} = 78.125'' - 1.875'' = 76.25''$$

This is excellent agreement assuming no wall thickness change.

2. Metallography shows no significant wall thickness reduction at 11 inches above bottom of Piece 1.

- Figure 1 WIS A (15-73) HL: Microscopic Examinations
- Figure 2 A(15-73), Upper End of Section 1, at Fracture, 4 Rotations (0°, 90°, etc.)
- Figure 3 A(15-73), Section 1, Double Axial Cross Section (90° and 270°) through Fracture. Depth of IGA Measures 0.016 in. (to Center of Field "AA") on the 270° Side.
- Figure 4 A(15-73), Continuation of Axial Metallography, on 270° Side, Section 1, Figure 3
- Figure 5 A(15-73), Continuation of Axial Metallography, Section 1, Figure 3
- Figure 6 A(15-73), Upper End of Section 1, Broken Out of Mount, Descaled, and Renovated as an Axial Section at approx. 210°
- Figure 7 A(15-73), Section 1, Axial Cross Section Through Fracture, approx. 210° Orientation. Depth of IGA Measures 0.010-0.012 in. (Measurement is Complicated by Necking Down of Tube at Fracture)
- Figure 8 A(15-73), Continuation of Axial Metallography of Figure 7
- Figure 9 A(15-73), Lower End of Section 2, at Fracture, 0°, 90°, etc.
- Figure 10 A(15-73), Section 2, Double Axial Cross Section (90° and 270°) through Fracture. "X's" Mark Upward Extent of Microscopic IGA
- Figure 11 A(15-73), Section 2, Axial Metallography, Areas A and B of Figure 10
- Figure 12 A(15-73), Continuation of Axial Metallography of Figures 10 & 11
- Figure 13 A(15-73), SEM Fractographs at Upper End of Piece 1, at 0° and 45°. OD Edges are at top. Both Areas Appear to be Shear Only
- Figure 14 A(15-73), SEM Fractographs at 90° and 135°. Shear Predominates at 90°; approx. 1/3 of Fracture at 135° is apparent IGA. (OD edges are at top)
- Figure 15 A(15-73), SEM Fractographs at 180° and 225°. At 180°, the IGA zone is approx. 3/4 of the fracture, and at 225°, IGA is about 2/3 of the fracture.
- Figure 16 A(15-73), SEM Fractographs at 235° and 250°. The zones of IGA appear to be approx. 1/2 of fracture in both areas.
- Figure 17 A(15-73), SEM Fractographs at 270°. IGA appears to be 1/4 of the fracture face.

predominantly shear only.

- Figure 19 A(15-73), Double Axial Micro at Top of Section 1, shown originally in Figure 3 (180° side). Electrolytically Descaled and Examined on OD by SEM at Areas A-G. (Lower 2 pictures are SEM's)
- Figure 20 A(15-73), SEM's of Descaled OD surfaces at Areas B and C of Figure 19
- Figure 21 A(15-73), SEM's of Descaled OD surfaces at Areas D and E of Figure 19
- Figure 22 A(15-73), SEM's of Descaled OD surfaces of Areas F and G of Figure 19
- Figure 23 A(15-73), 11 in. above bottom end of Section 1, Transverse Cross Section. Depth of IGA in lower photomicrograph measures 0.009 in.
- Figure 24 A(15-73), 11 in. above bottom. Areas B and C of Figure 23.
- Figure 25 A(15-73), 1-1/2 in. below Fracture. Transverse Cross Section.
- Figure 26 A(15-73), 1-1/2 in. below Fracture Areas B and C of Figure 25. The OD conditions at B represents intergranular penetrations of about 1 grain in depth (Approx. 0.006 in. or 0.6 mil)
- Figure 27 A(15-73), Double Axial Cross Section, 1 in. long, centered at 7-1/4 in. above the fracture. "Chatter marks" from tube removal equipment were present on ID surface.
- Figure 28 A(15-73), Axial Cross Section 6-3/4 to 7-3/4 in. above fracture. Areas A-D of Figure 29.
- Figure 29 A(15-73), Fracture Surface of Section 1, showing materials analyzed by EDAX at Degree Orientations Indicated
- Figure 30 A(15-73), EDAX at 45°, Figure 29
- Figure 31 A(15-73), EDAX at 90°, Figure 29
- Figure 32 A(15-73), EDAX at 135°, Figure 29
- Figure 33 A(15-73), EDAX at 180°, Figure 29
- Figure 34 A(15-73), EDAX at 225°, Figure 29
- Figure 35 A(15-73), EDAX at 270°, Figure 29
- Figure 36 A(15-73), EDAX at 315°, Figure 29

WESTINGHOUSE ELECTRIC CORPORATION

WIS A (15-73) HL: Microscopic Examinations

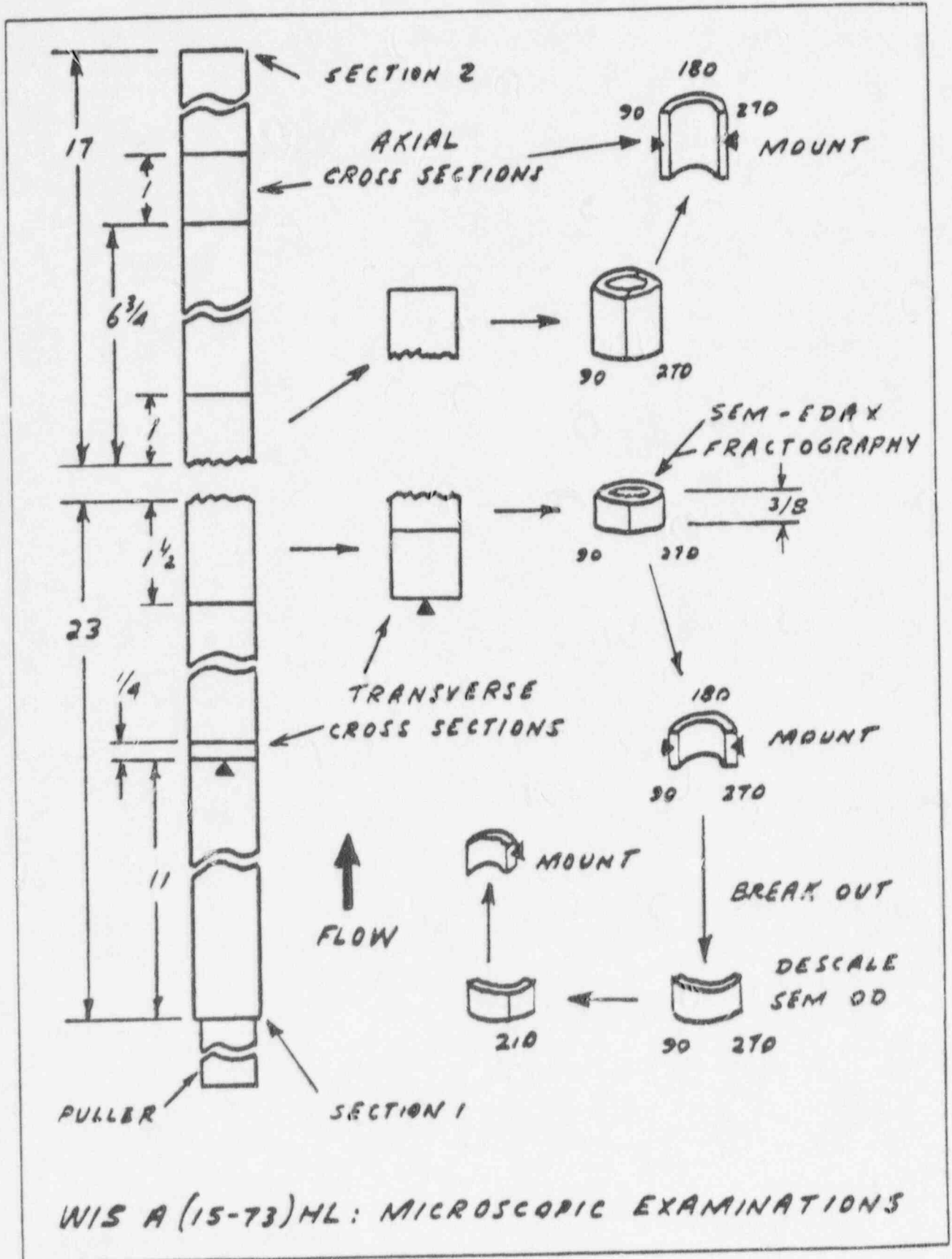


Figure 1

A(15-73), Upper End of Section I, at
Fracture, 4 Rotations (0° , 90° , etc.)

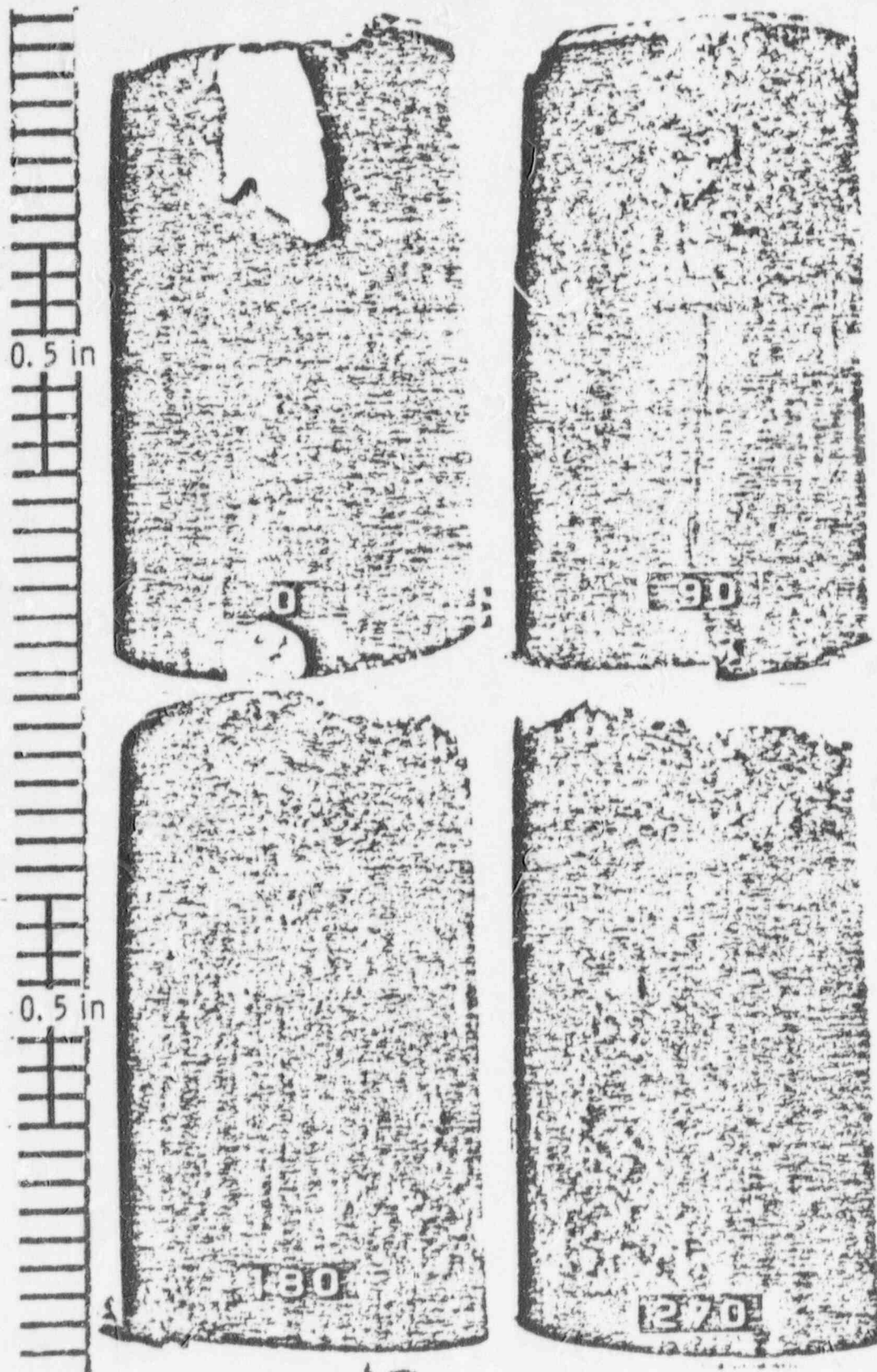


Figure 2

A (15-73), Section 1, Double Axial Cross
 Section (90° and 270°) through Fracture. Depth of IGS Measures
 0.016 in. (to Center of Field "AA") on the 270° Side)

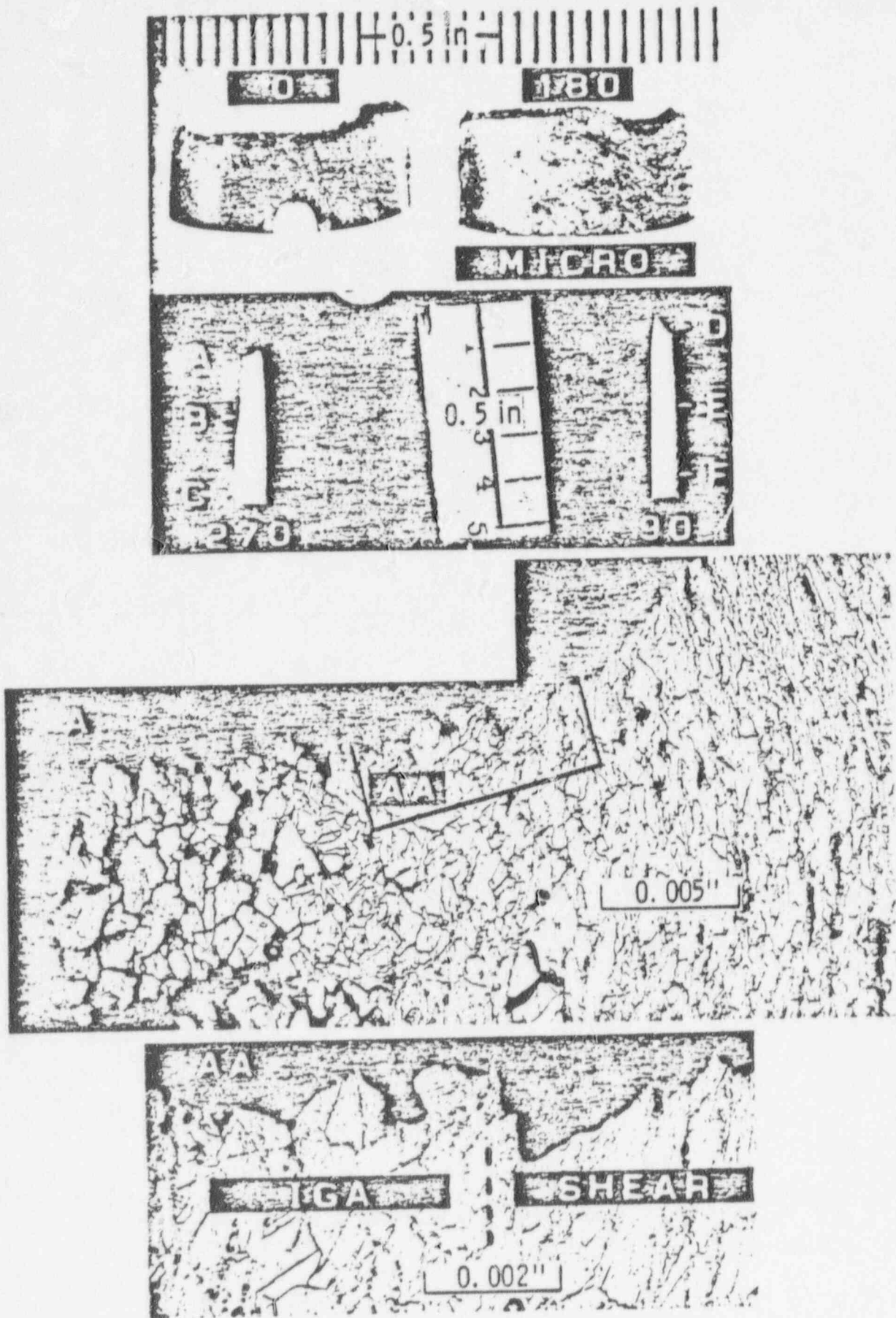


Figure 3

A (15-73), Continuation of Axial Metallography, on 270° Side, Section 1, Figure 3

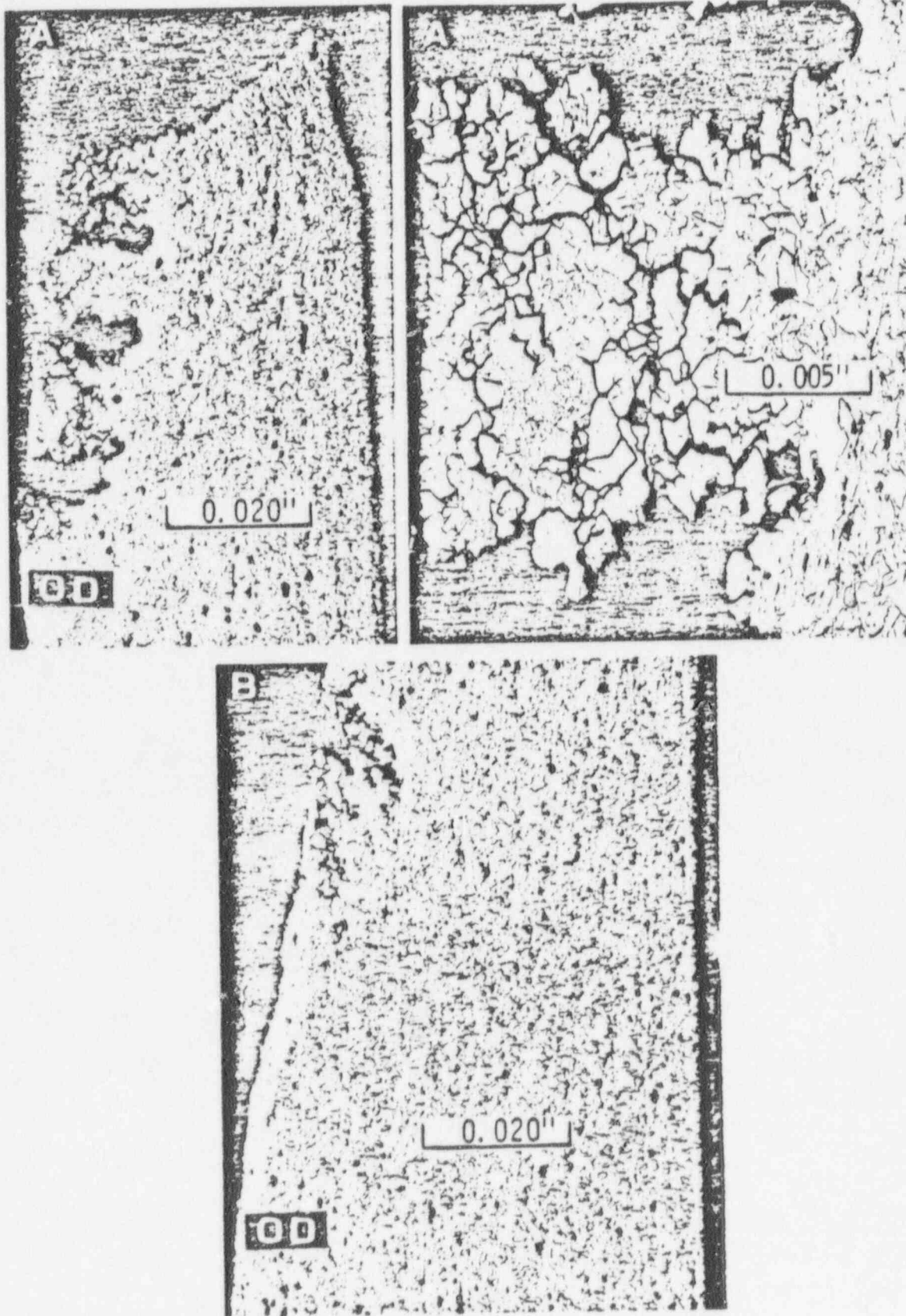


Figure 4

A (15-73), Continuation of Axial Metallography, Section 1, Figure 3

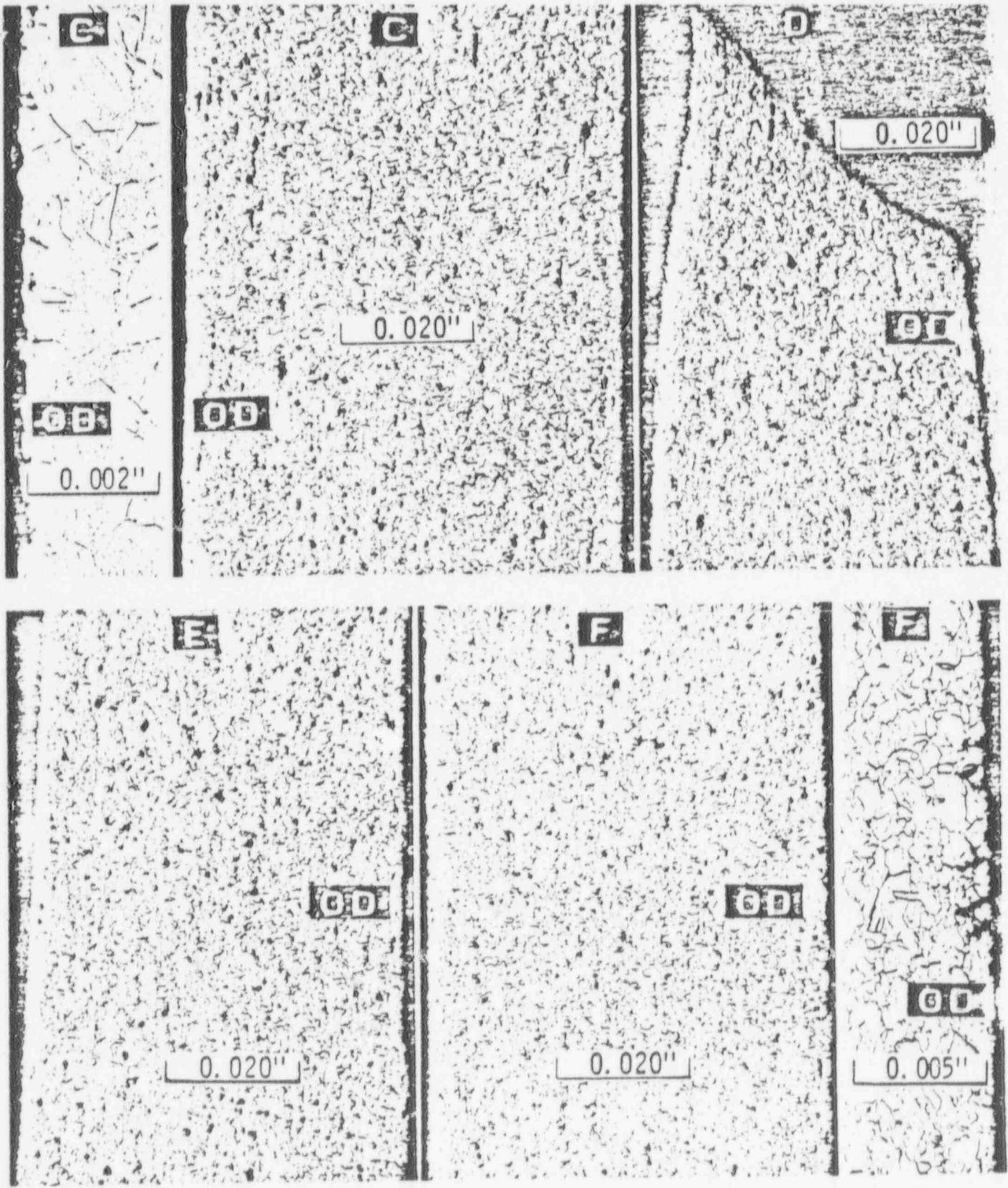


Figure 5

A (15-73), Upper End of Section 1,
Broken Out of Mount, Descaled, and
Renovated as an Axial Section at
approx. 210°

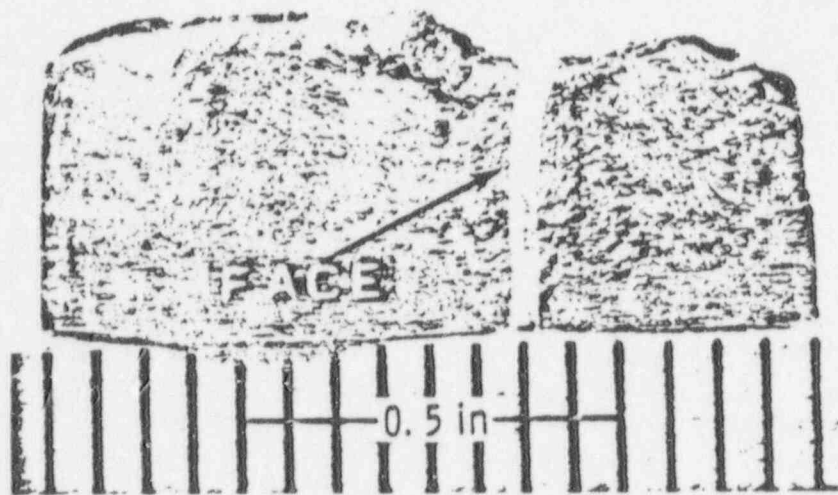


Figure 6

A (15-73), Section 1, Axial Cross Section
Through Fracture, approx. 210° Orientation.
Depth of IGAs Measures 0.010-0.012 in.
(Measurement is complicated by necking
down of tube at fracture)

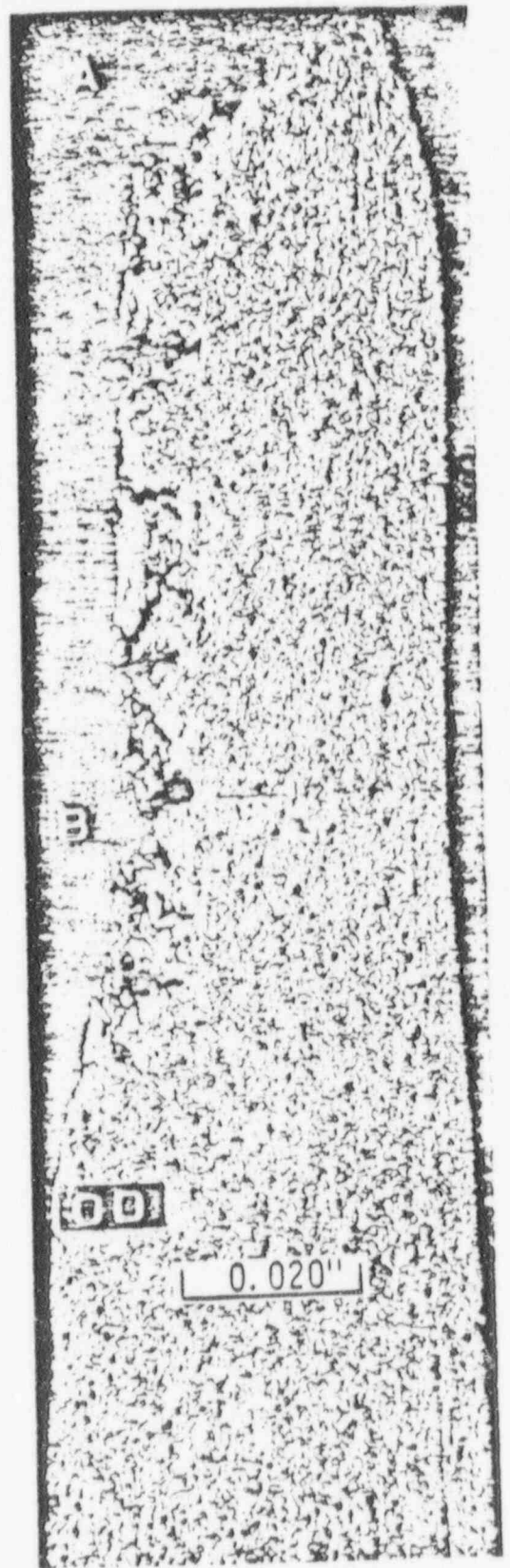
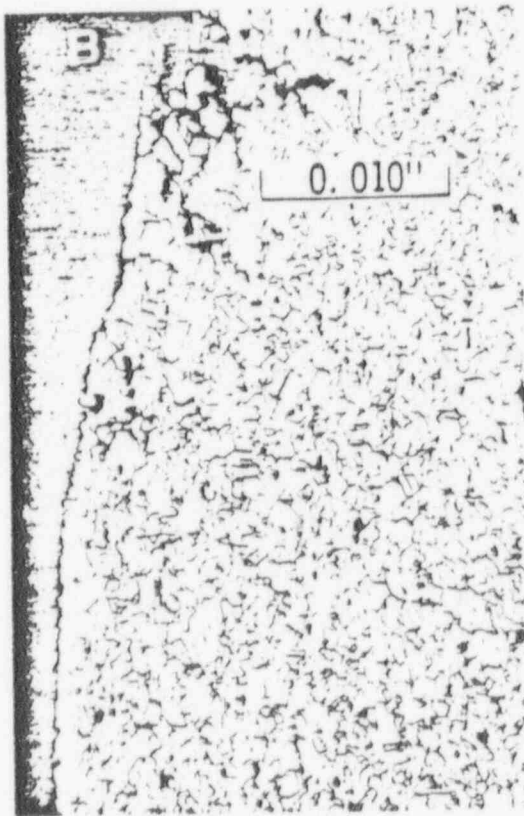
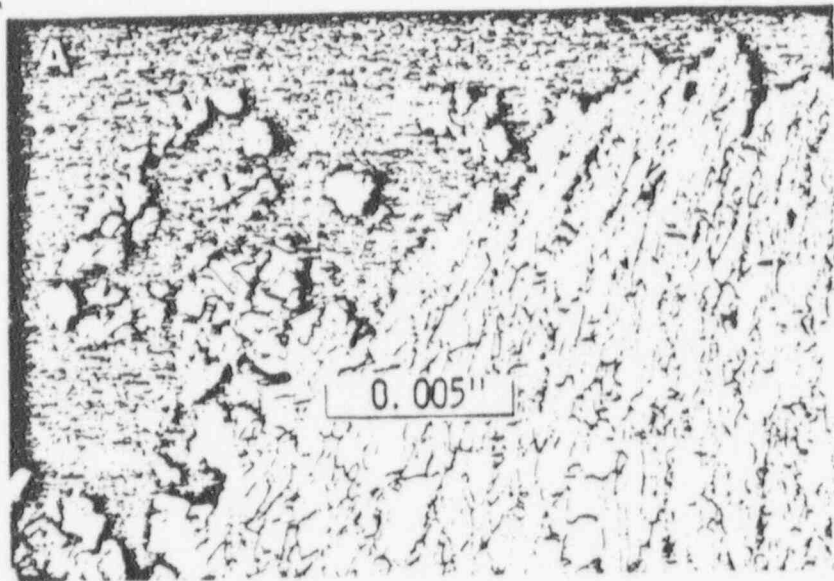


Figure 7

A (15-73), Continuation of Axial
Metallography of Figure 7

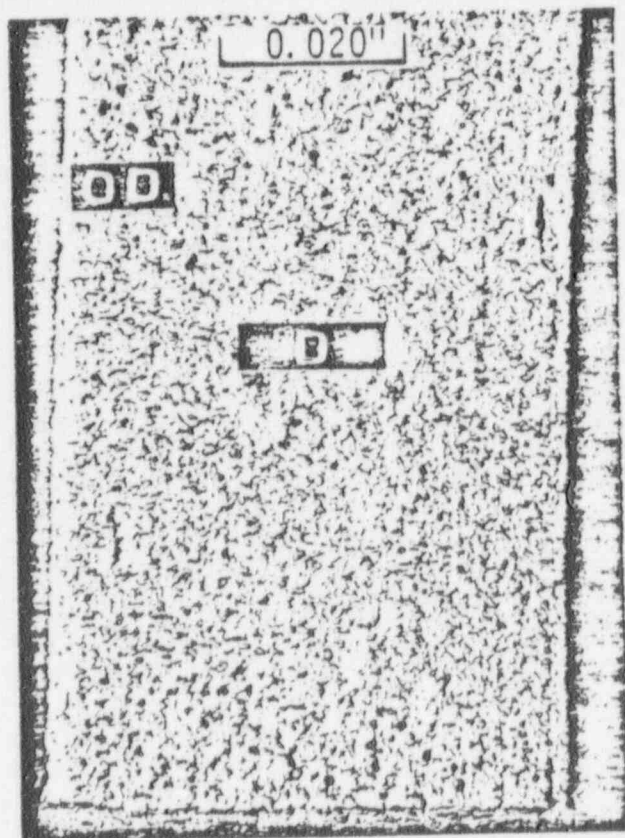
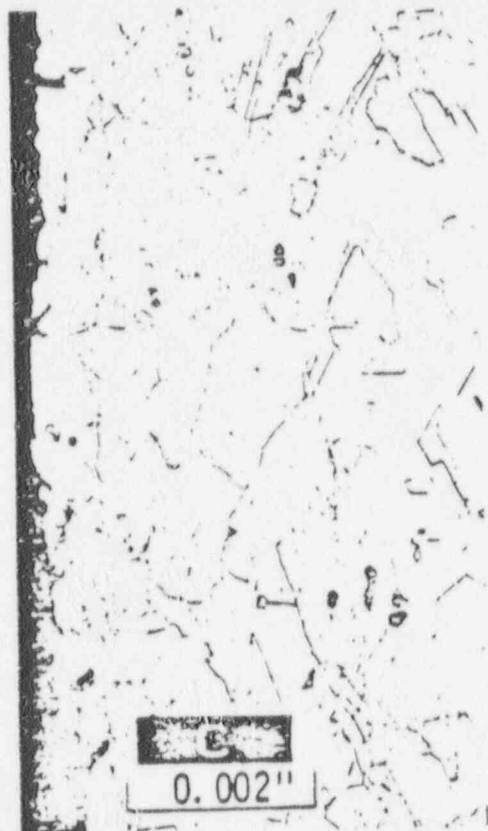
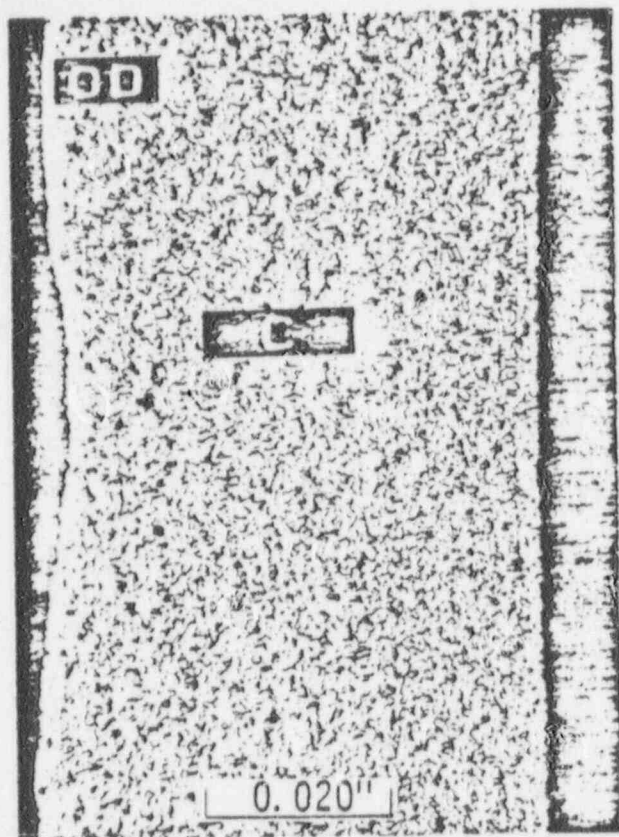


Figure 8

A (15-73), Lower End of Section 2,
at Fracture, 0°, 90°, etc.

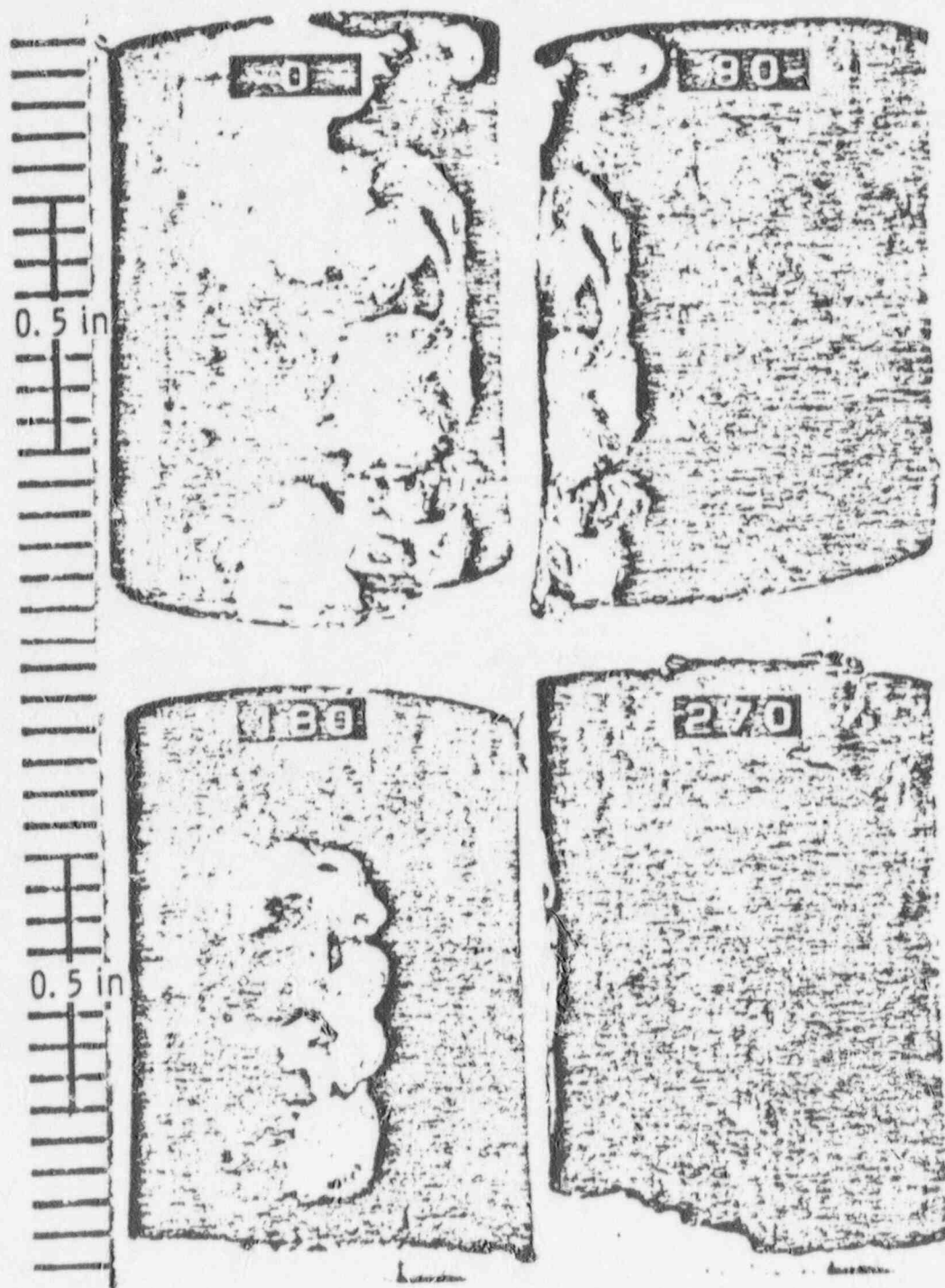


Figure 9

A (15-73), Section 2, Double Axial
Cross Section (90° and 270°) through
Fracture. "X's" Mark Upward Extent
of Microscopic IGA

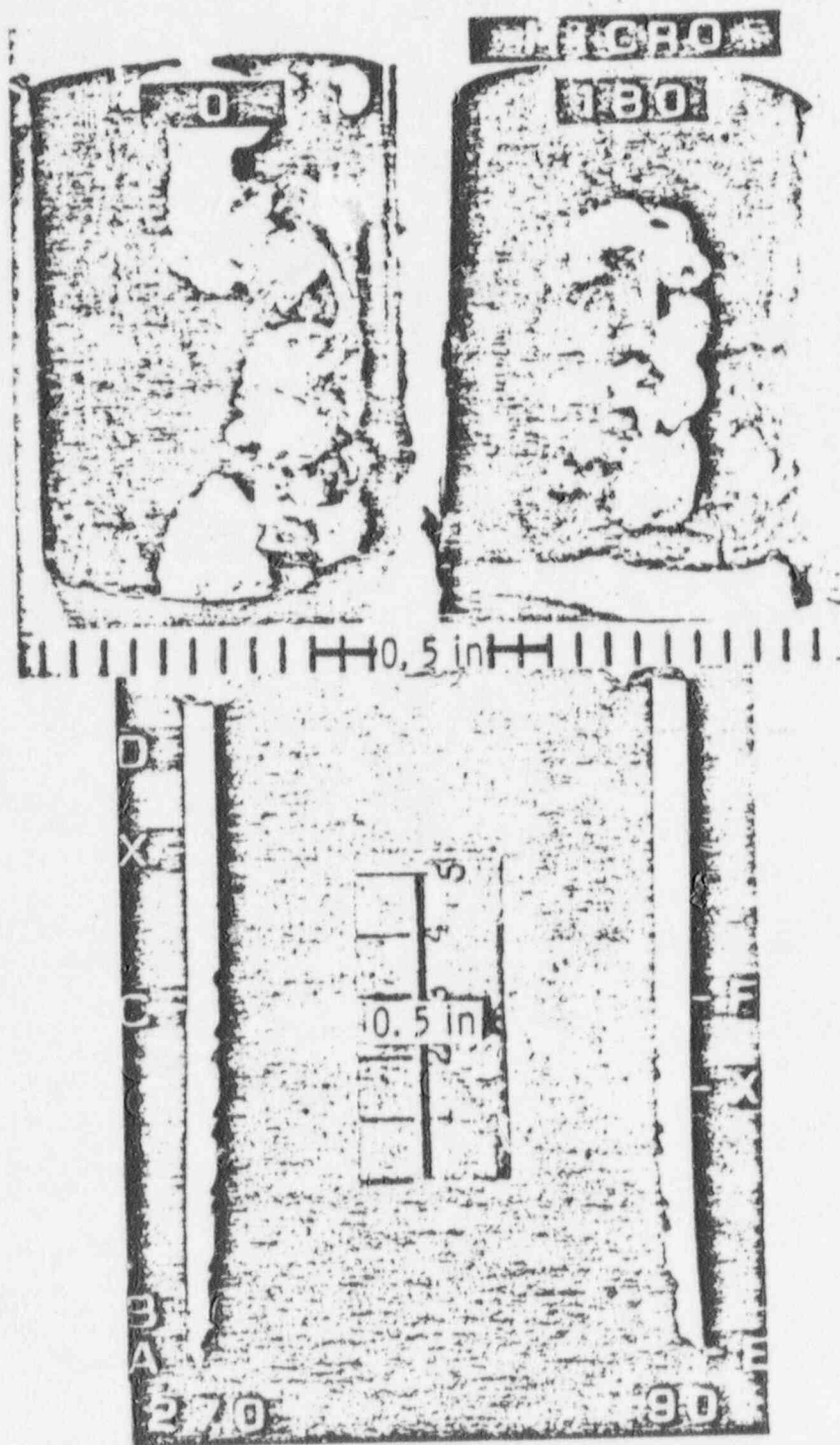


Figure 10

A (15-73), Section 2, Axial Metallography,
Areas A and B of Figure 10

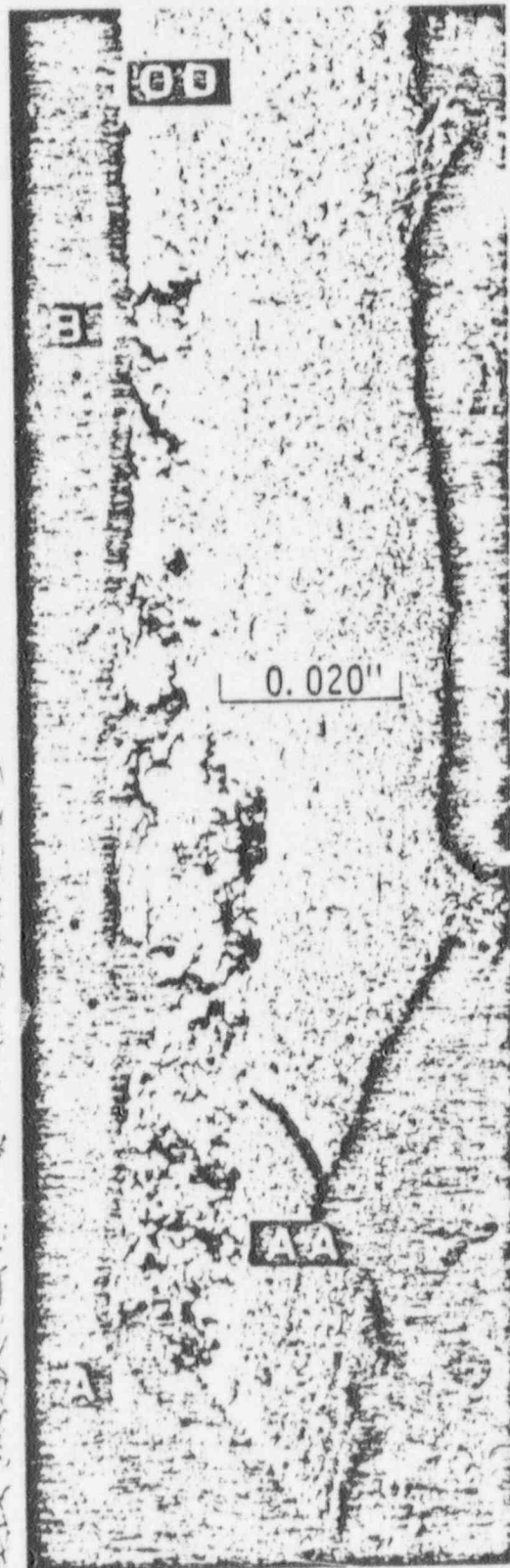
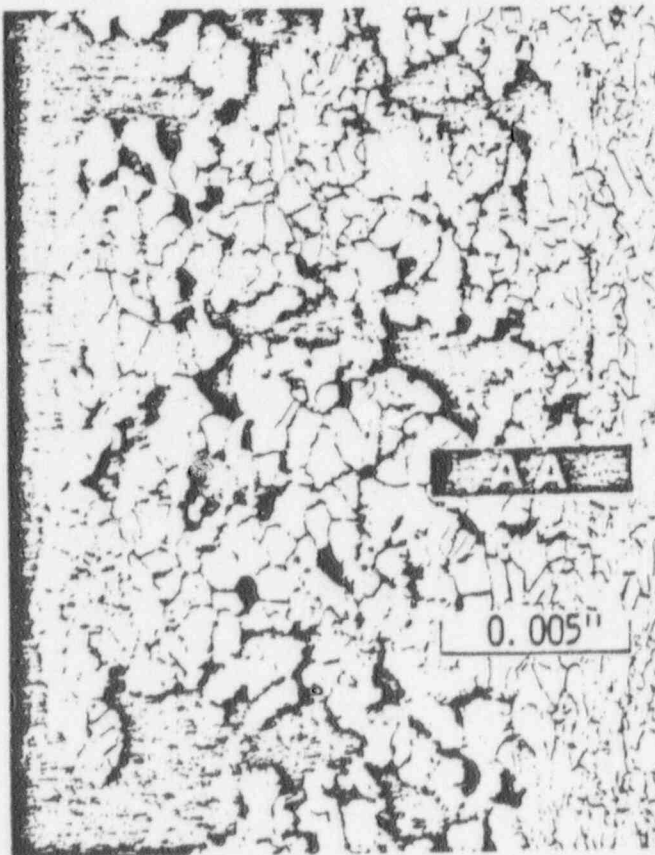


Figure 11

A (15-73), Continuation of Axial
Metallography of Figures 10 & 11

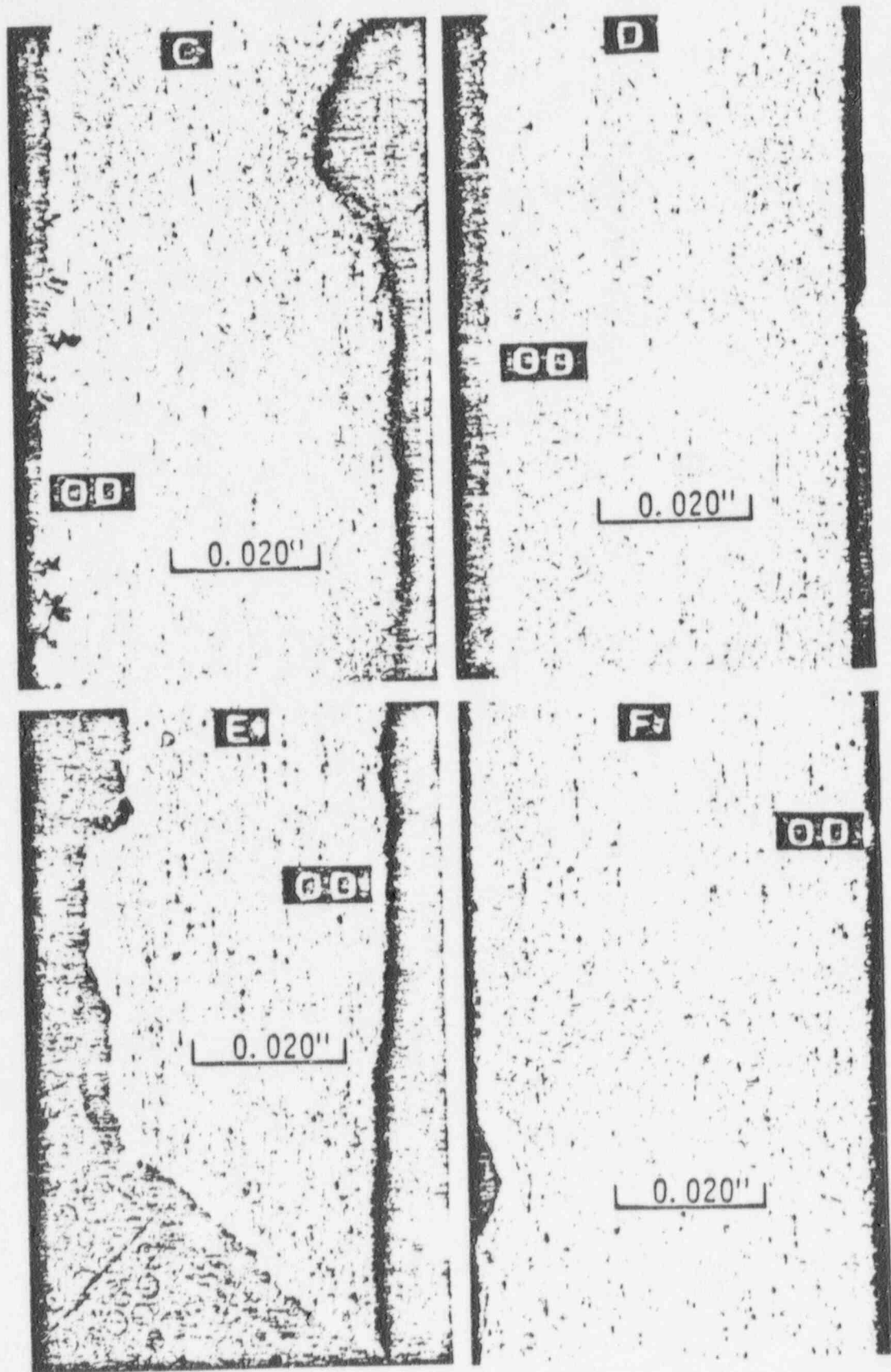


Figure 12

A (15-73), SEM Fractographs at Upper End
of Piece 1, at 0° and 45° OD Edges are
at top. Both areas appear to be shear only

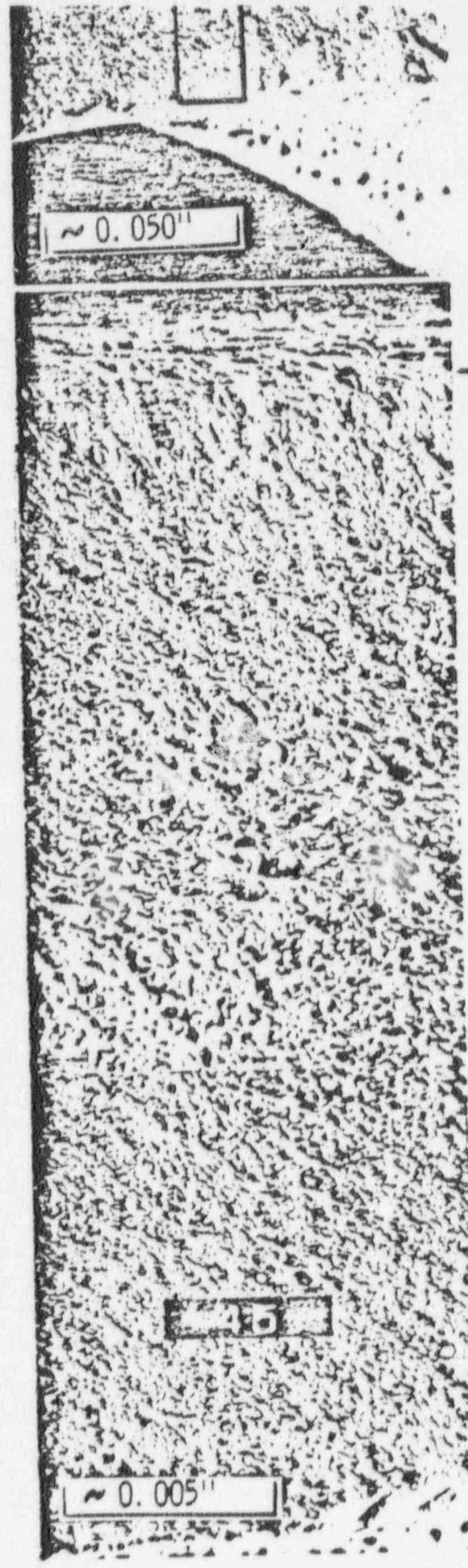
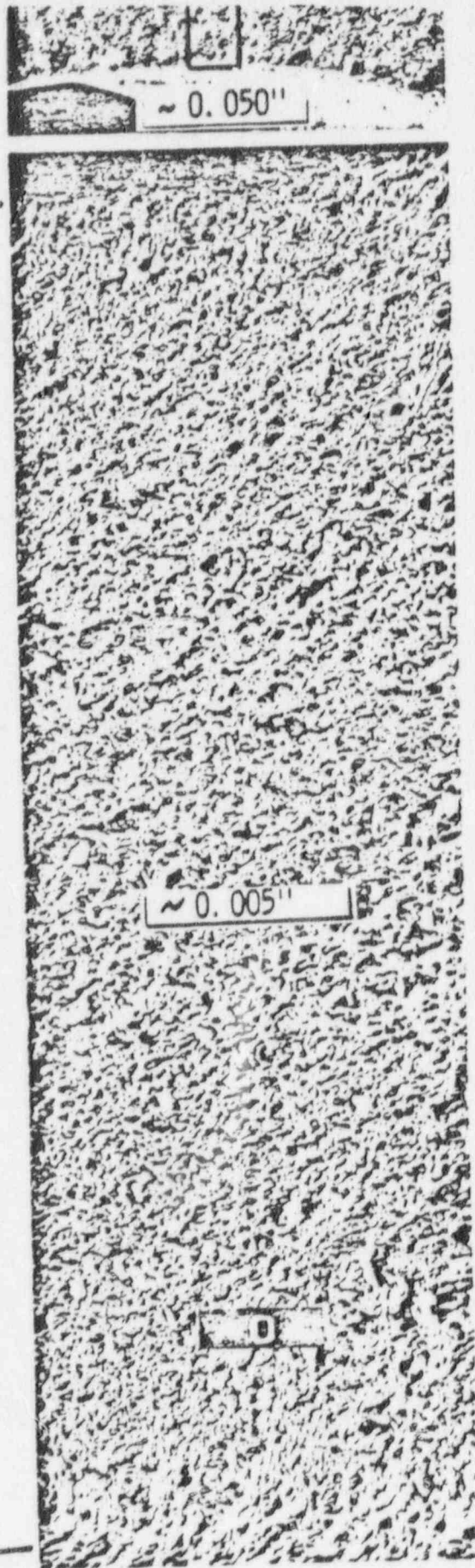


Figure 13

A (15-73), SEM Fractographs at 90° and 135° . Shear predominates at 90° ; approx. 1/3 of fracture at 135° is apparent IGA. (OD edges are at top)

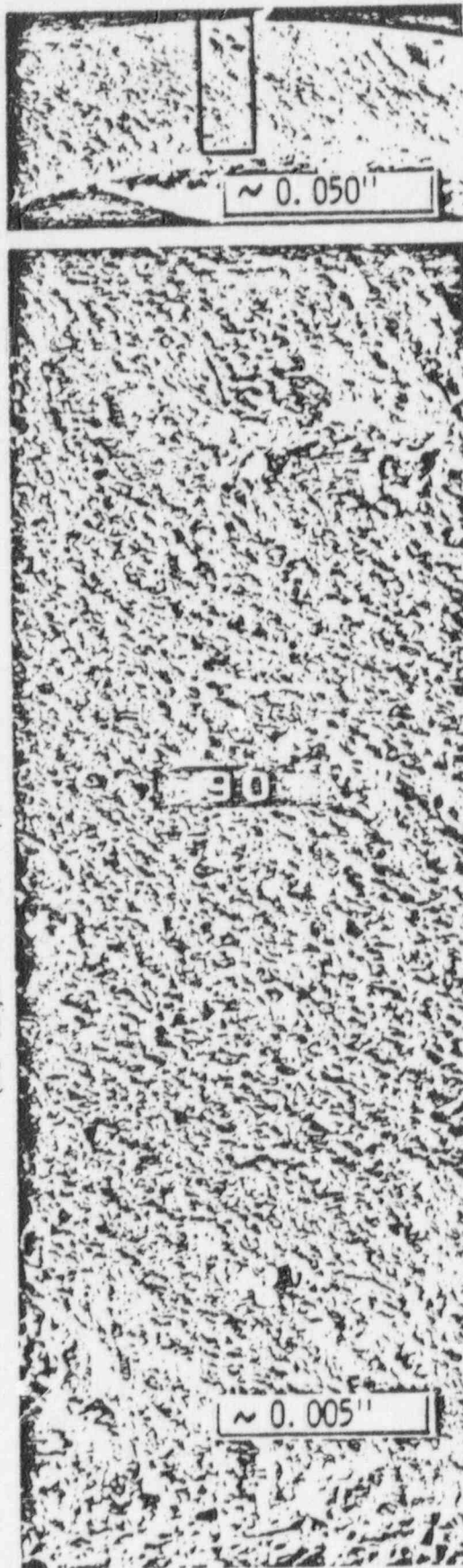


Figure 14

A (15-73), SEM Fractographs at 180° and 225° . At 180° , the IGA zone is approx. $3/4$ of the fracture, and at 225° , IGA is about $2/3$ of the fracture

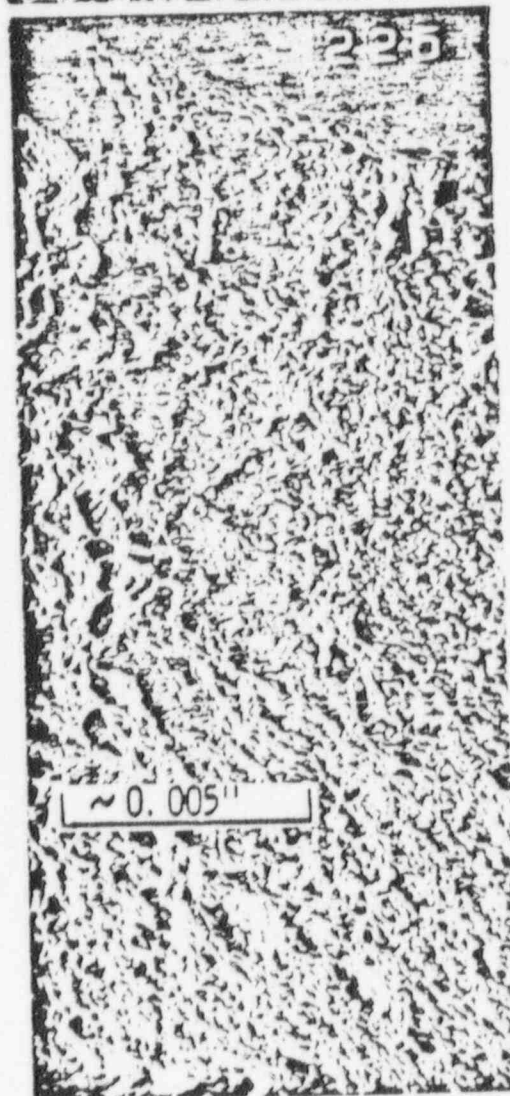
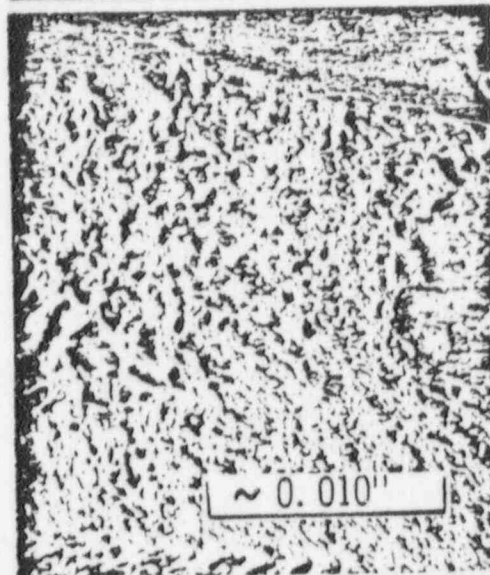
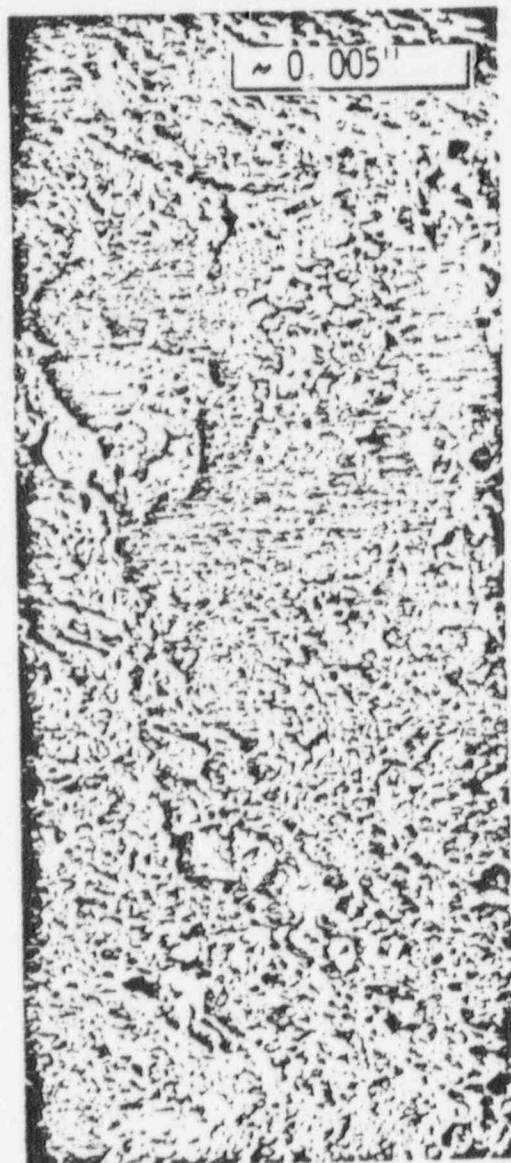
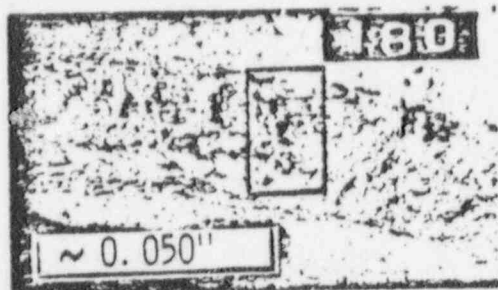


Figure 15

A (15-73), SEM Fractographs at 235° and 250°. The zones of 16A appear to be approx. 1/2 of fracture in both areas.

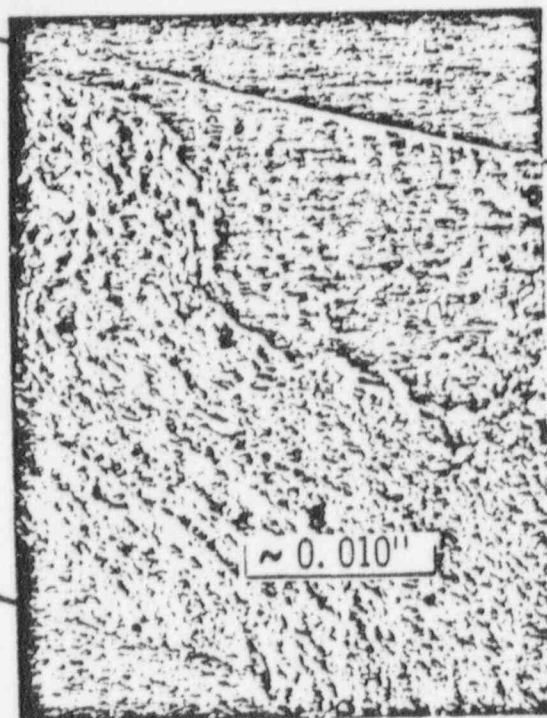
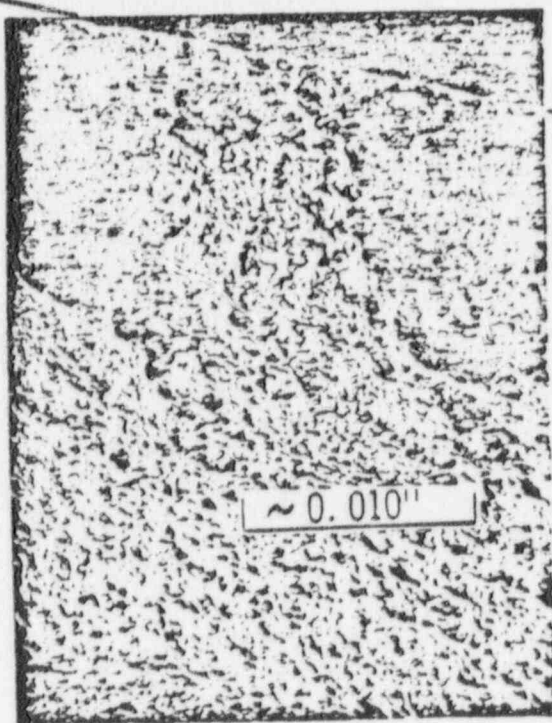
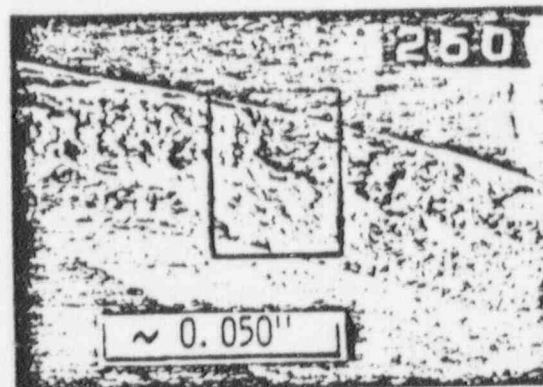
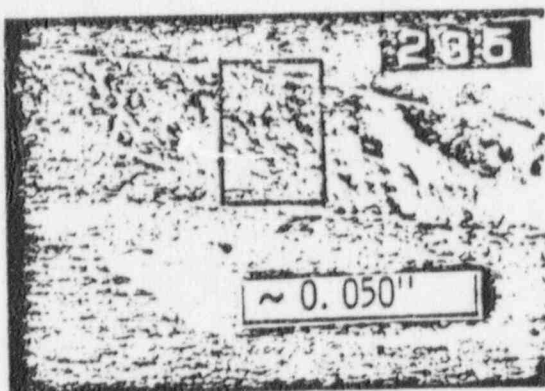


Figure 16

Λ (15-73), SEM Fractographs at 270° .
16A appears to be $\geq 1/4$ of the fracture
face.

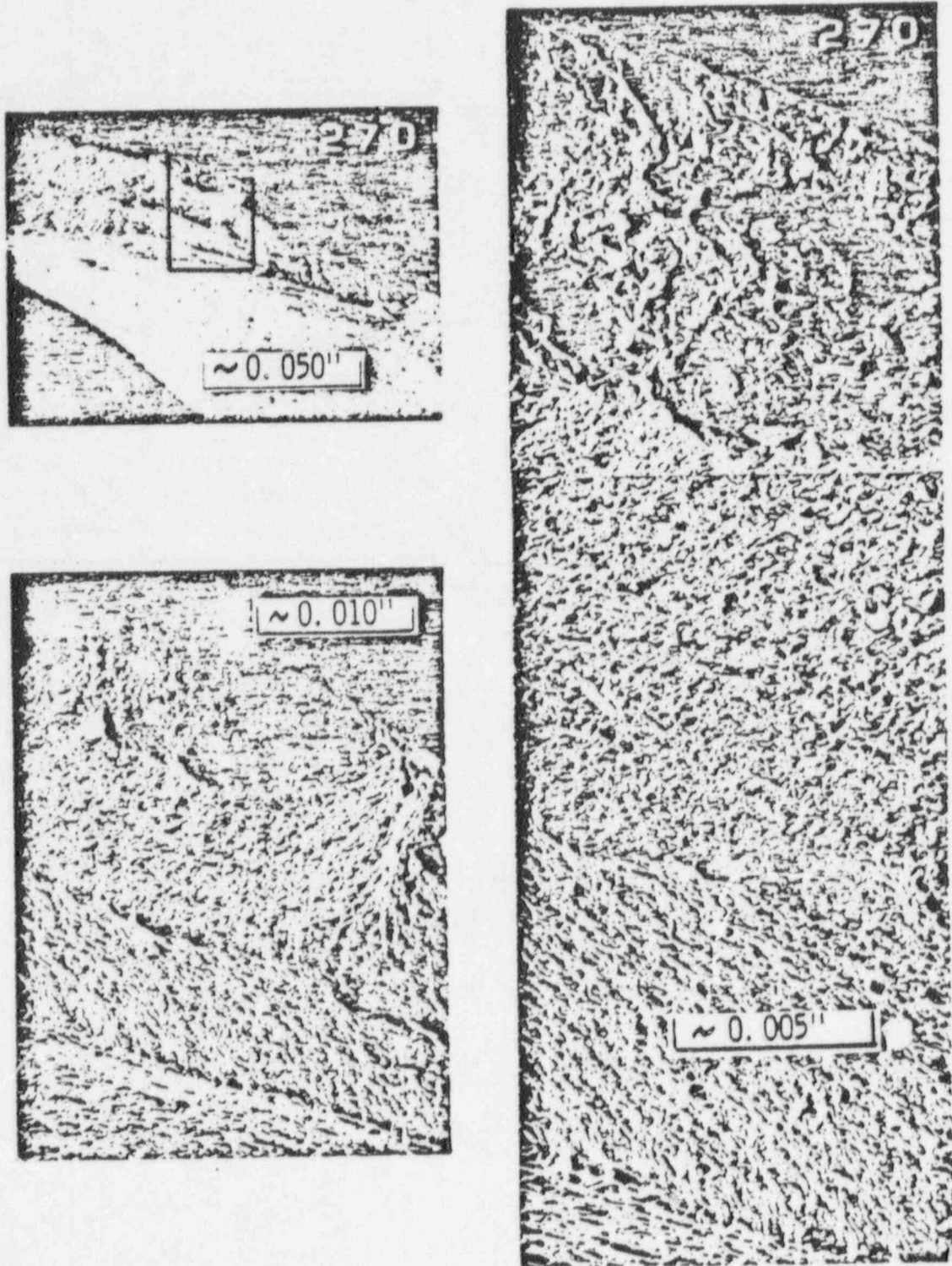


Figure 17

A (15-73), SEM Fractographs at 315°
Fracture appears to be predominantly
shear only

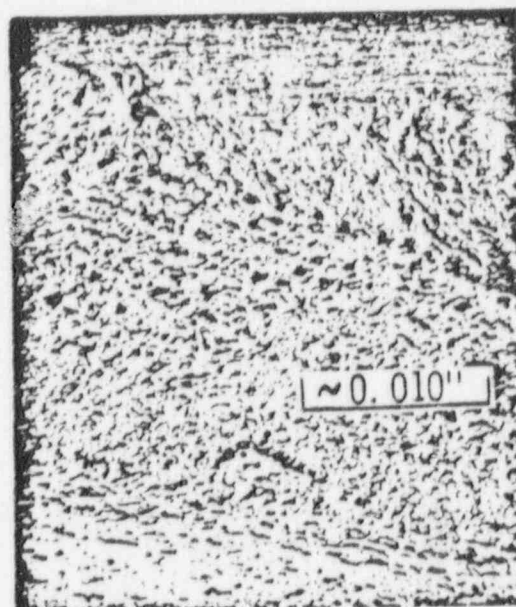
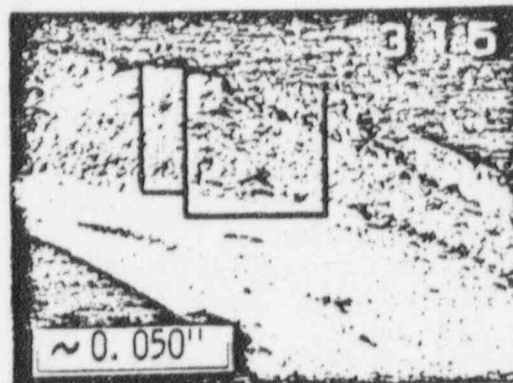
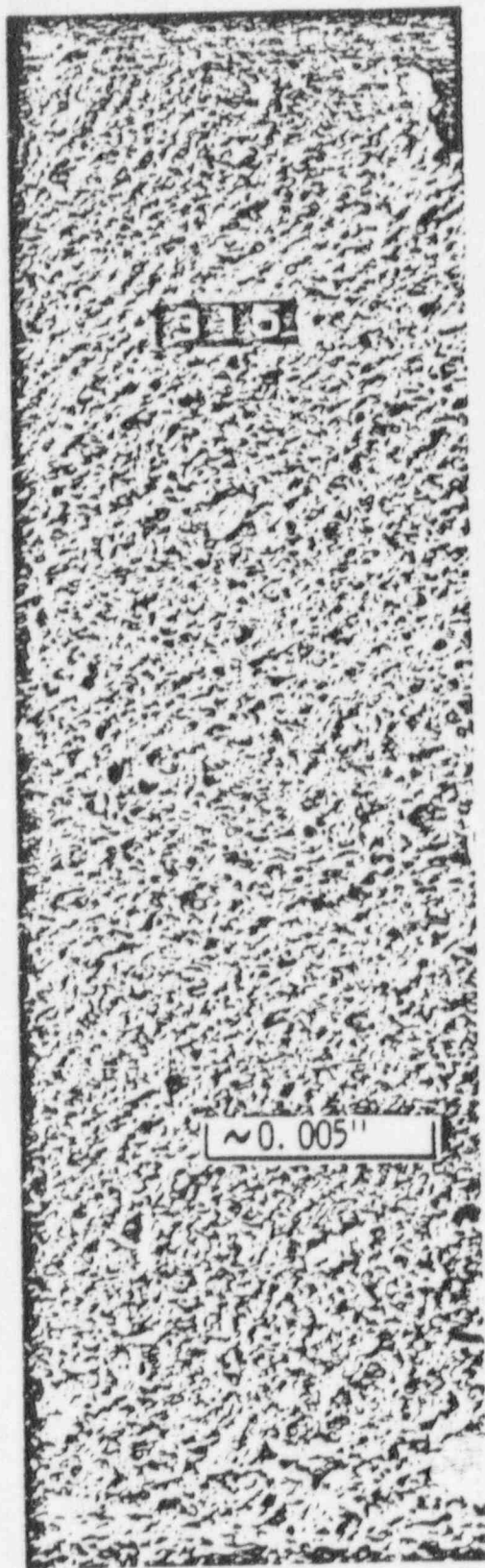


Figure 18

A (15-73), Double Axial Micro at Top of Section 1,
 shown originally in Figure 3 (180° side). Electrolytically
 Descaled & examined on OD by SEM at Areas A-G. (Lower
 2 pictures are SEM's)

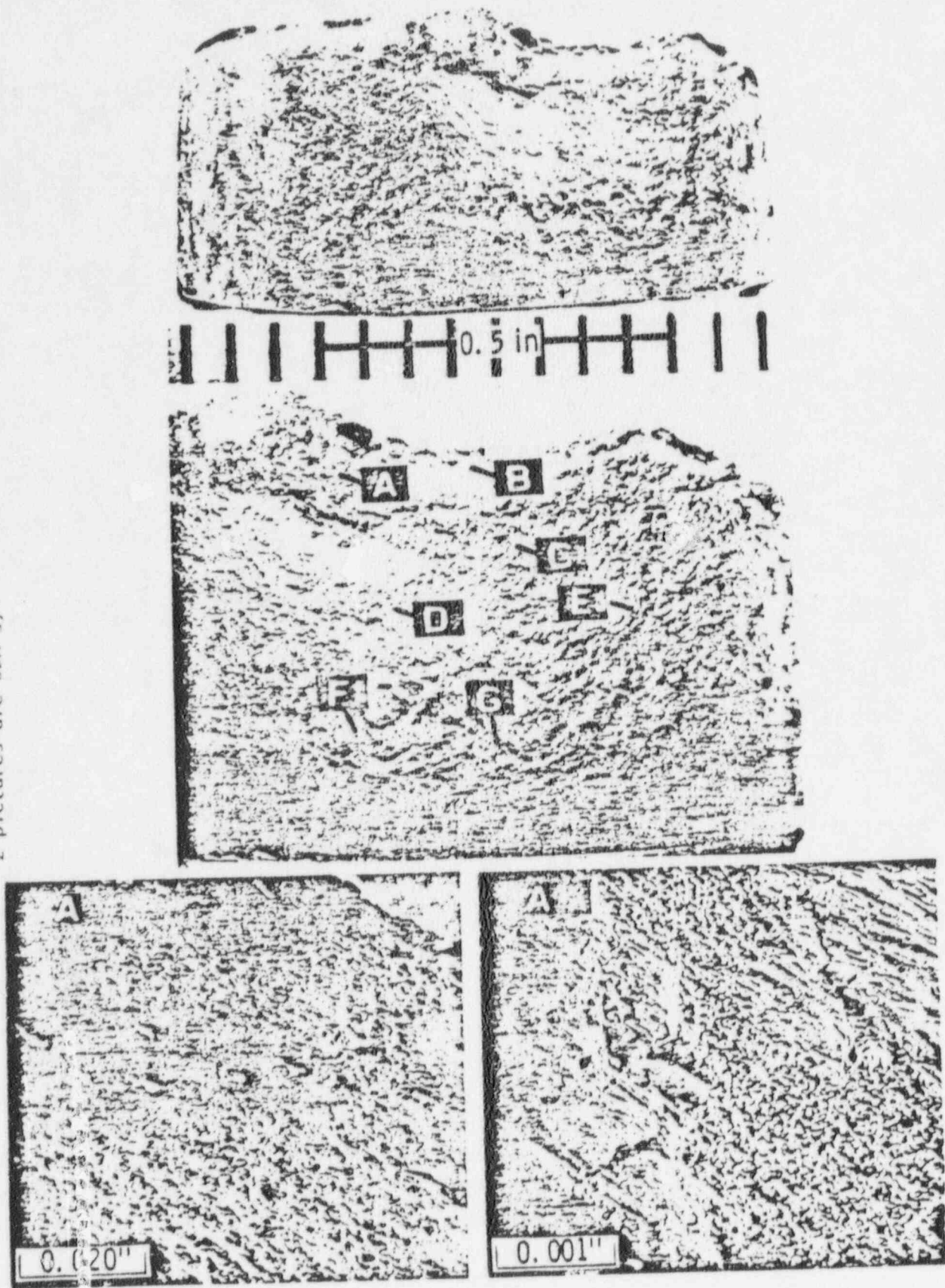


Figure 19

A (15-73), SEM's of descaled OD Surfaces
at Areas B & C of Figure 19

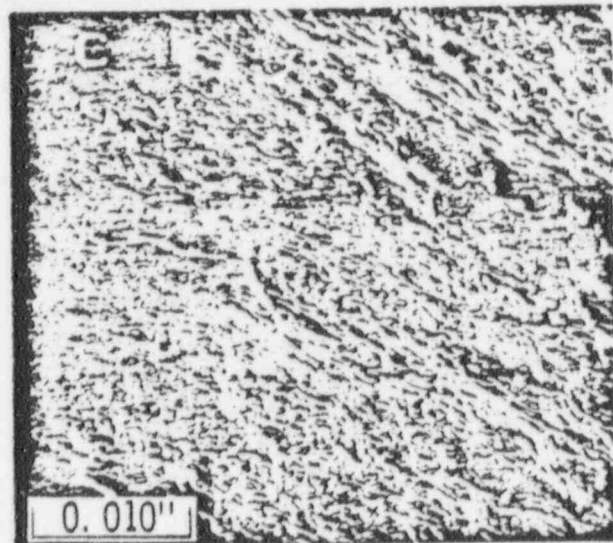
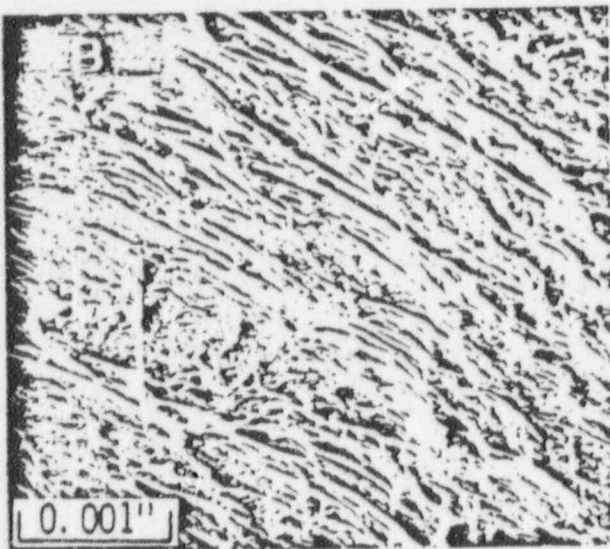
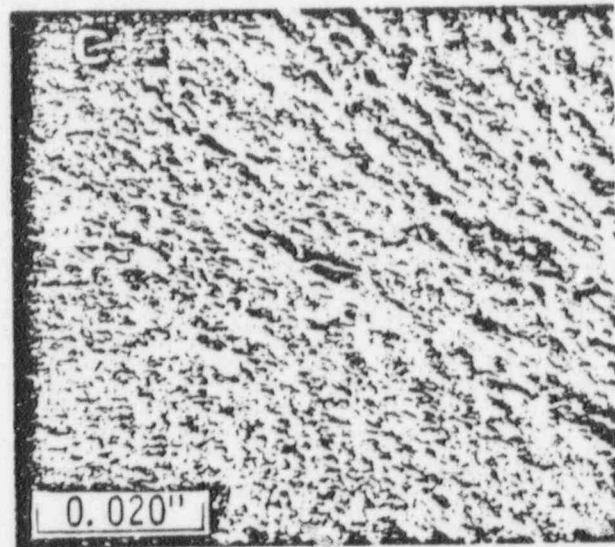
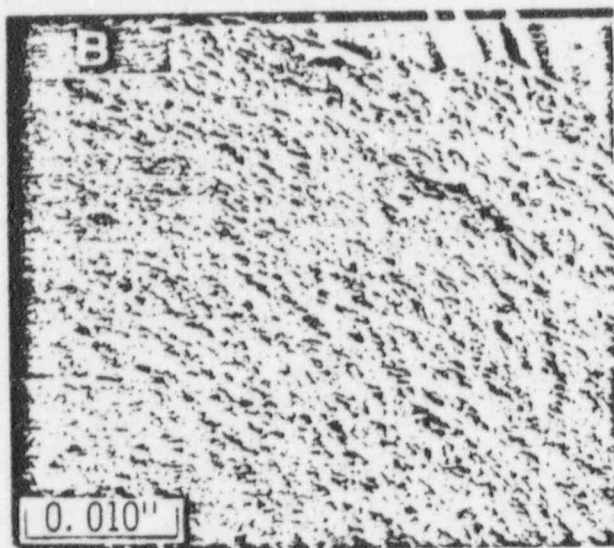


Figure 20

A (15-73), SEM's of Descaled OD surfaces
at Areas D and E of Figure 19

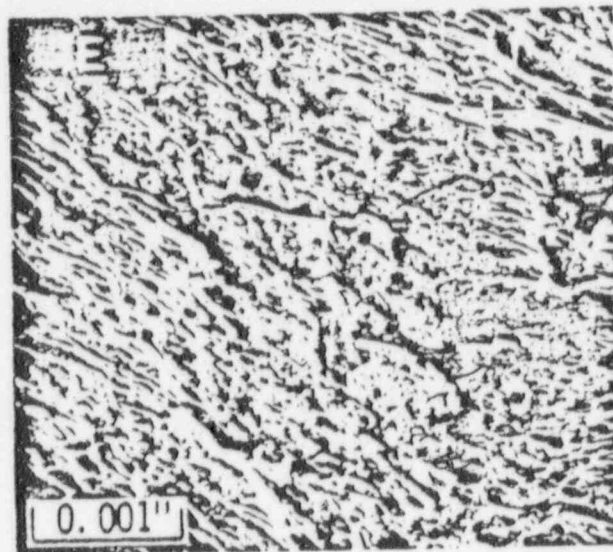
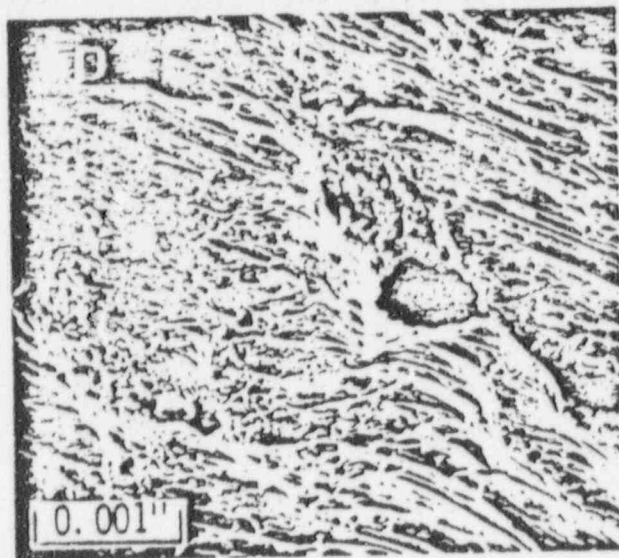
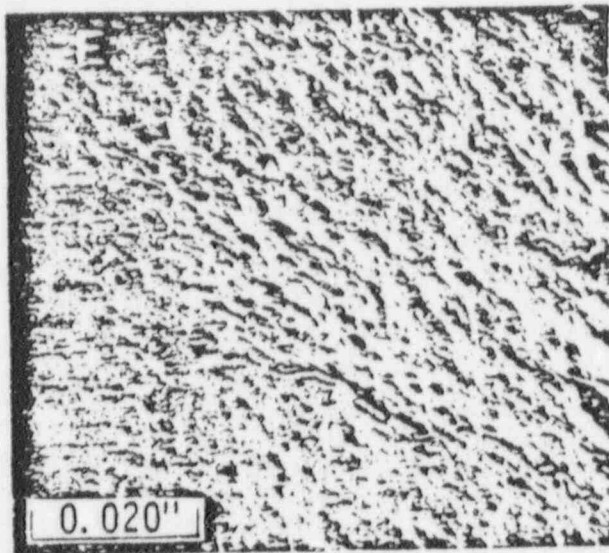
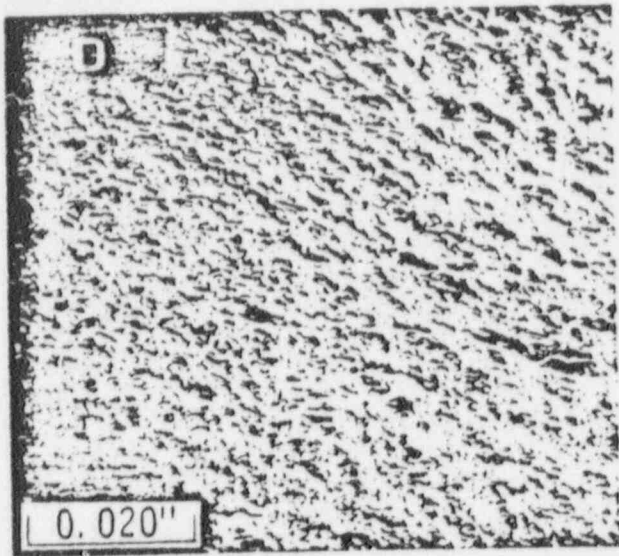


Figure 21

A (15-73), SEM's of Descaled OD surfaces
at Areas F & G of Figure 19

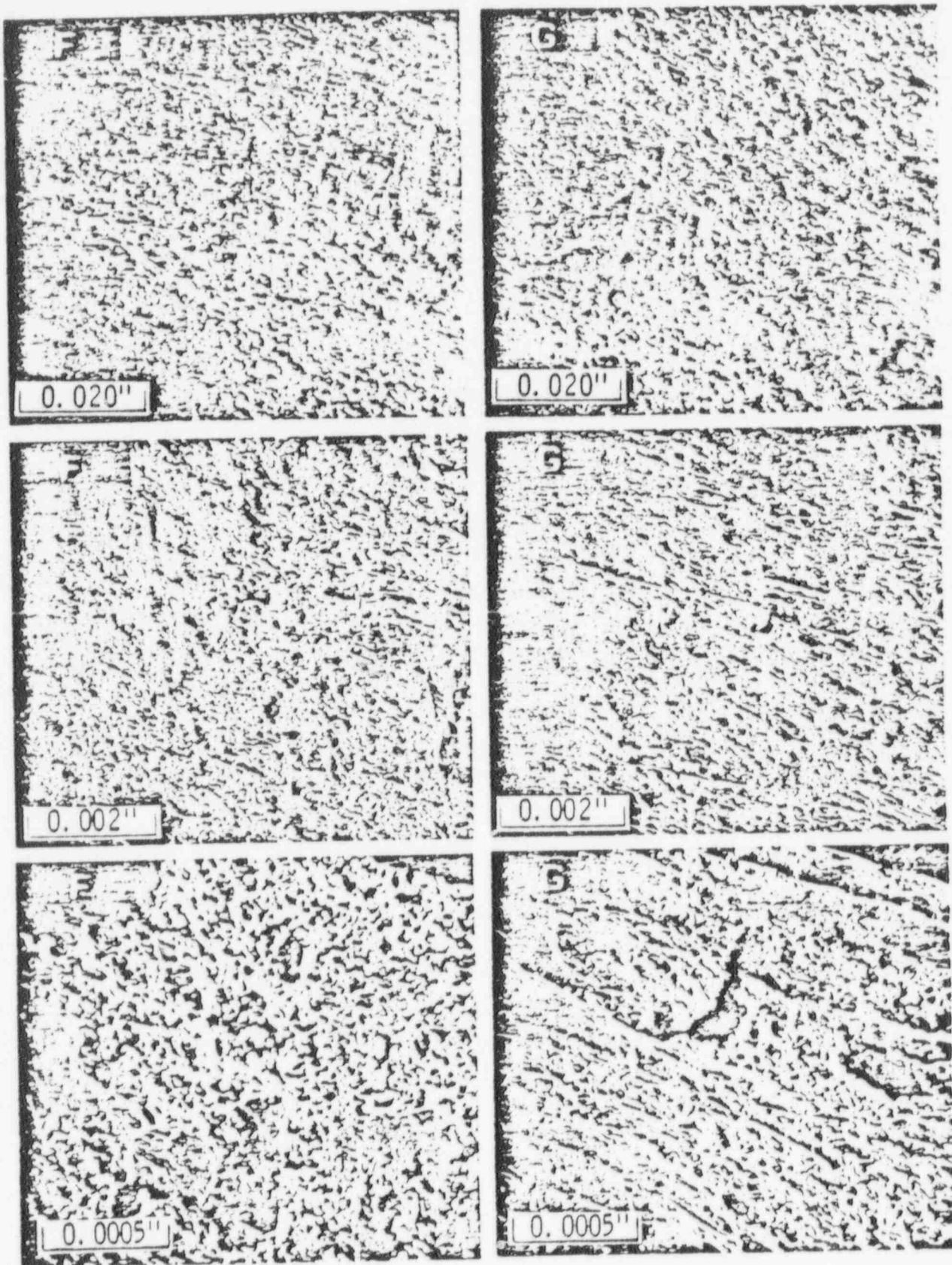


Figure 22

A (15-73), 11 in. above bottom end of Section 1,
 Transverse Cross Section. Depth of IGA in lower
 photomicrograph measures 0.009 in.

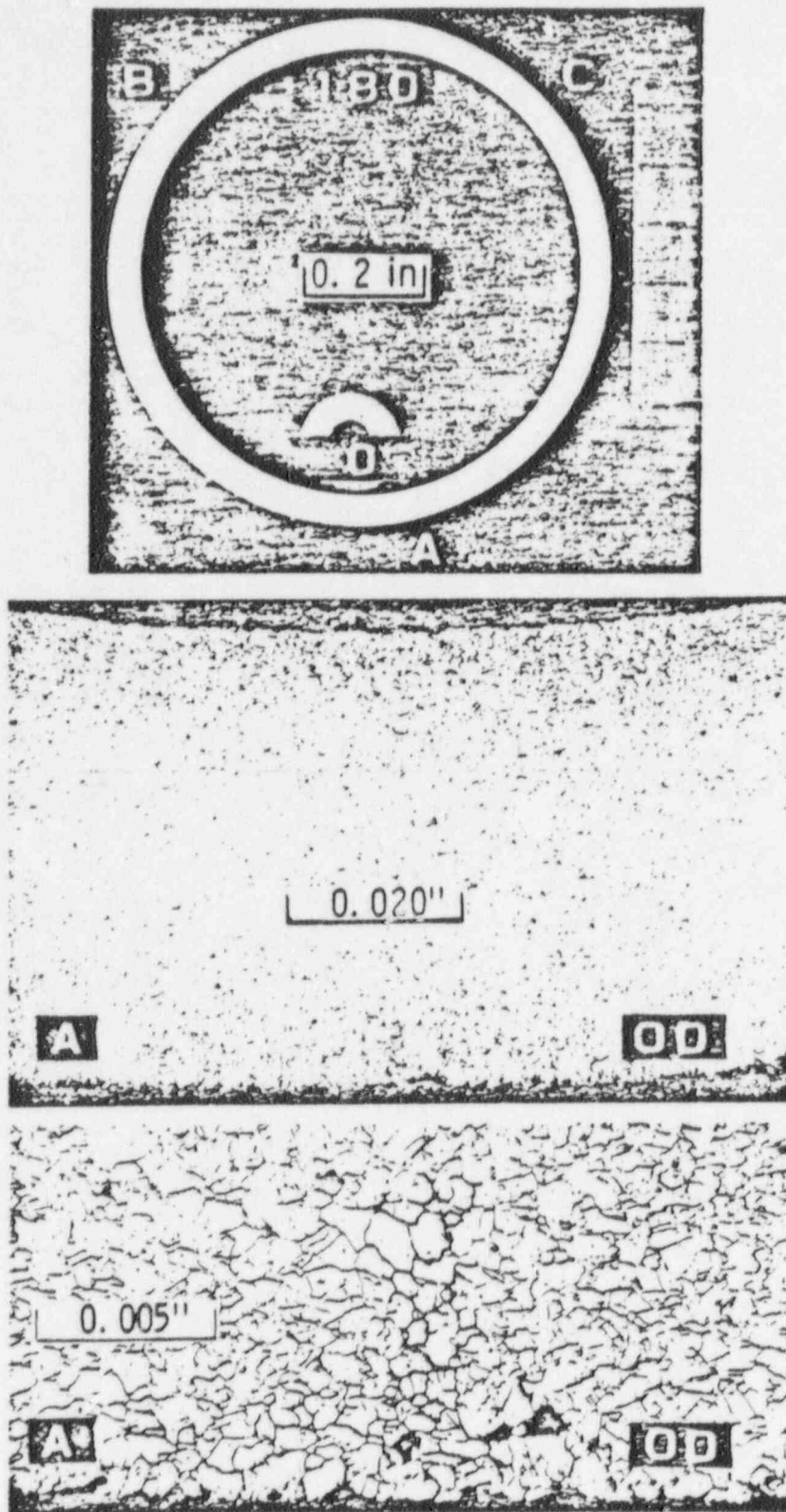


Figure 23

A (15-73), 11 in. above bottom. Areas B
and C of Figure 23.

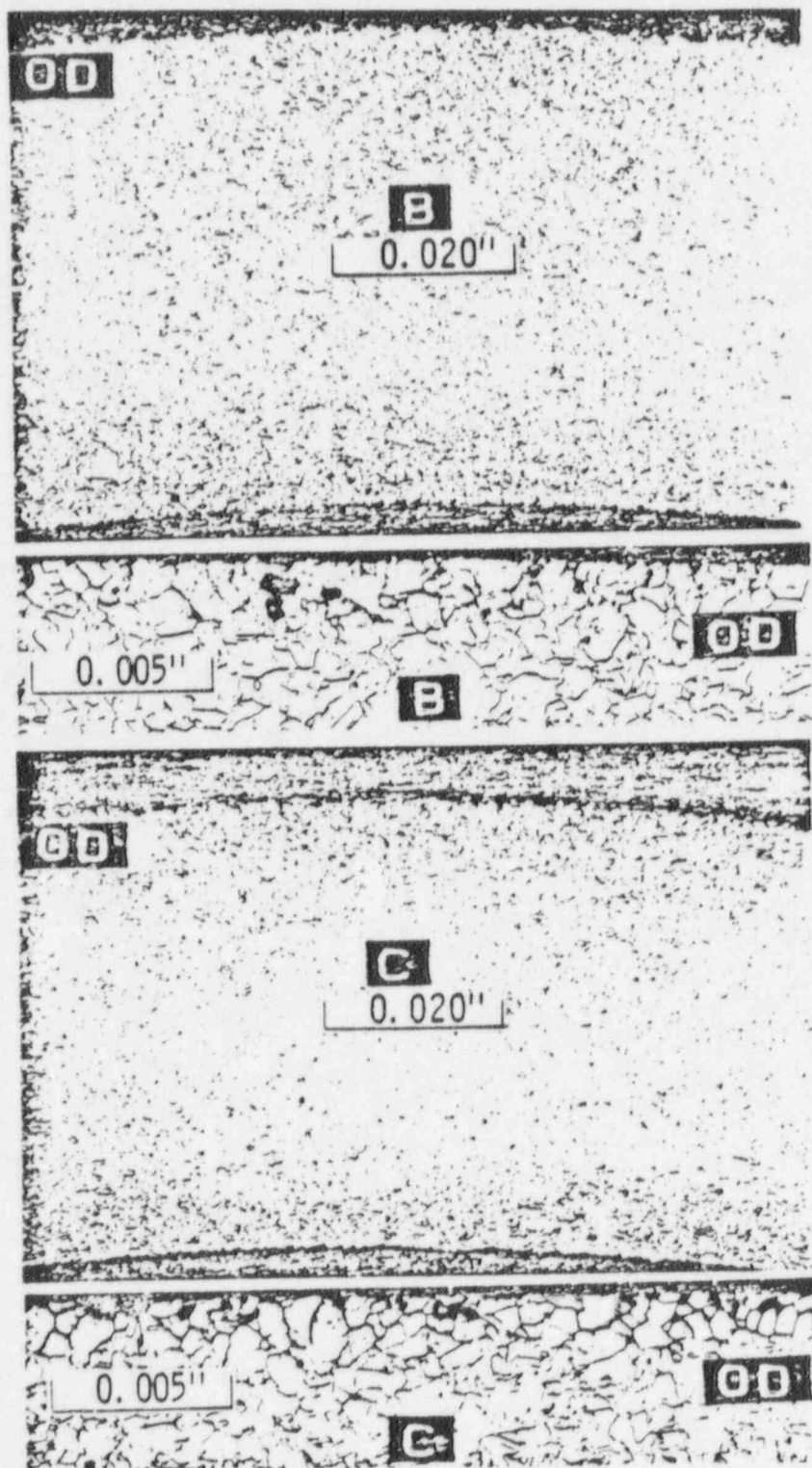


Figure 24

A (15-73), 1-1/2 in. below Fracture,
Transverse Cross Section.

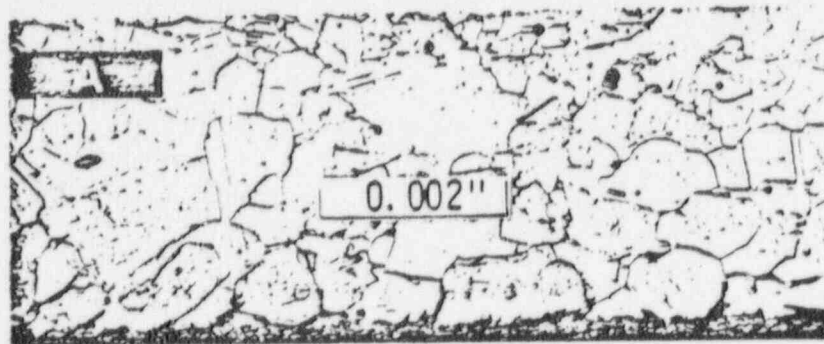
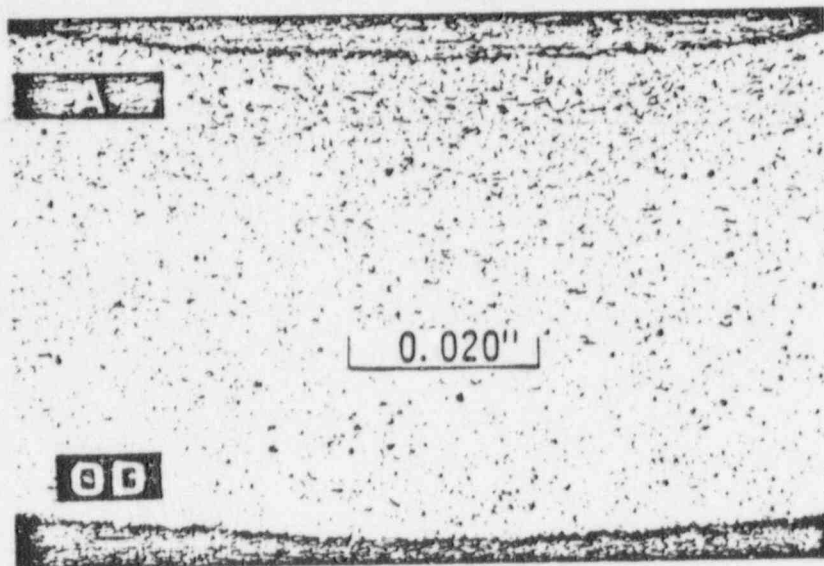
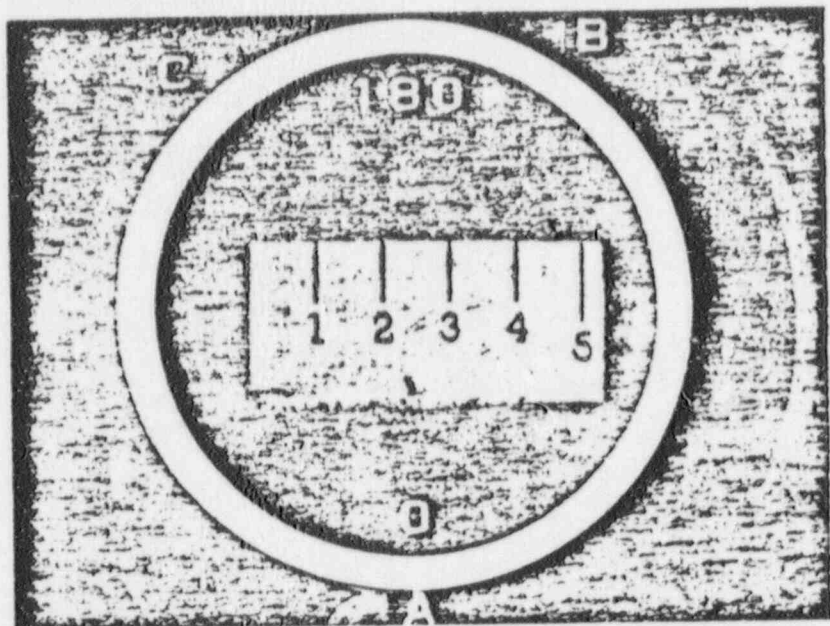


Figure 25

A (15-73), 1-1/2 in. below Fracture Areas B
& C of Figure 25. The OD conditions at B
represents intergranular penetrations of
about 1 grain in depth (approx. 0.006 in.
or 0.6 mil)

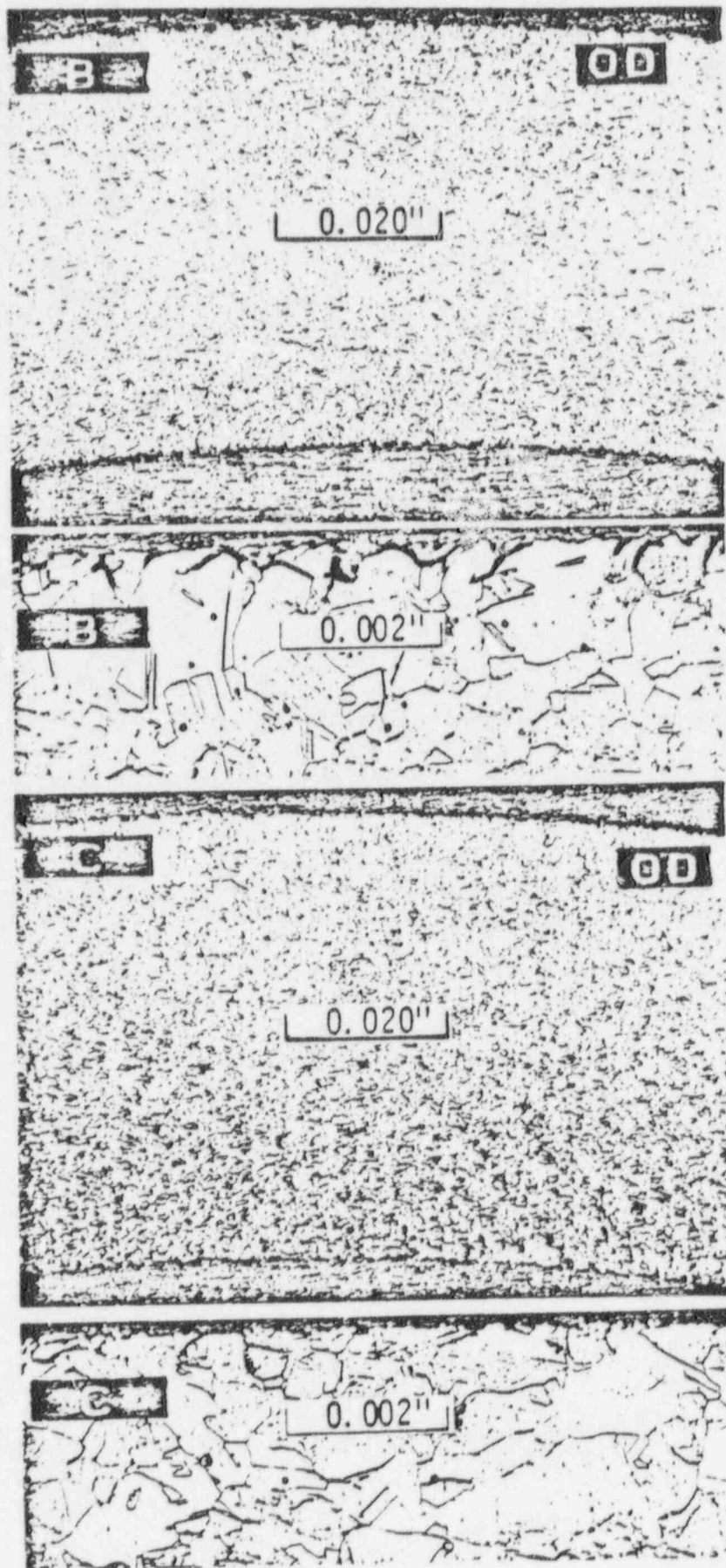


Figure 26

A (15-73), Double Axial Cross Section, 1 in. long, centered at 7-1/4 in. above the fracture. "Chatter marks" from tube removal equipment were present on ID surface.

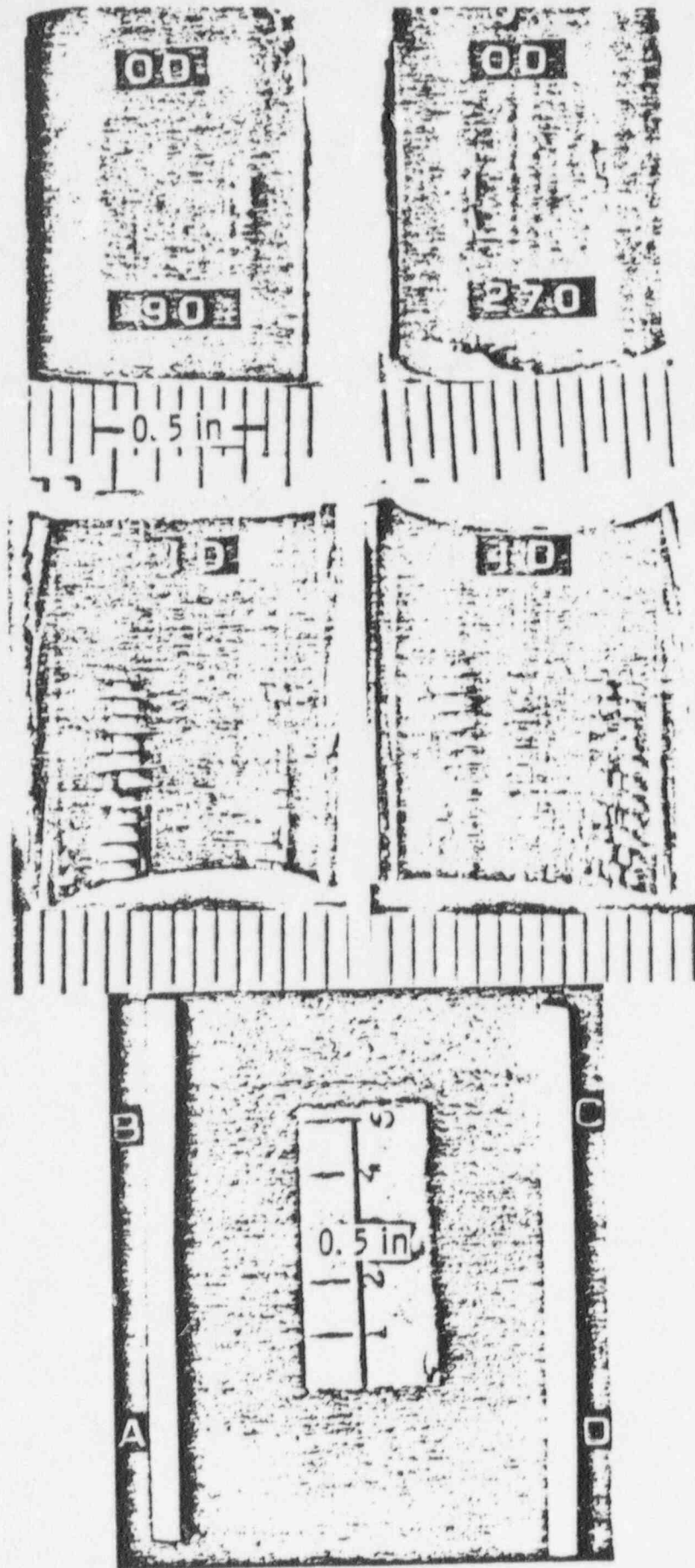


Figure 27

WIS (15-73) 7 1/4 IN ABOVE FRACTURE

A (15-73), Double Axial Cross Section 6-3/4 to 7-3/4 in. above fracture.
Areas A-D of Figure 29.

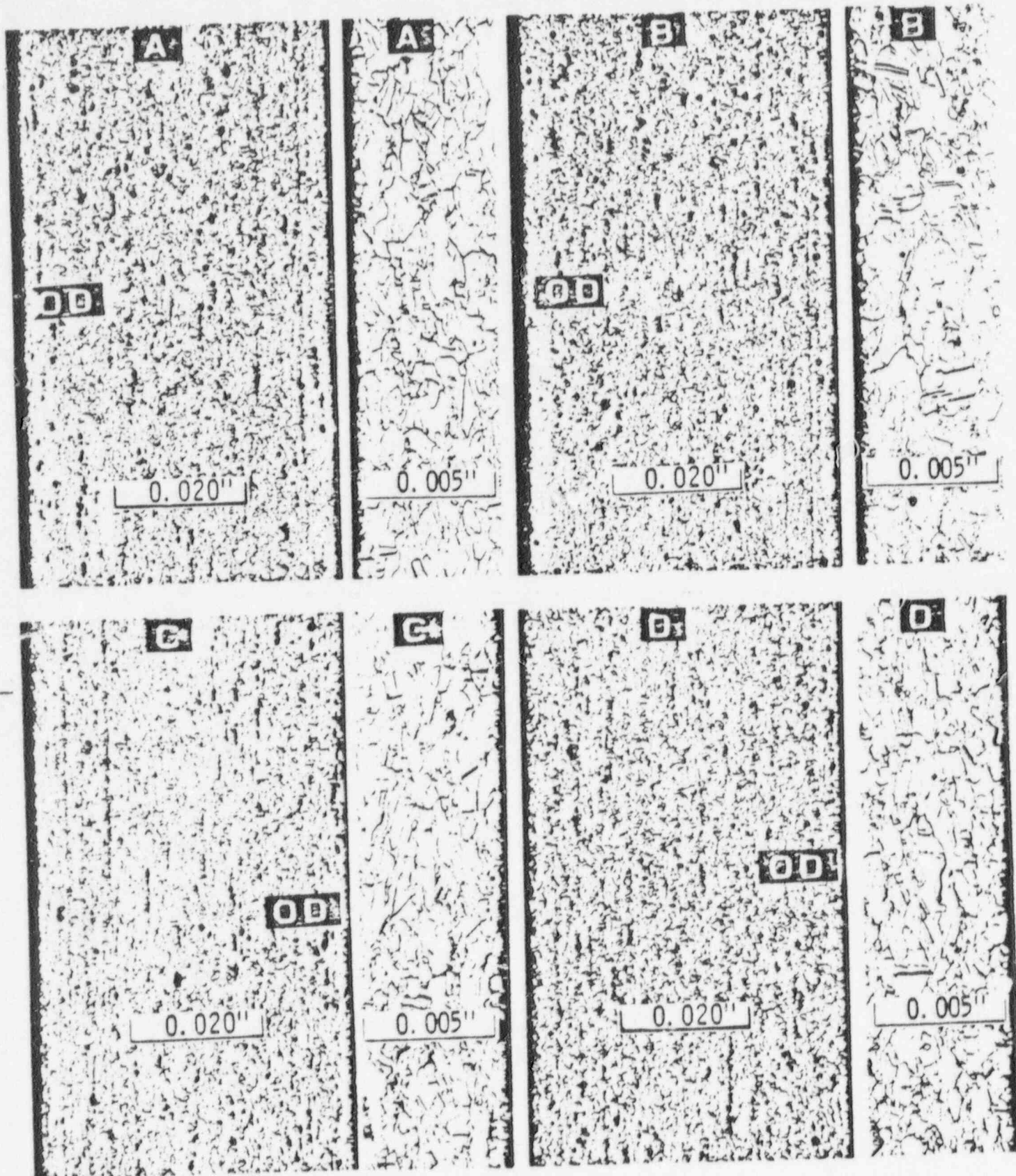


Figure 28

A (15-73), Fracture Surface of Section 1, showing materials analyzed by EDAX at Degree Orientations indicated

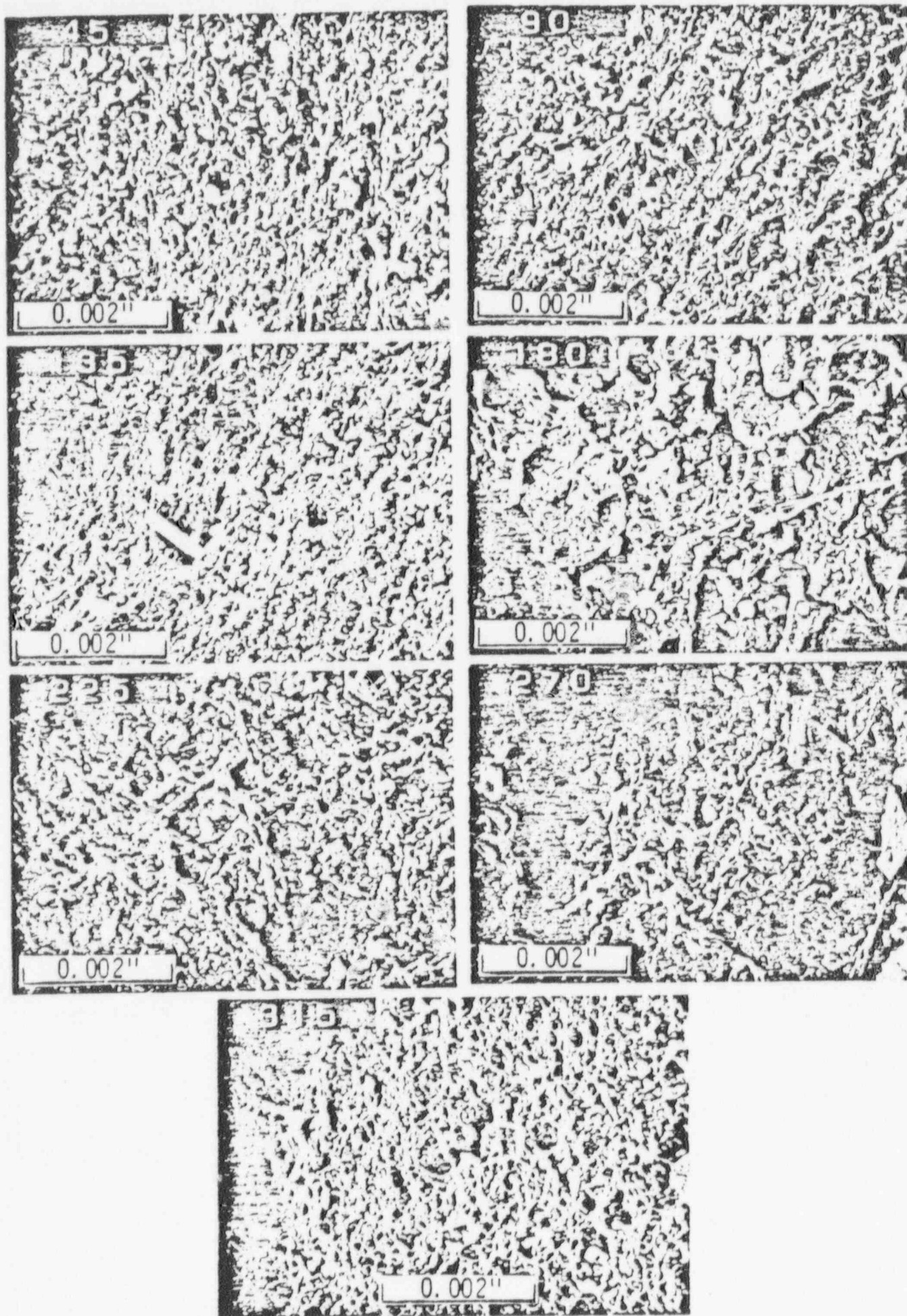


Figure 29

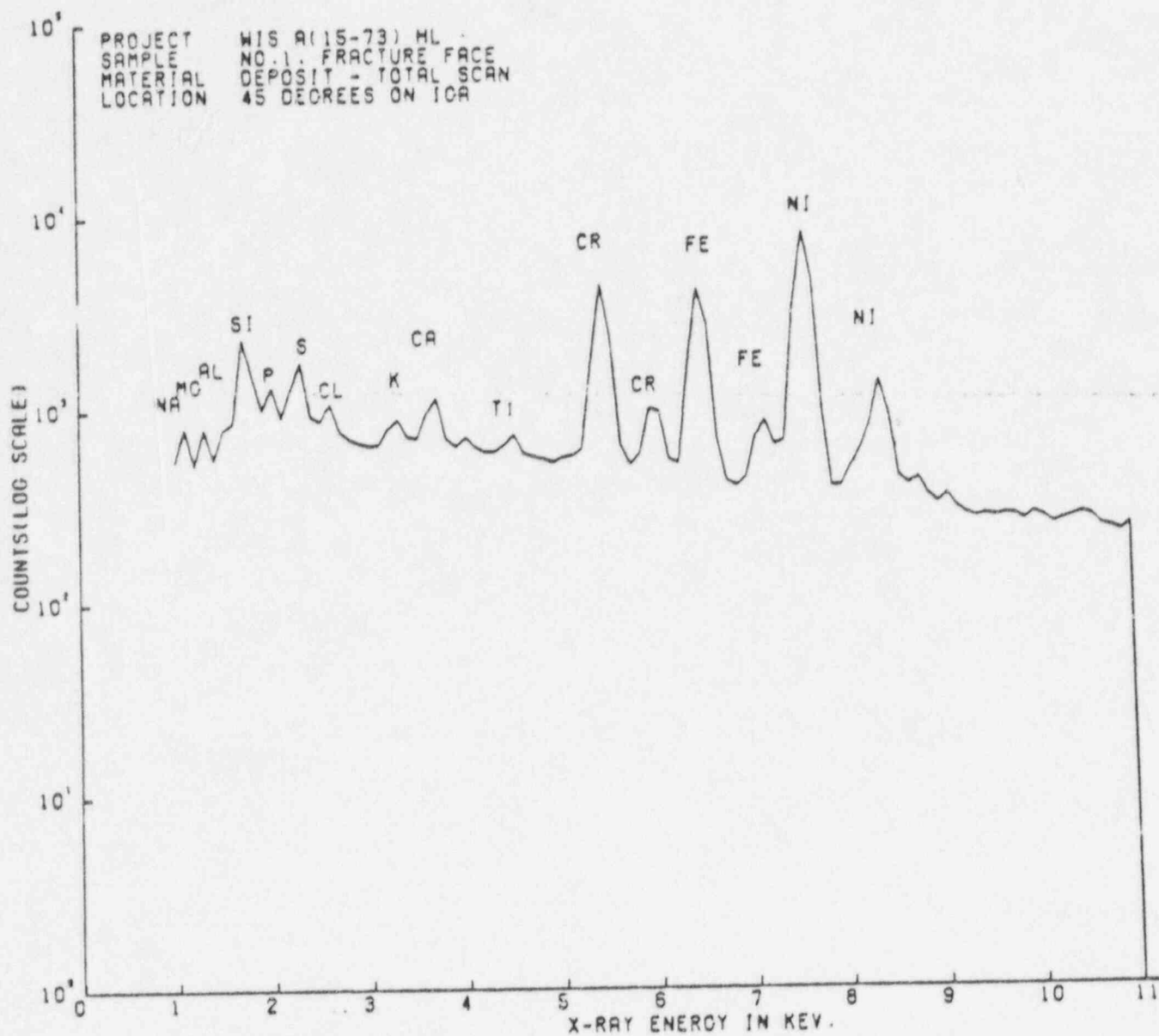


Figure 30

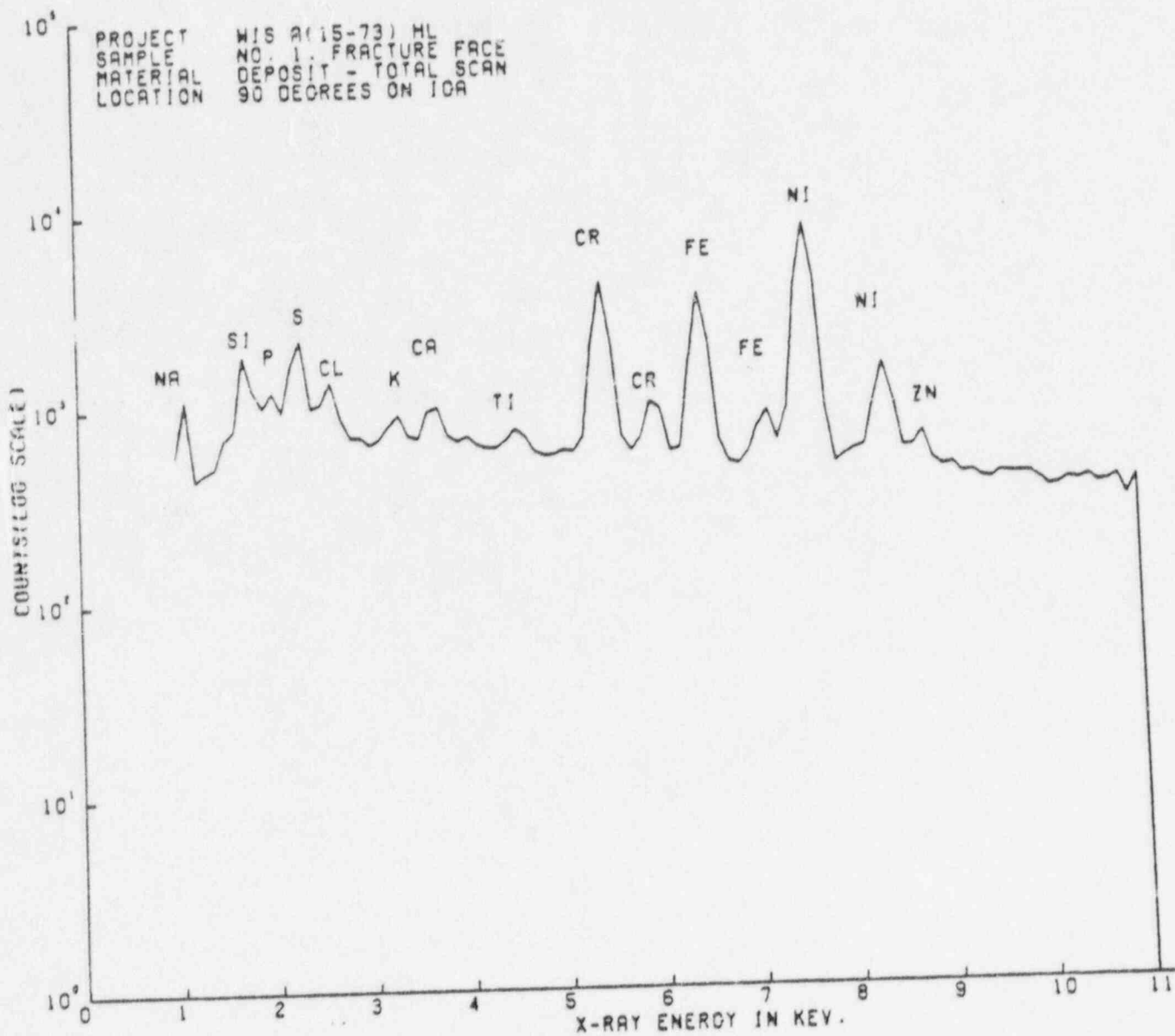


Figure 31

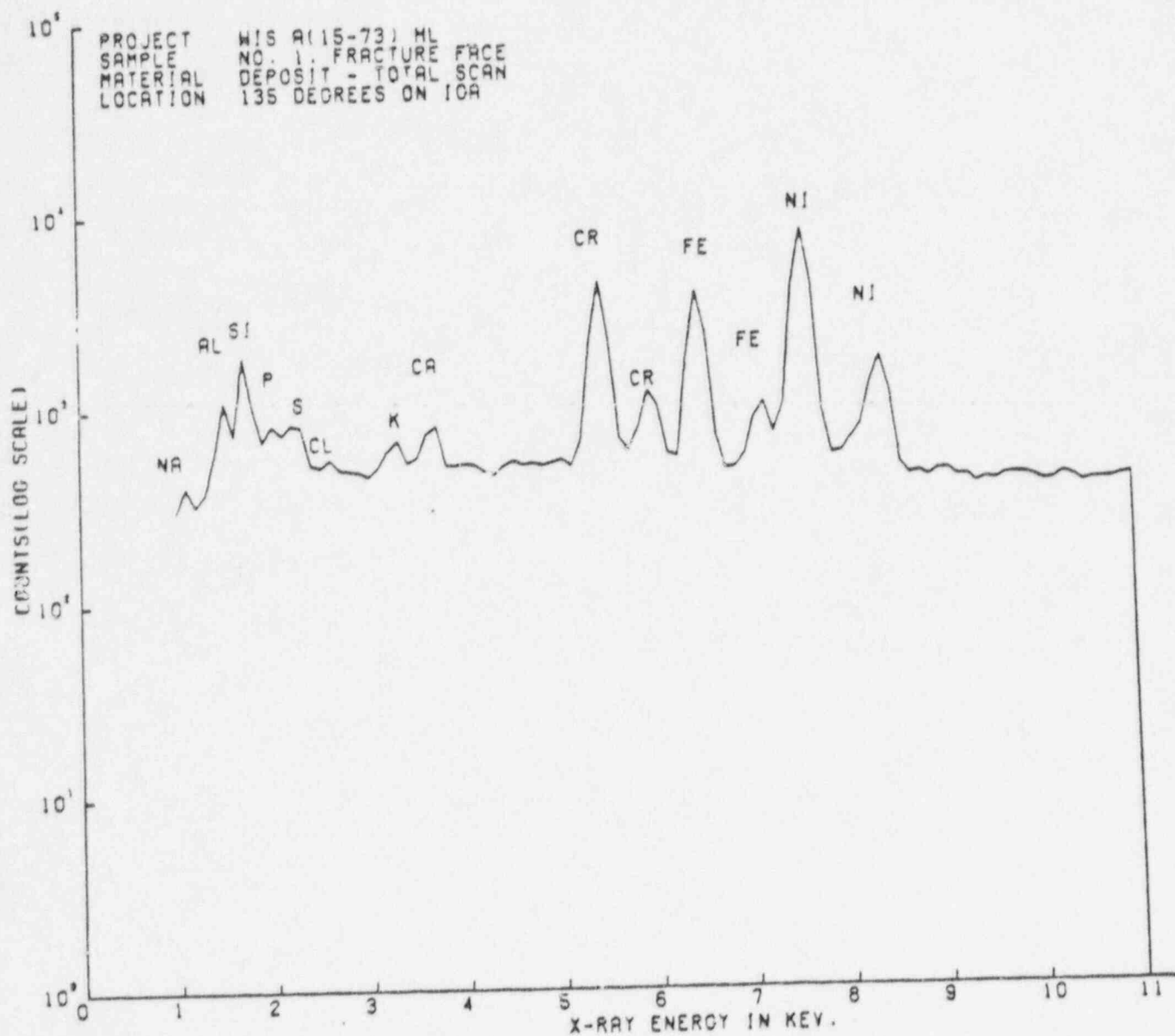


Figure 32

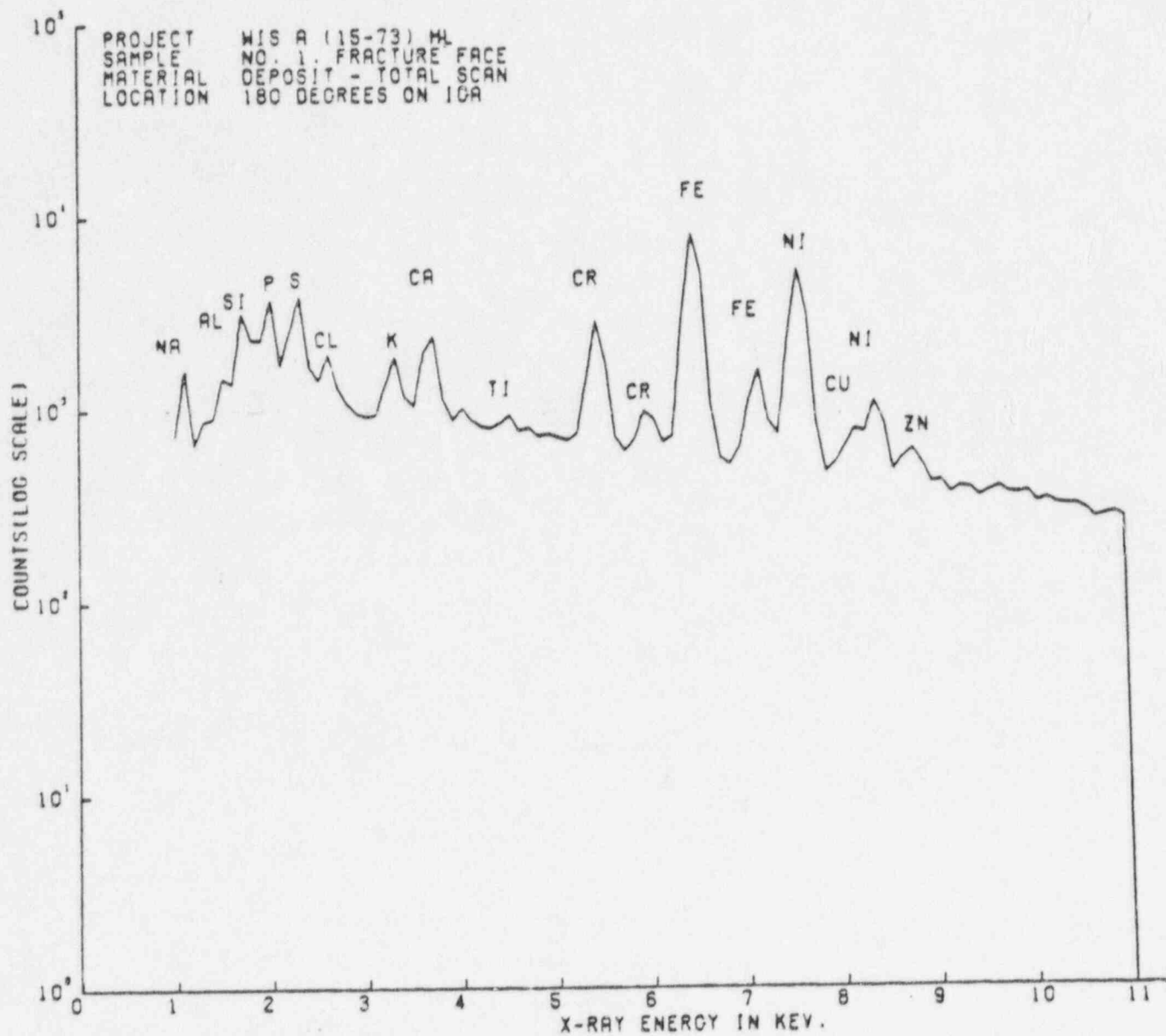


Figure 33

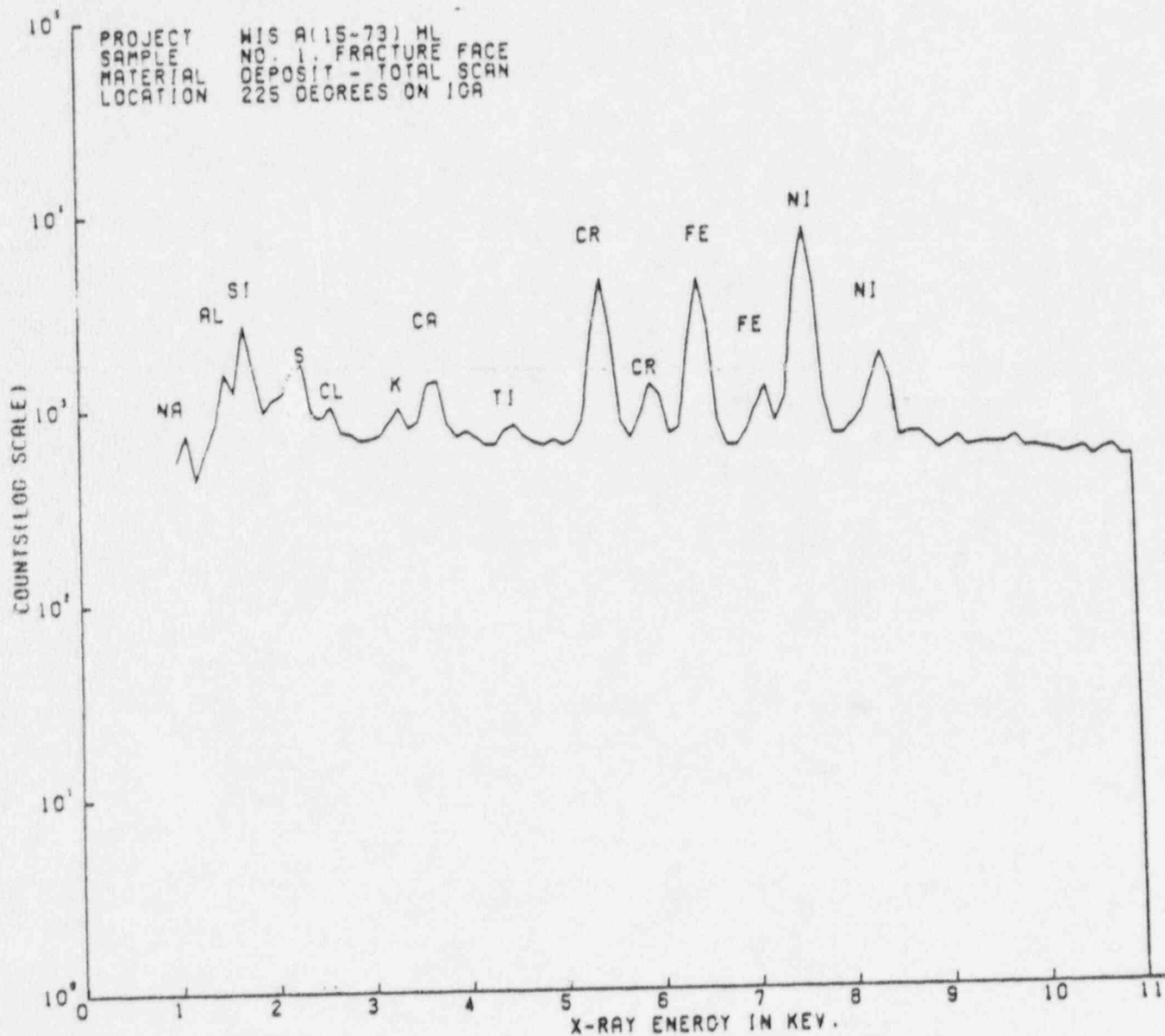


Figure 34

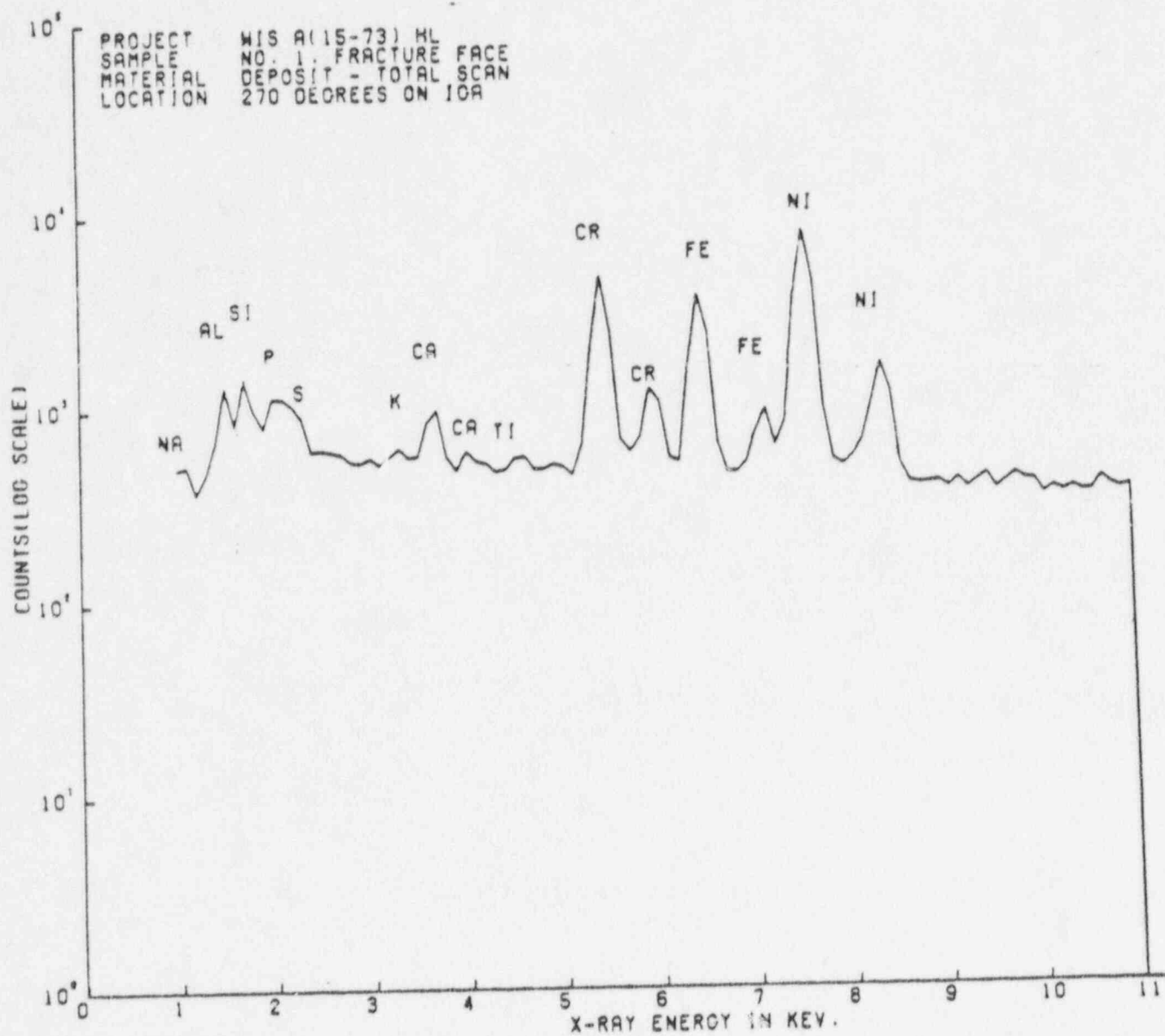


Figure 35

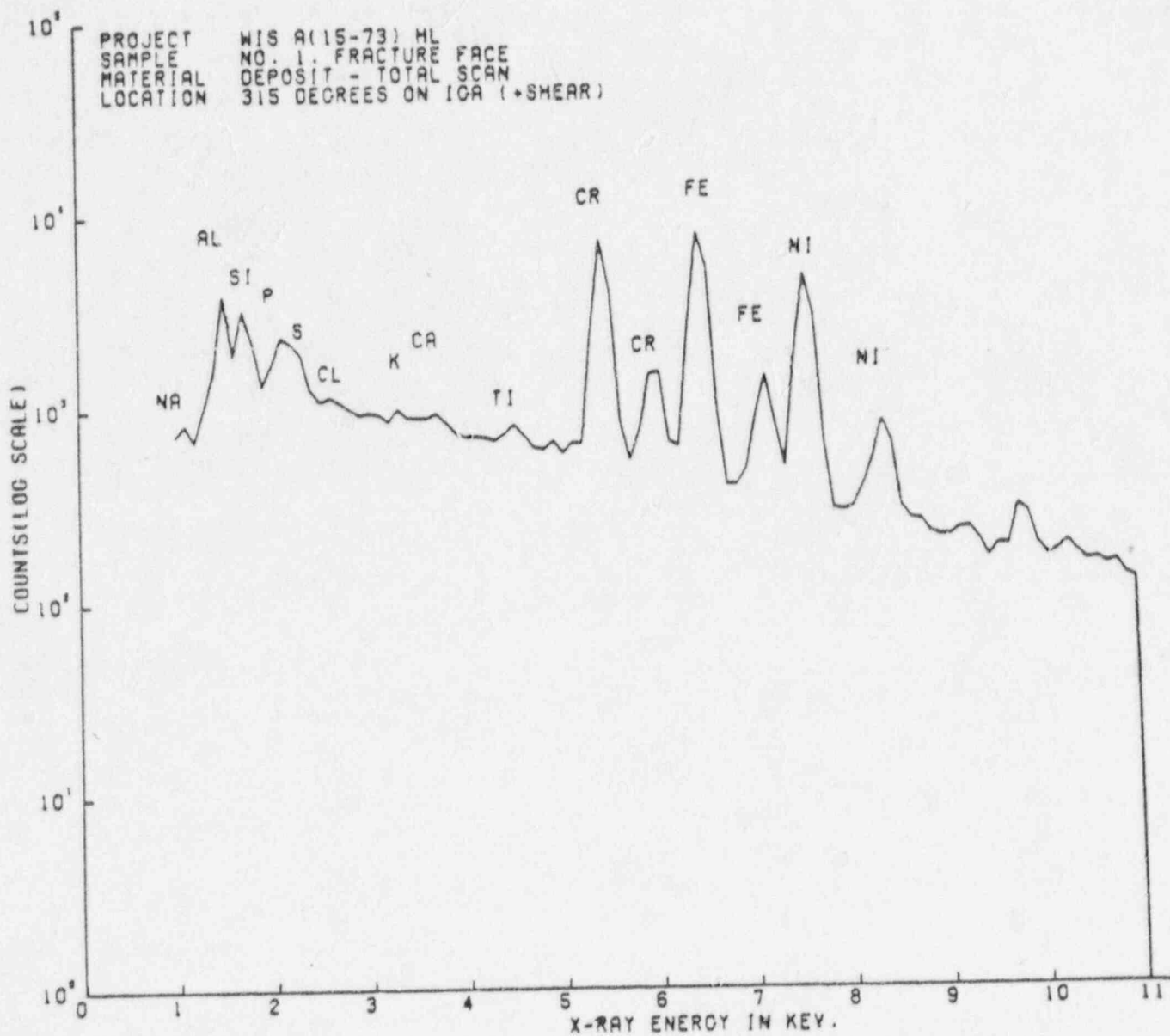


Figure 36

POINT BEACH UNIT 2 (WIS)
ANALYSIS OF APRIL, 1981
EDDY CURRENT INSPECTION RESULTS

INTRODUCTION

An evaluation of the April, 1981 eddy current inspection results, was made at the request of Wisconsin Electric Power Company. The principal objective of the evaluation was to determine the average growth of the reported eddy current indications (ECI's) since the previous May, 1980 inspection. Comparisons of the ECI growth data as well as photographs of the eddy current signals were also made in the evaluation.

DISPLAY OF EDDY CURRENT INDICATIONS REPORTED AT APRIL, 1981 INSPECTION

Figures 1 and 2 are histograms of the numbers of inlet side indications arranged according to the reported percent wall penetration, steam generators A and B, respectively (Note that the vertical scale of Figure 1 is twice that of Figure 2). Inspection of the histograms shows that the majority of the indications are observed at the lowest range of wall penetration (20-29%) with successively smaller numbers reported at the higher percentages of penetration. This type of behavior is typical of the thinning phenomenon, as shown in a number of previous evaluations of inspection data from other units.

COMPARISON OF GROWTH OF EDDY CURRENT INDICATIONS IN SUCCESSIVE INSPECTION INTERVALS

A statistical evaluation of the change in reported tubesheet eddy current indications (ECI) between successive inspections from 1974 to 1981 was made for the inlet data from each of the two Point Beach Unit 2 steam generators. Only those tubes for which ECI's of 20% or greater in each of the pair of inspections compared were used in the data base. The results of the calculations are summarized for each of the steam generators in Tables 1 and 2 respectively, and are graphically displayed in the form of histograms for each steam generator in Figures 3 and 4 respectively for the 1980-1981 period. Figure 3 for Steam Generator A shows rather well behaved data, clustered about the 0 to 5% growth range in a generally bell-shaped curve. In the case of Steam Generator B inlet, Fig. 4, the same general trends are observed, although the data are not as continuous as those of Fig. 3, presumably due to the considerably smaller data base.

TABLE 1
POINT BEACH UNIT 2 (WIS)
STEAM GENERATOR A (INLET)

Growth of Eddy current Indications \geq 20%
in Successive Inspection Intervals

<u>INSPECTION</u> <u>INTERVAL</u>	<u>NUMBER OF TUBES</u> <u>COMPARED</u>	<u>CALCULATED AVERAGE</u> <u>GROWTH IN ECI (%)</u>	<u>STANDARD DEVIATION</u> <u>%</u>
10/74 - 3/76	21	1.8	6.3
3/76 - 3/77	24	-0.3	3.0
3/77 - 3/78	19	-2.4	4.4
3/78 - 3/79	8	-0.9	3.1
3/79 - 3/80	4	10.5	7.1
3/80 - 4/81	164	5.5	6.5

TABLE 2
POINT BEACH UNIT 2 (WIS)
STEAM GENERATOR B (INLET)

Growth of Eddy Current Indications $\geq 20\%$
in Successive Inspection Intervals

<u>INSPECTION</u> <u>INTERVAL</u>	<u>NUMBER OF TUBES</u> <u>COMPARED</u>	<u>CALCULATED AVERAGE</u> <u>GROWTH IN ECI (%)</u>	<u>STANDARD DEVIATION</u> <u>%</u>
10/74 - 8/75	2	-8	0
8/75 - 3/76	2	8	0
3/76 - 3/77	5	-1.4	4.0
3/77 - 3/78	8	2.6	2.3
3/78 - 3/79	5	-4.2	3.8
3/79 - 3/80	4	2.5	7.1
3/80 - 4/81	22	4.9	7.9

For Steam Generator A (inlet), the unit in which a sufficient data base is present, the data over the seven year period indicate little change in ECI's. In the comparison between the March, 1979 and March, 1980 inspections, a 10.5% average change was calculated. However, this can be disregarded since only four tubes could be compared (i.e., only four tubes exhibited ECI's of $\geq 20\%$ in both inspections). For the March, 1980 to April, 1981 interval, an average ECI growth of 5.5% was determined for a calculated growth rate of 0.48%/EFPM over the latest inspection intervals of 11.5 EFPM. For Steam Generator B (inlet) the data base is generally too small to permit any conclusions to be drawn from the calculations for the inspection intervals up to March, 1980. For the March, 1980 to April, 1981 inspection interval, an average ECI growth of 4.9% was determined for a calculated growth rate of 0.43%/EFPM over the latest inspection interval of 11.5 EFPM.

A Westinghouse re-evaluation of the March, 1980 data from SG-A compared to reported values in April, 1981, was made on a sample of 68 inlet tubes from the data tapes. Some differences were noted for the March, 1980 data. On the basis of the Westinghouse estimates, an apparent growth of 3.4% was calculated for the 68 tube sample for the March, 1980-April, 1981 operating period. This compares with the higher estimate of 5.5% quoted above.

PHOTOGRAPHIC COMPARISON OF CURRENT AND PRIOR EDDY CURRENT SIGNALS

A comparison of the April, 1981 eddy current signals from a sample of ten tubes, selected from the central region of Steam Generator A inlet, was made with the corresponding signals recorded for those tubes in previous inspections. The tubes compared were selected on the basis of location in the region of greatest reported activity, reported wall penetration of 20% or greater, and consecutive inspection history traceable as far back in time as possible. Except for a few cases where a selected tube was not inspected in March, 1979, eddy current signals were retrieved from tape storage for each tube from the March, 1980, March, 1979, March, 1978, March, 1977, March, 1976, and October, 1974 inspections.

The photographs of the eddy current signal CRT displays for each of the ten steam generator tubes selected are shown in the Appendix to this report. In

the April, 1981 and March, 1980 inspections, multifrequency (400 kHz and 100 kHz singly and mixed, in the differential mode) data were obtained, as labeled on each figure. The 400 kHz tubesheet signal is shown at the upper left, the 100 kHz signal is displayed at the upper right, and the mixed signal appears at the lower center of the photographs from these inspections. In the other inspections noted, only single frequency, 400 kHz data were obtained. The percent wall penetration data as reported by Zetec are included on the CRT photographs for reference purposes. In some cases, either no evaluation was reported (left blank on photo), or distorted tubesheet signals (DTS) were noted. It is evident from a visual comparison of the photographs that the 400 kHz signals have the same general shape in successive inspections from October, 1974 to April, 1981 for each of the ten tubes examined. Since it was concluded in October, 1974 that the indications reported were due to tube wall thinning, the photo comparisons suggest that the April, 1981 indications can also be attributed to the same phenomenon, or alternatively that the intergranular attack (IGA) observed in the pulled tube (R15C73 HL) has not contributed in a significant manner to the observed eddy current signals at the top of the tubesheet. As for the 10 tubes compared, the 1980 and 1981 signals for R15C73 also show no notable differences, (See Figure 5).

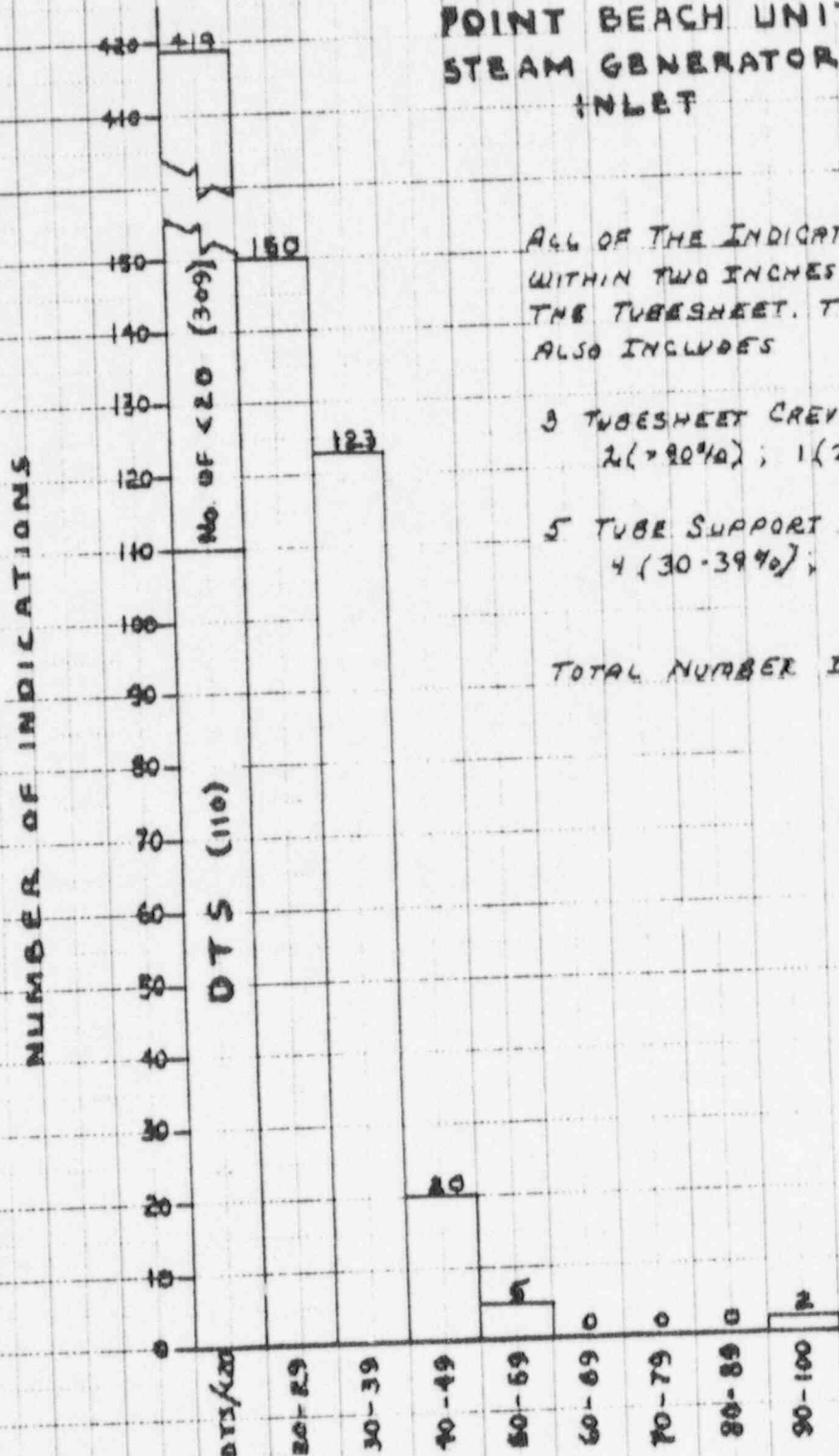
SUMMARY AND CONCLUSIONS

Evaluation of the April, 1981 eddy current inspection data suggests no more than a small increase in penetration for the affected inlet tubing of Steam Generators A and B, as indicated by the data of Tables 1 and 2. On the basis of the reported data, the growth rates over the operating interval between the March, 1980 and April, 1981 inspection are calculated as 0.48%/EFPM for Steam Generator A, and 0.43%/EFPM for Steam Generator B. Comparisons of these rates with those of the previous inspection intervals cannot be made with any degree of certainty due to small data base for the previous intervals. However, photocomparison of eddy current signals from selected tubes generally shows little or no change in signals since October, 1974. In addition, Westinghouse believes that the calculated rates based on the Zetec data are too high by up to about 2%, so that the above corrosion rates are probably lower. In view of these observations, Westinghouse believes that the corrosion rate indicated for the 3/80-4/81 period is not substantially changed from that of previous years for this unit. Indeed it is not clear that the total data assemblage for the top of the tubesheet region supports any detectable progression over the 1974-1981 period.

FIGURE 1

DISTRIBUTION OF ALL EDDY CURRENT INDICATIONS REPORTED AT THE APRIL 1981 INSPECTION

POINT BEACH UNIT 2 STEAM GENERATOR A INLET



ALL OF THE INDICATIONS ARE REPORTED
WITHIN TWO INCHES FROM THE TOP OF
THE TUBESHEET. THIS DISTRIBUTION
ALSO INCLUDES

3 TUBESHEET CREVICE INDICATIONS
2 (> 90%) ; 1 (21%)

5 TUBE SUPPORT INDICATIONS
4 (30-39%) ; 1 (21%)

TOTAL NUMBER INDICATIONS = 719

SIZE OF INDICATIONS (% WALL PENETRATION)

5/12/81 HEN

POINT BEACH UNIT 2
STEAM GENERATOR B
INLET

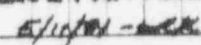
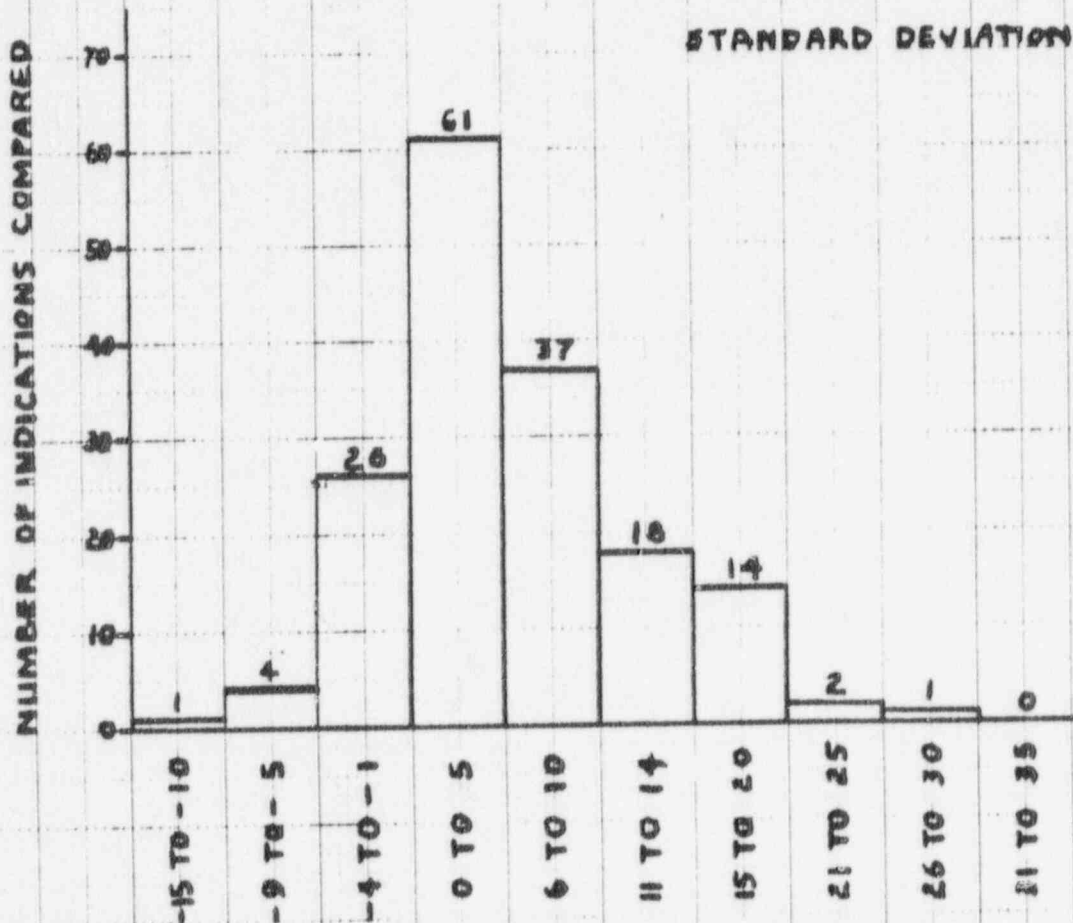


FIGURE 3

DISTRIBUTION OF THE CHANGE IN SIZE OF INDICATIONS REPORTED AS 220% AT THE TOP OF THE TUBESHEET IN BOTH MARCH 1980 AND APRIL 1981

POINT BEACH UNIT 2
STEAM GENERATOR A
INLET

NUMBER OF INDICATIONS
COMPARED = 164
MEAN CHANGE IN SIZE = 5.5%
STANDARD DEVIATION = 6.5%



CHANGE IN SIZE OF INDICATION (% WALL PENETRATION)

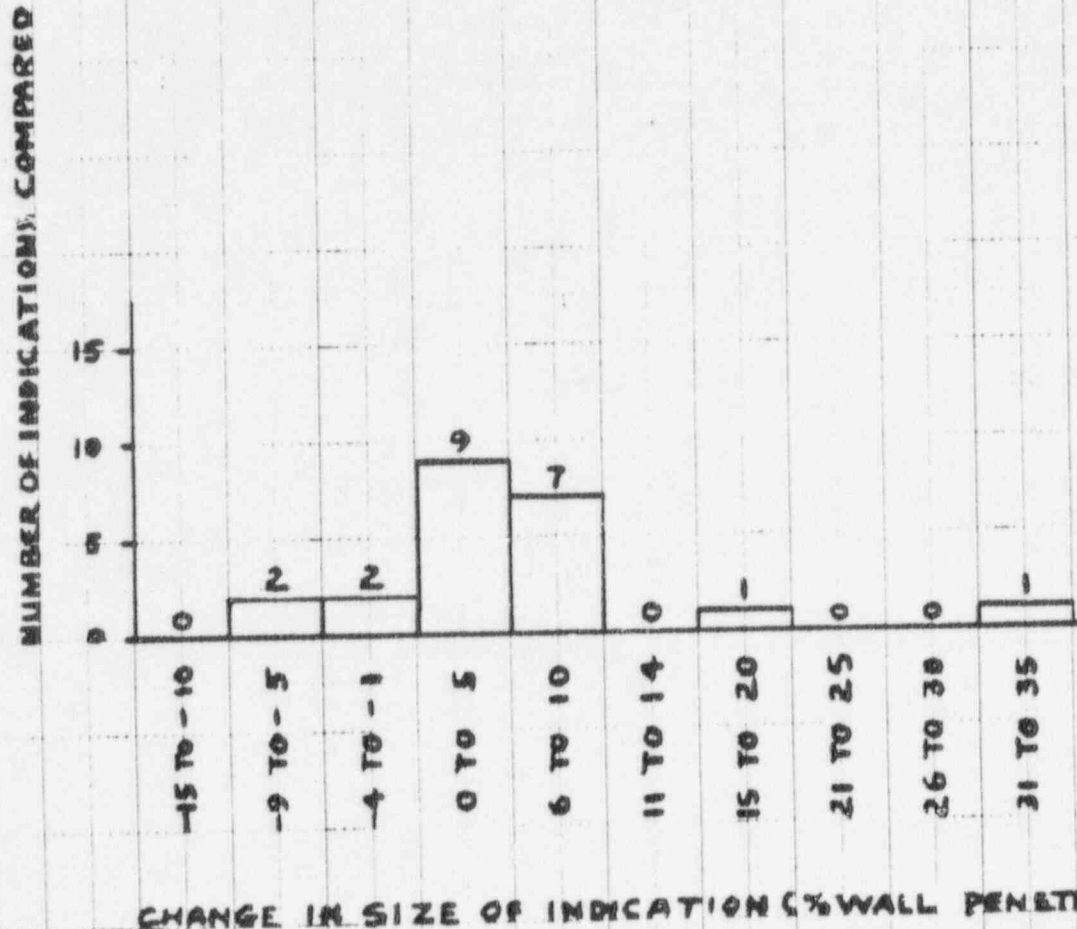
6/15/81
[Signature]

FIGURE 4

DISTRIBUTION OF THE CHANGE IN SIZE
OF INDICATIONS REPORTED AS $\geq 20\%$
AT THE TOP OF THE TUBESHEET IN
BOTH MARCH 1980 AND APRIL 1981

POINT BEACH UNIT 2
STEAM GENERATOR B
INLET

NUMBER OF INDICATIONS
COMPARED = 22
MEAN CHANGE IN SIZE = 4.91
STANDARD DEVIATION = 7.92



CHANGE IN SIZE OF INDICATION (% WALL PENETRATION)

5/15/81
WAK

FIGURE 5

POINT BEACH UNIT 2 (WIS)
STEAM GENERATOR A-INLET

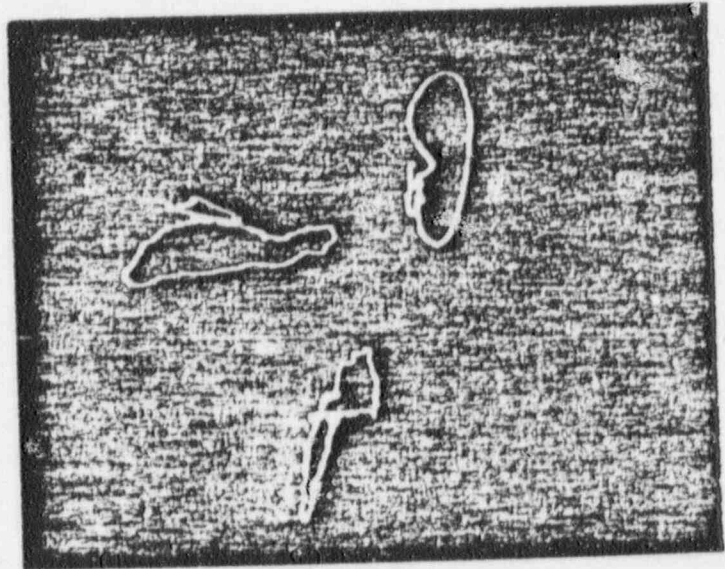
EDDY CURRENT SIGNALS
RI5C73

(Pulled 4/81)

400 kHz

3/80

100 kHz



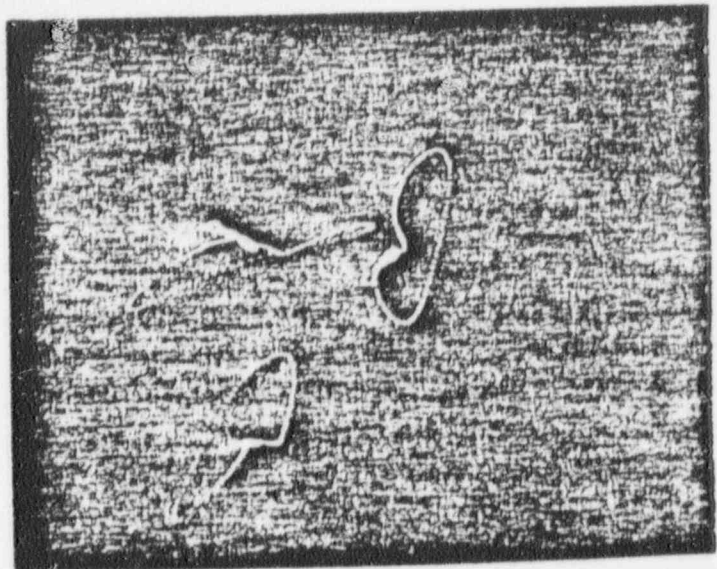
400 - 100 MIX

400 kHz

4/81

100 kHz

400 kHz



400 - 100 MIX

APPENDIX

Photographic Comparison of Eddy Current Signals
From Successive Inspections for a Selection of
Steam Generator Tubes. Point Beach Unit 2, Steam
Generator A - Inlet.

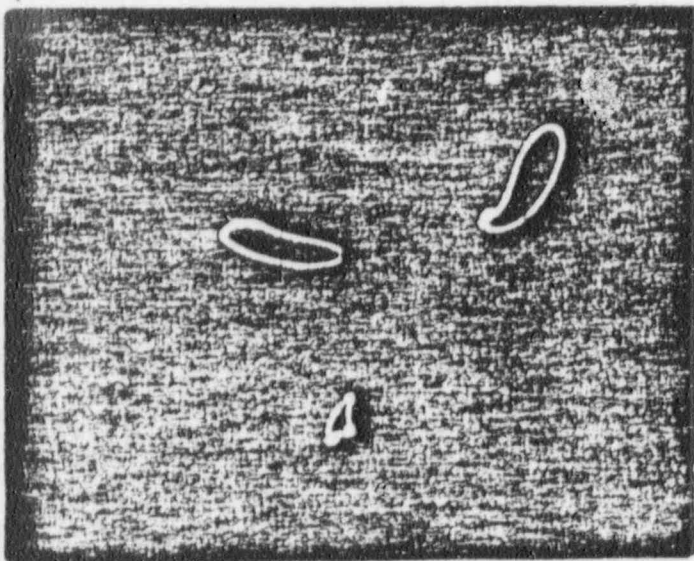
POINT BLANK UNIT 2 (WILD)
SILAM GENERATOR A INLET

R22044

400 KHz

4/81

100 KHz

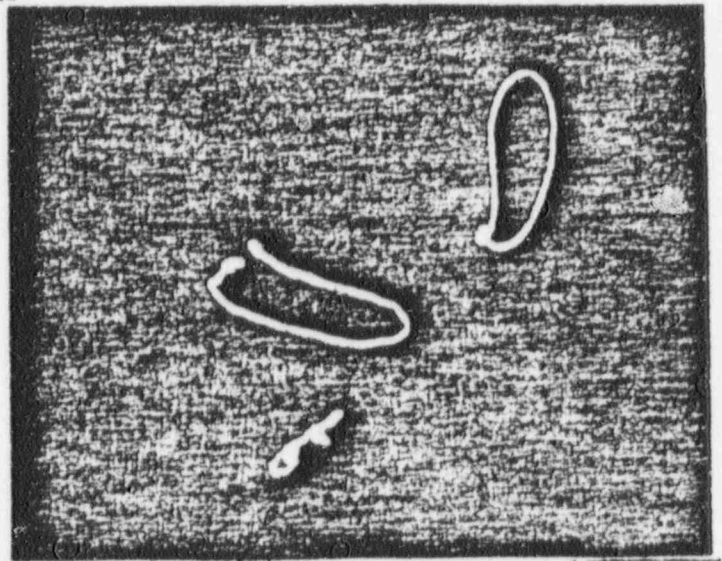


400 - 100 MIX
49 %

400 KHz

3/80

100 KHz



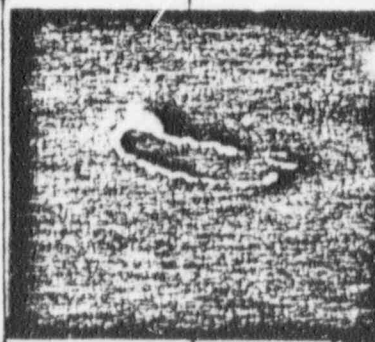
400 - 100 MIX
< 20 %

3/79

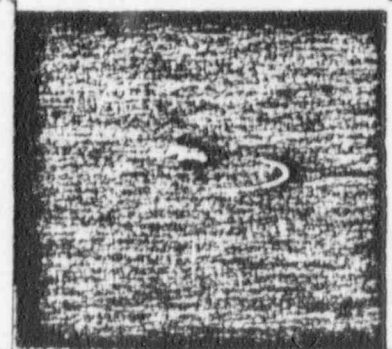
NOT
INSPECTED

400 KHz

3/78

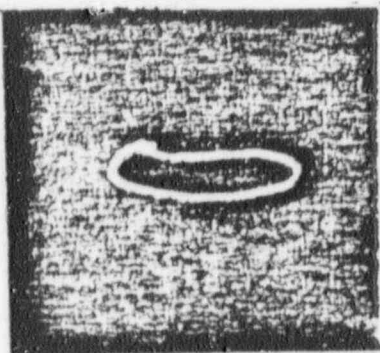


3/77



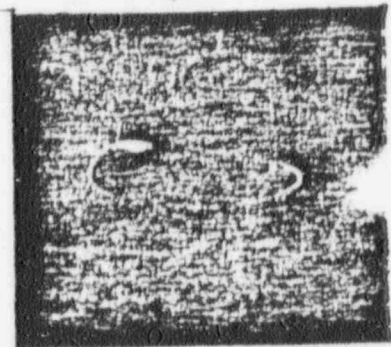
DTS

3/76



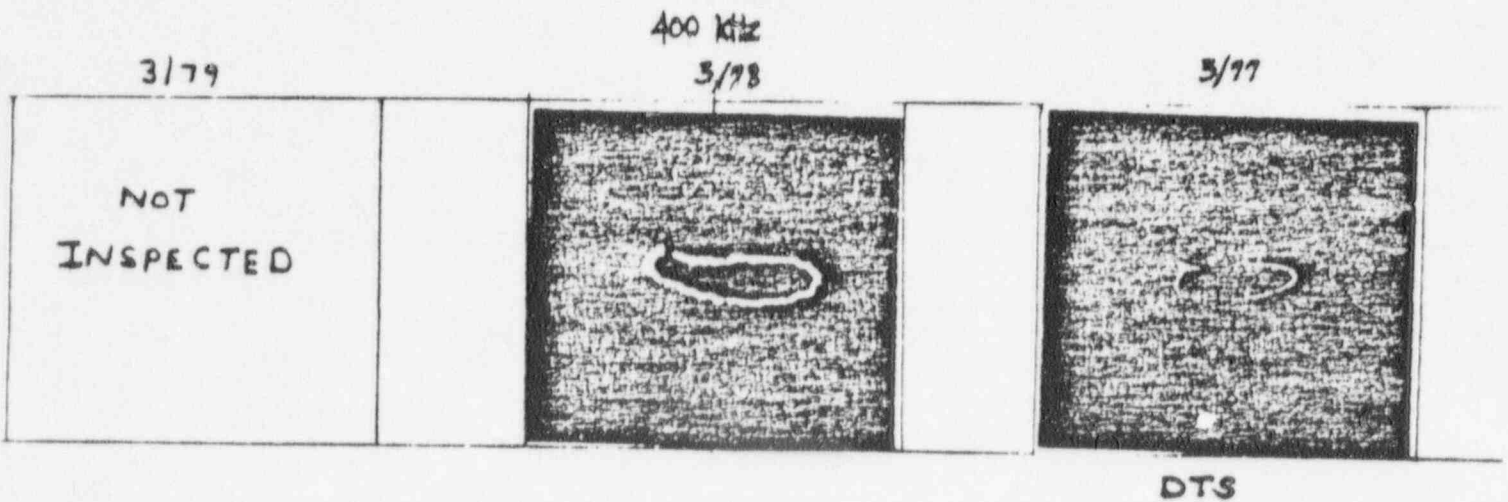
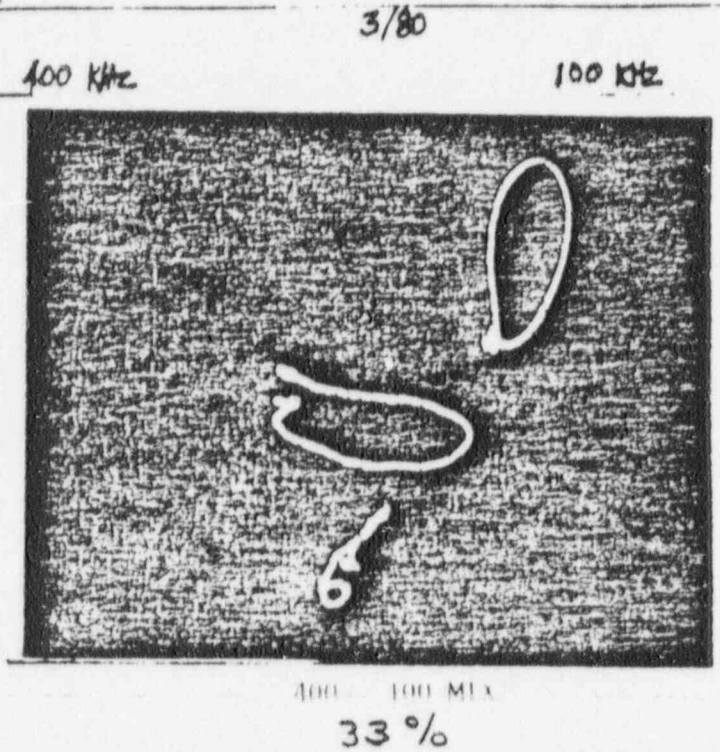
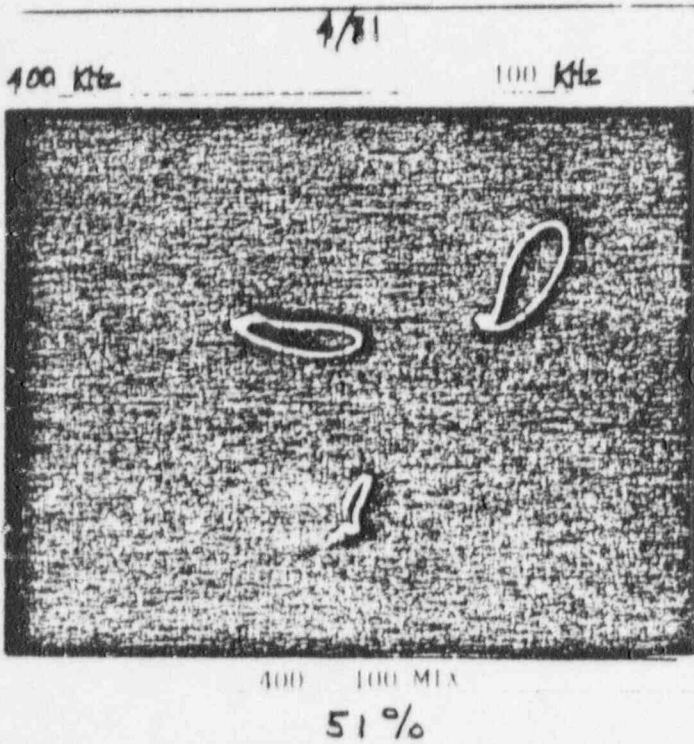
DTS

10/74



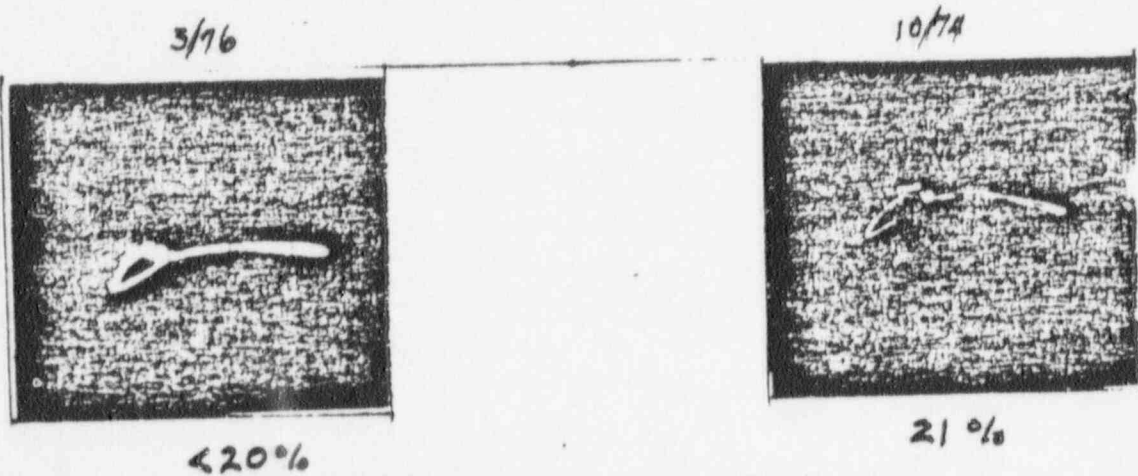
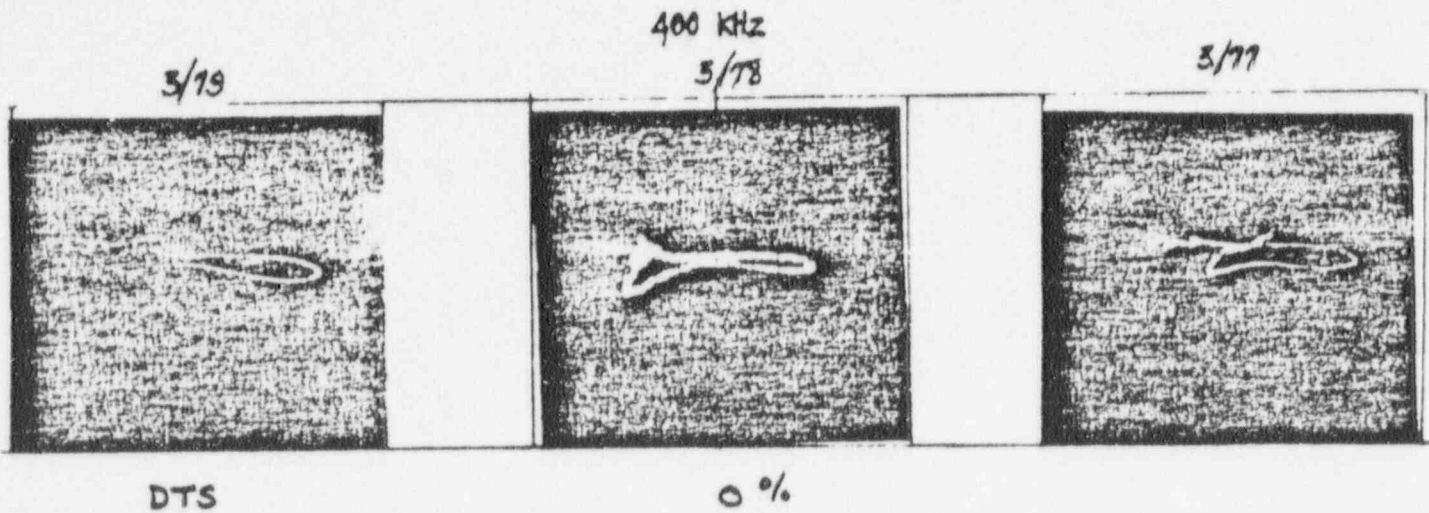
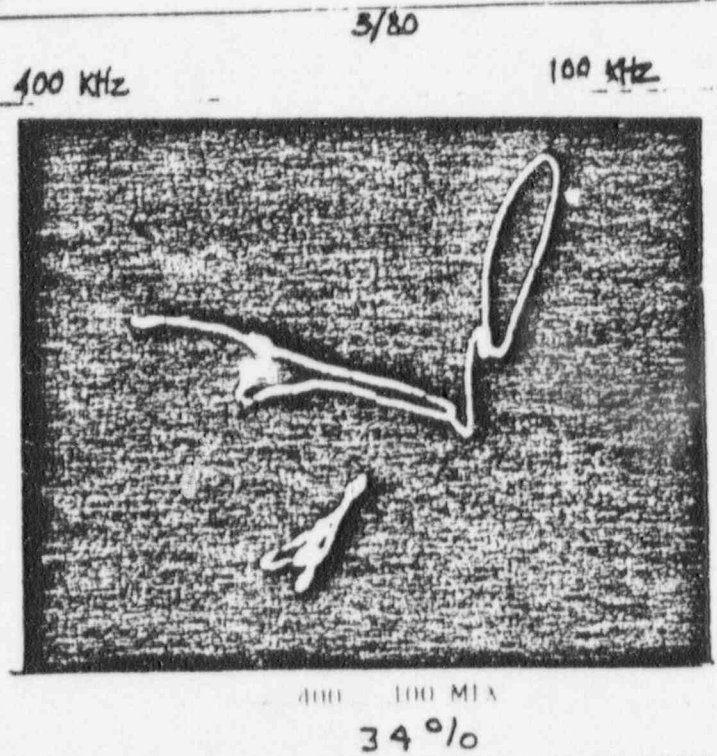
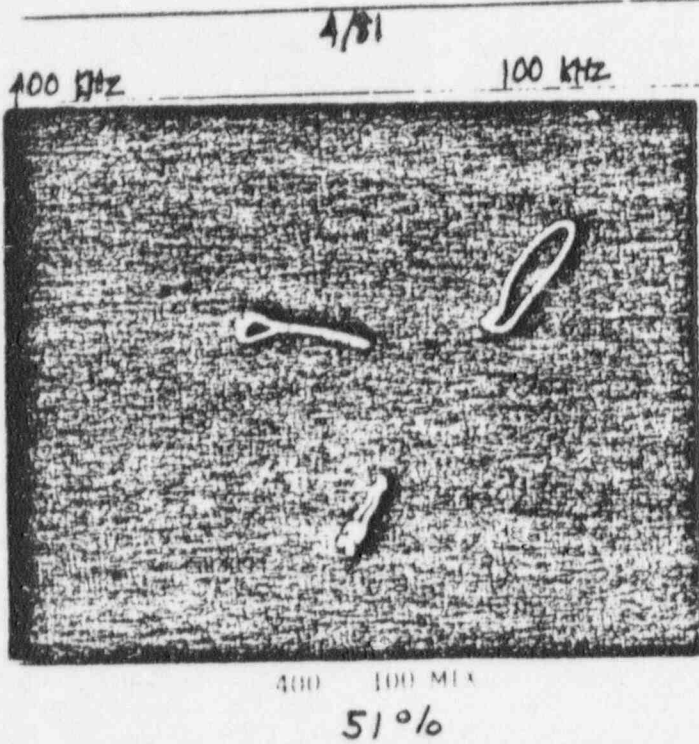
POINT BLACK UNIT (W/1)
STEAM GENERATOR A INLET

R21C44



POINT BEACH UNIT 2 (WIND)
STEAM GENERATOR A-INLET

R19C44



POINT BEACH UNIT 2 (WEST)
STEAM GENERATOR A INLET

219243

4/81

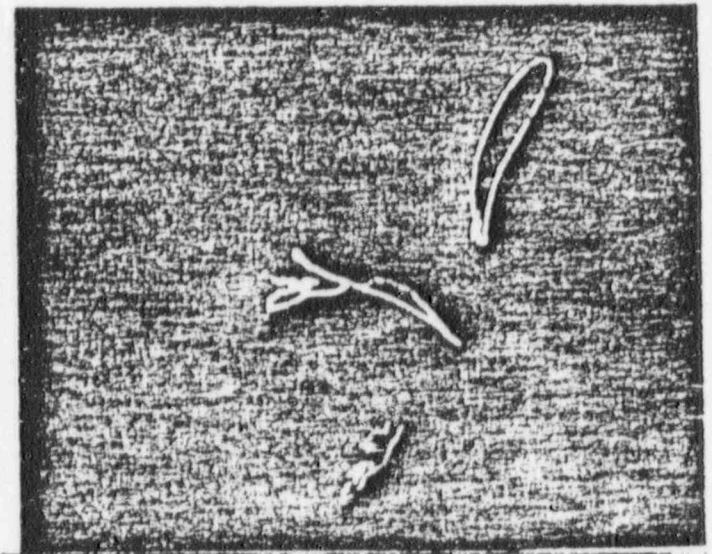
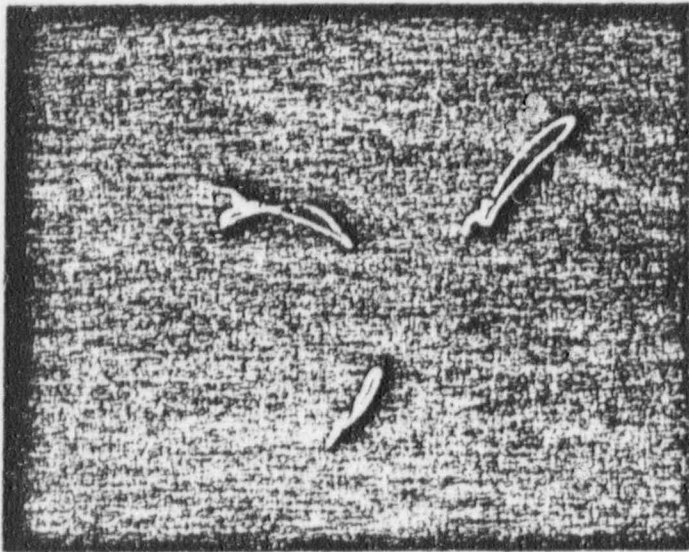
3/80

400 kHz

100 kHz

400 kHz

100 kHz



400 100 MIX

36 %

400 100 MIX

34 %

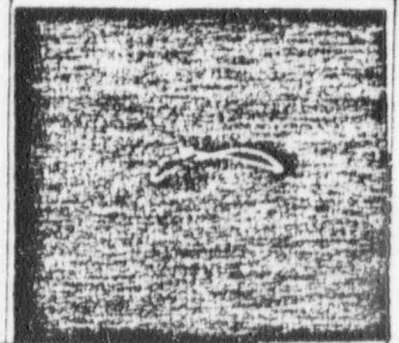
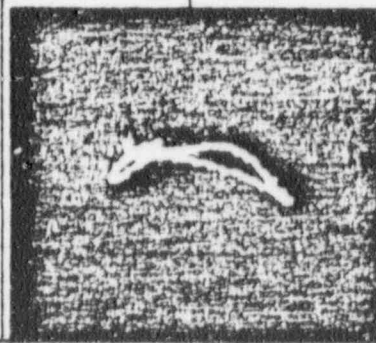
3/79

400 kHz

3/78

3/77

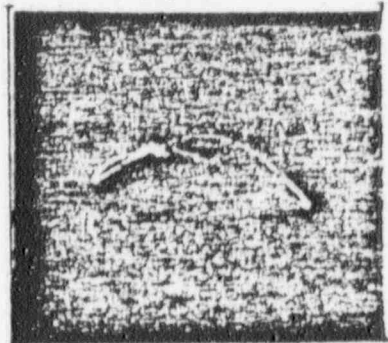
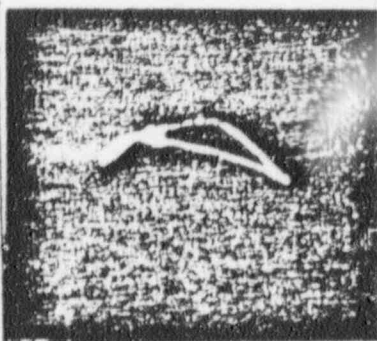
NOT
INSPECTED



< 20 %

3/76

10/74

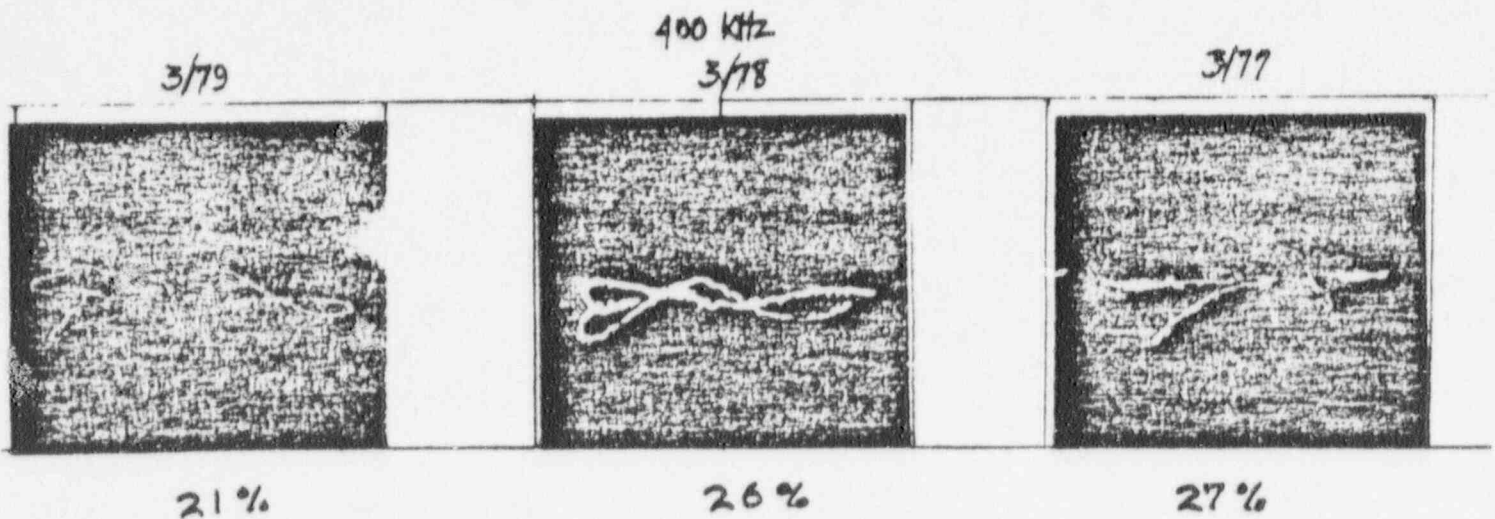
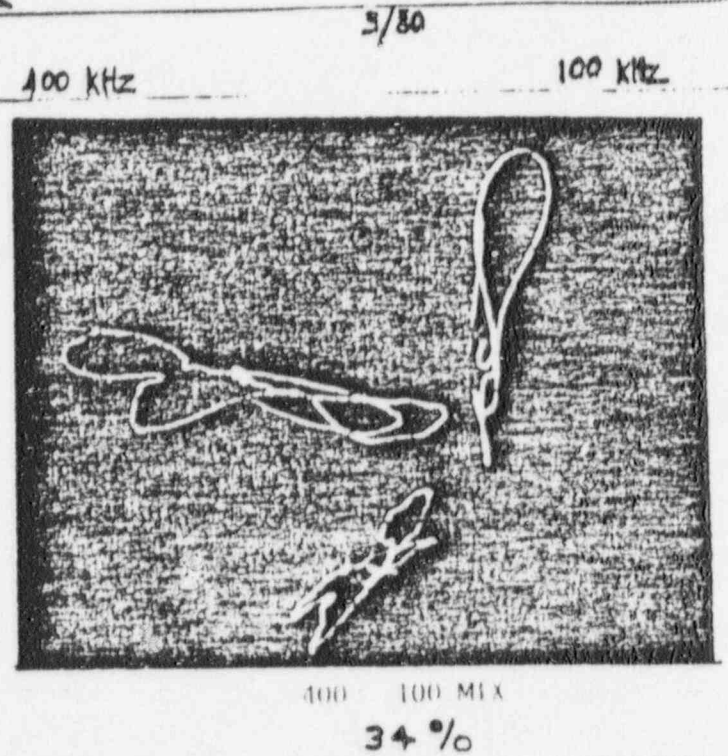
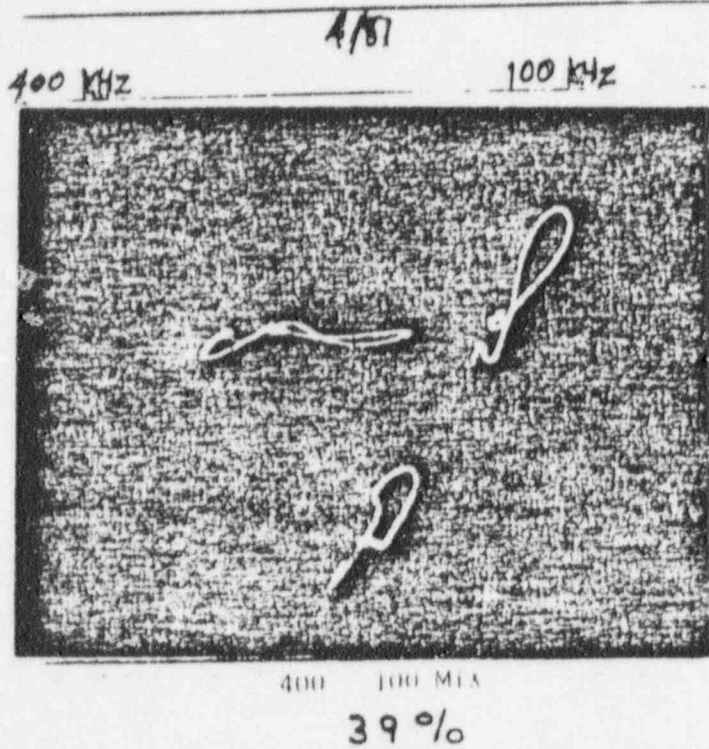


< 20 %

< 20 %

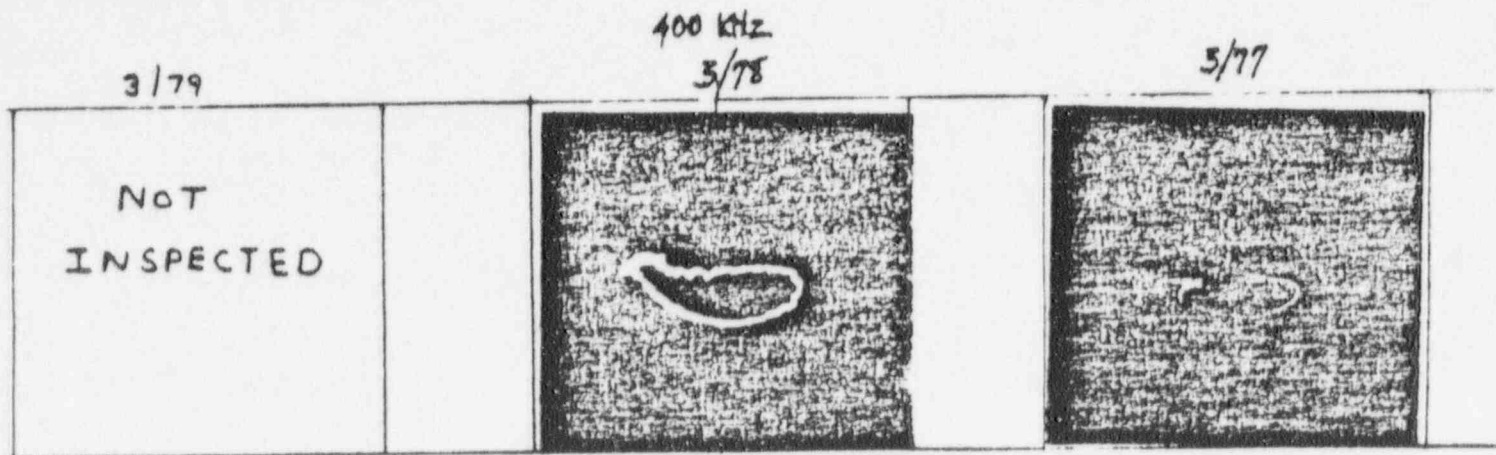
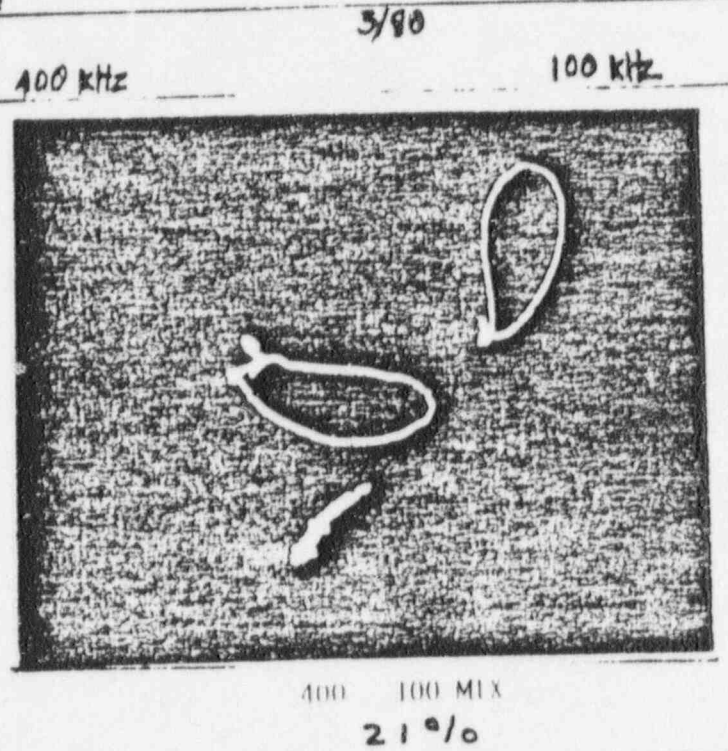
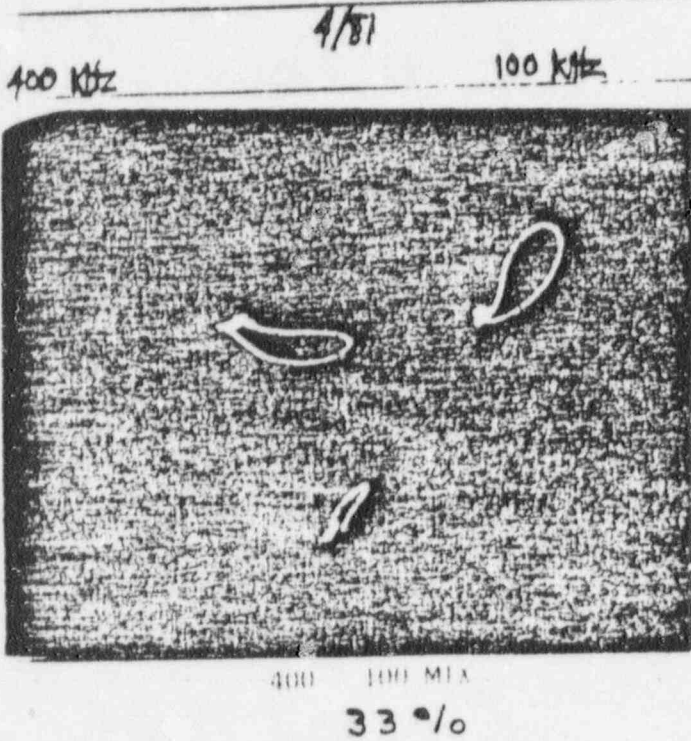
POINT BEACH UNIT 2 (WIS)
STEAM GENERATOR A INLET

R200A2

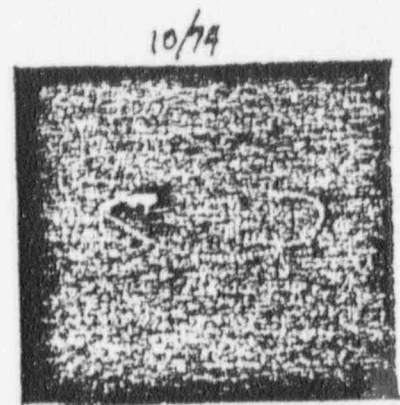
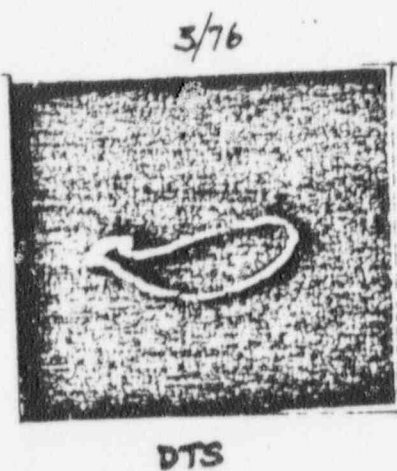


POINT BEAM UNIT 2 (WIS)
SILAM GENERATOR A-INLET

R20CAA



DTS



POINT REACT UNIT 2 (WIS)
STEAM GENERATOR A-INLET

R20C46

4/81

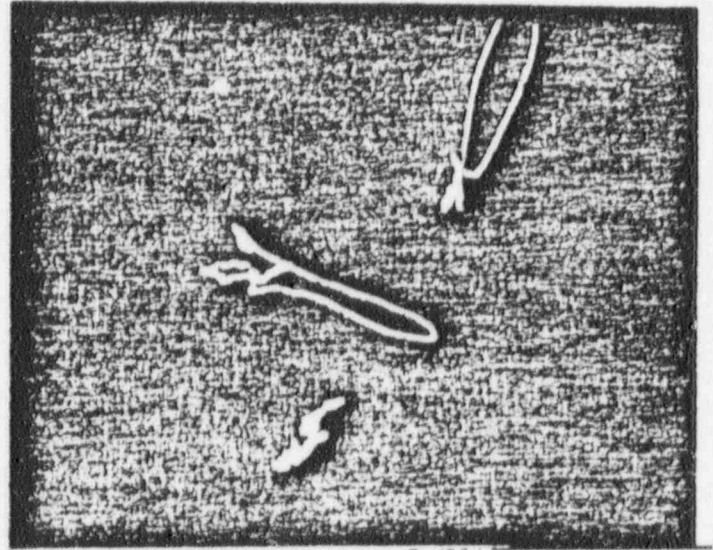
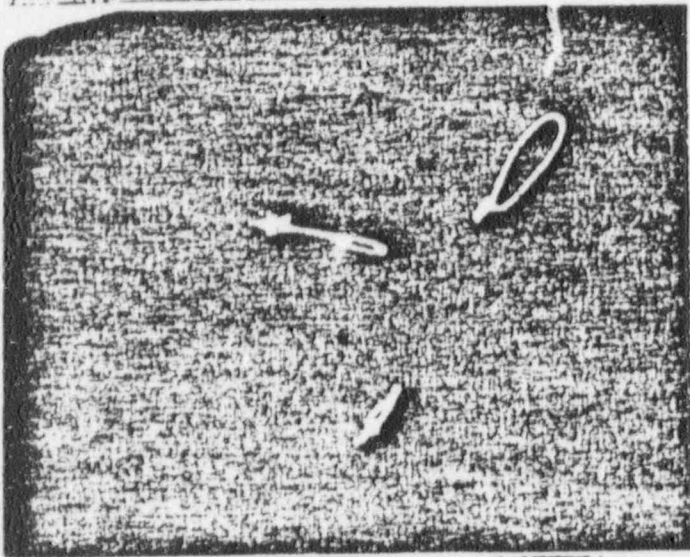
5/80

400 kHz

100 kHz

400 kHz

100 kHz



400 100 MIX
36%

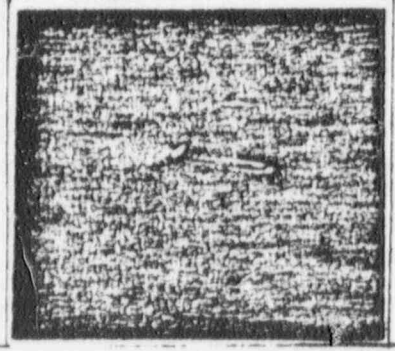
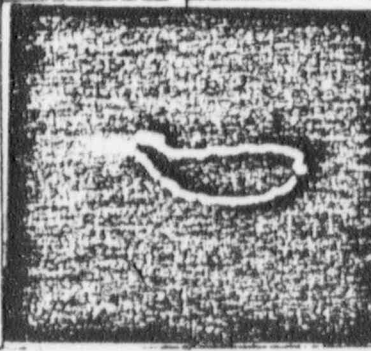
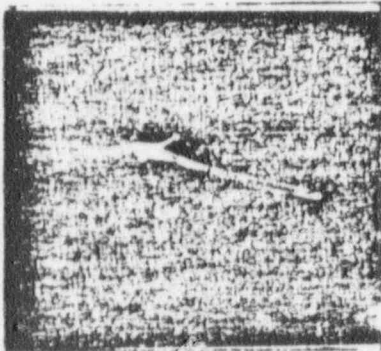
400 100 MIX
29%

5/79

400 kHz

5/78

5/77



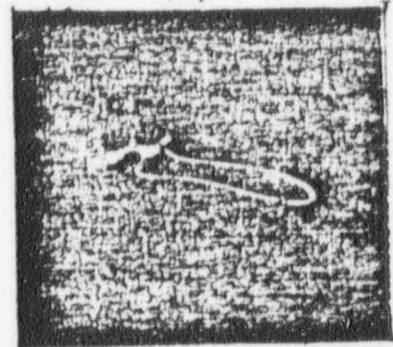
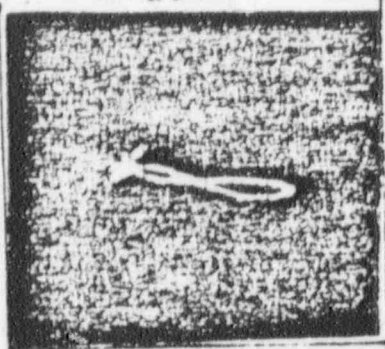
29%

31%

30%

3/76

10/74

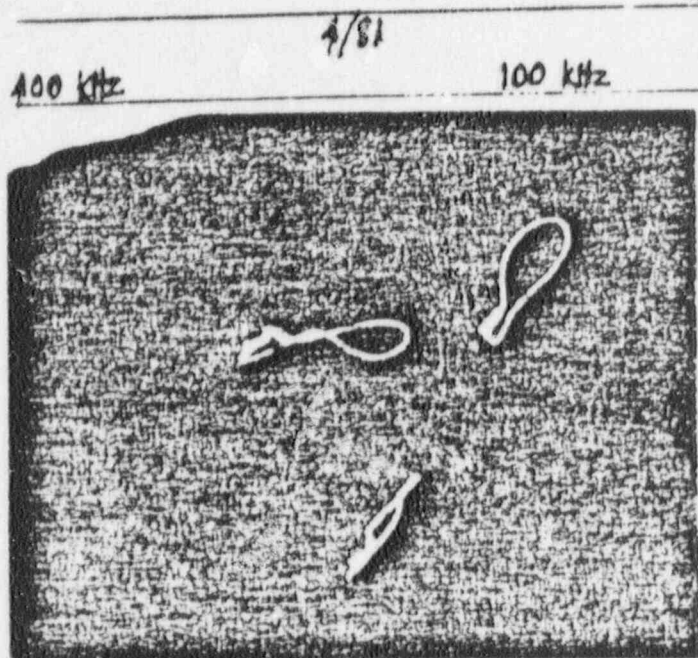


20%

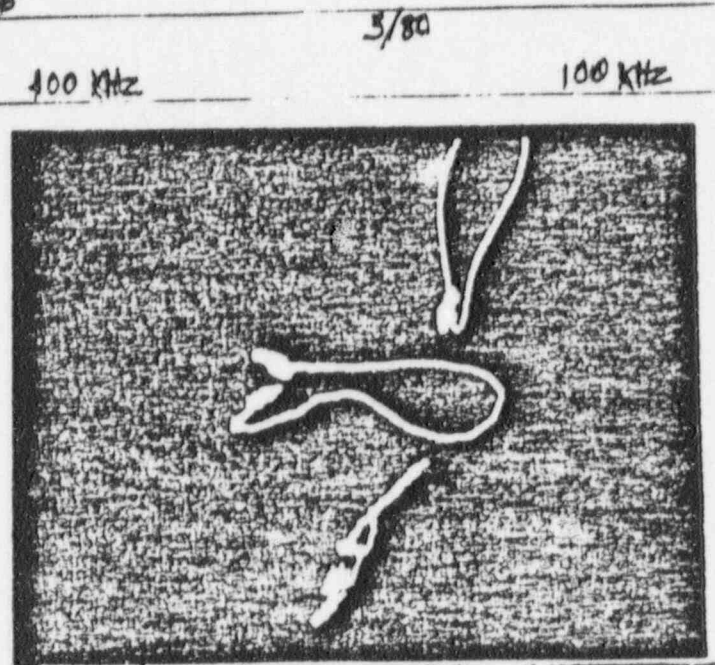
20%

POINT BEACH UNIT 2 (WFO)
STEAM GENERATOR A INLET

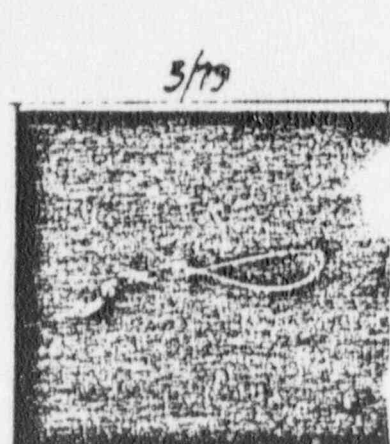
R21C46



400 100 MIX
36 %



400 100 MIX
37 %



30 %



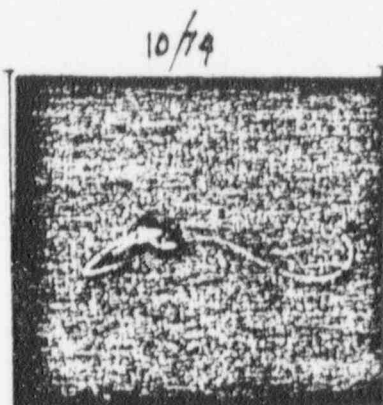
21 %



26 %



24 %



<20 %

POINT REACTOR UNIT 2 (WIS)
STEAM GENERATOR A INLET

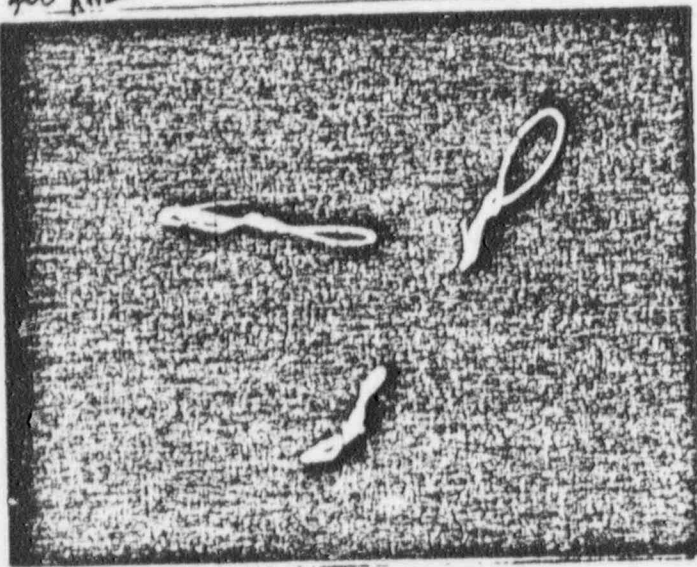
R17C59

5/80

400 KHz

4/81

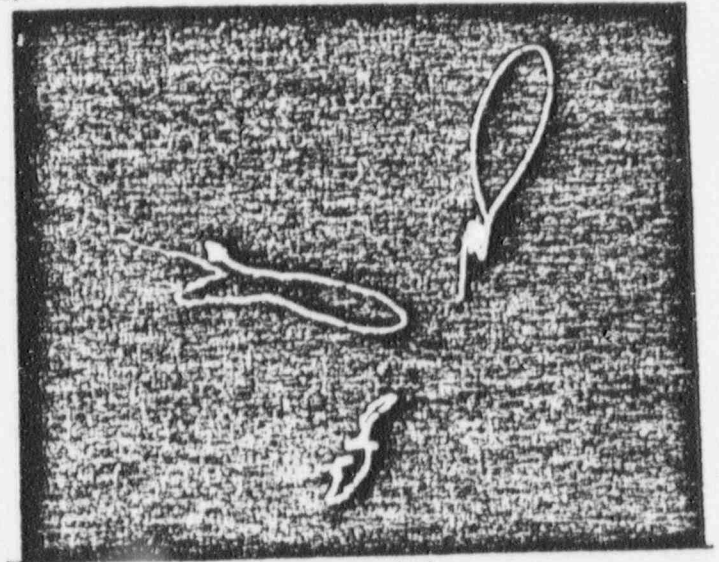
100 KHz



400 100 MIX
39%

400 KHz

100 KHz



400 100 MIX
36%

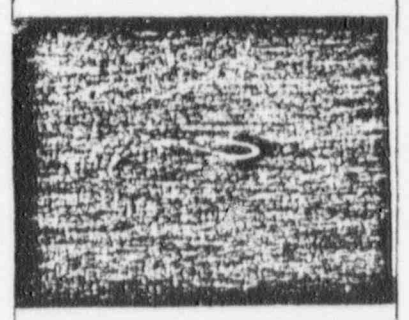
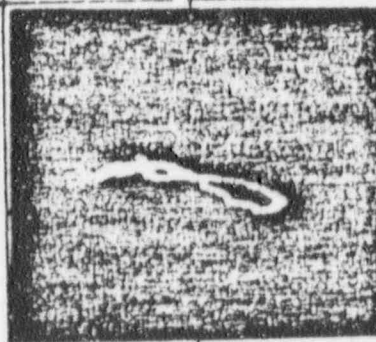
400 KHz

2/79

3/78

3/77

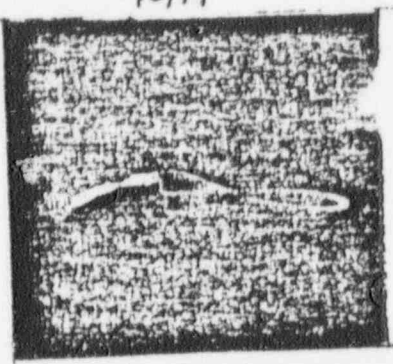
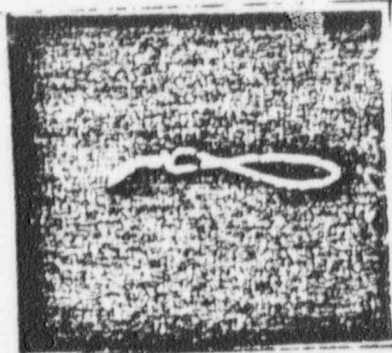
NOT
INSPECTED



<20%

3/78

10/74



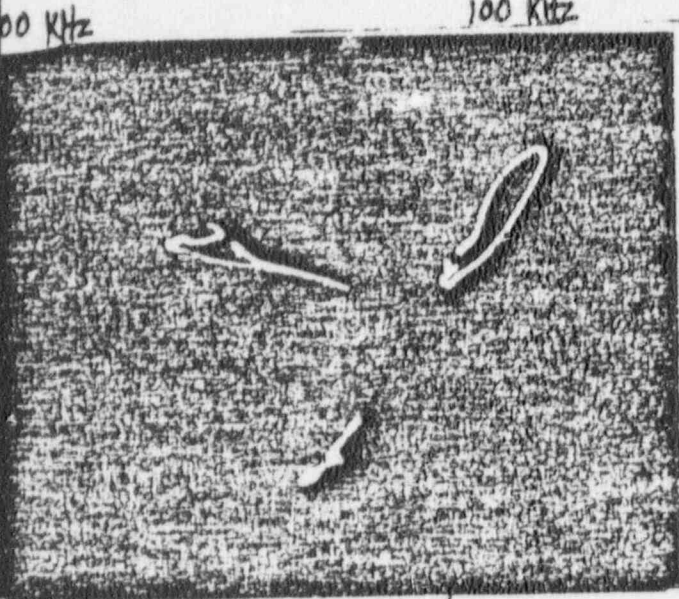
<20%

<20%

POINT BEACH UNIT 2 (W15)
STEAM GENERATOR A INLET

R16C38

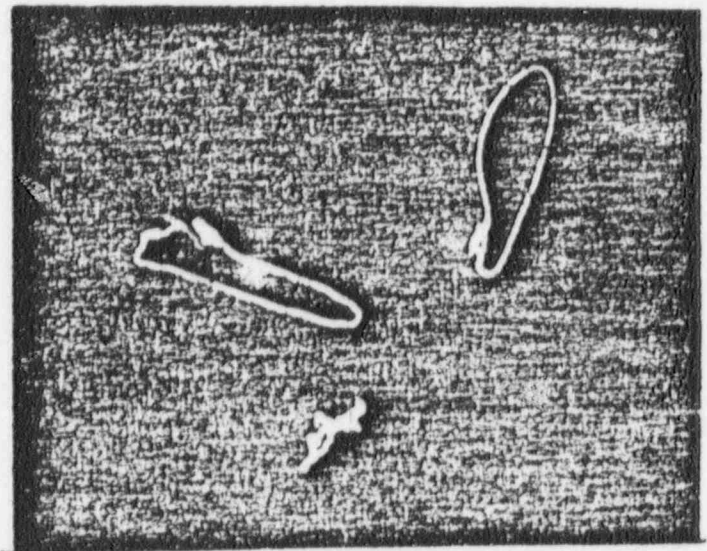
3/80



400 - 100 MIX
36%

400 KHz

100 KHz



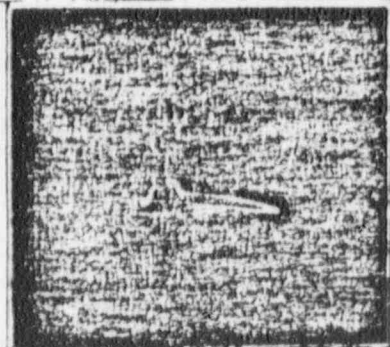
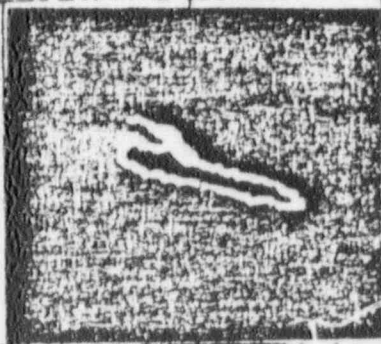
400 100 MIX
26%

3/79

100 KHz
3/78

3/77

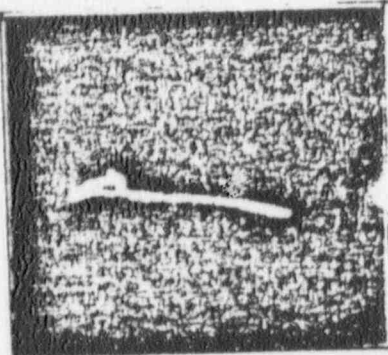
NOT
INSPECTED



DTS

3/76

10/74



DTS

